SPRINGER BRIEFS IN APPLIED SCIENCES AND TECHNOLOGY
AUTOMOTIVE ENGINEERING: SIMULATION AND VALIDATION METHODS

Daniel Watzenig
Bernhard Brandstätter *Editors*

Comprehensive Energy Management - Safe Adaptation, Predictive Control and Thermal Management

Springer

SpringerBriefs in Applied Sciences and Technology

Automotive Engineering: Simulation and Validation Methods

Series editors

Anton Fuchs, Graz, Austria
Hermann Steffan, Graz, Austria
Jost Bernasch, Graz, Austria
Daniel Watzenig, Graz, Austria

More information about this series at http://www.springer.com/series/11667

Daniel Watzenig · Bernhard Brandstätter
Editors

Comprehensive Energy Management - Safe Adaptation, Predictive Control and Thermal Management

Springer

Editors
Daniel Watzenig
Forschungsgesellschaft Mbh
Virtual Vehicle Research Center
Graz
Austria

Bernhard Brandstätter
Virtual Vehicle Research Center
Graz
Austria

ISSN 2191-530X ISSN 2191-5318 (electronic)
SpringerBriefs in Applied Sciences and Technology
Automotive Engineering: Simulation and Validation Methods
ISBN 978-3-319-57444-8 ISBN 978-3-319-57445-5 (eBook)
DOI 10.1007/978-3-319-57445-5

Library of Congress Control Number: 2017937931

© The Author(s) 2018
This work is subject to copyright. All rights are reserved by the Publisher, whether the whole or part of the material is concerned, specifically the rights of translation, reprinting, reuse of illustrations, recitation, broadcasting, reproduction on microfilms or in any other physical way, and transmission or information storage and retrieval, electronic adaptation, computer software, or by similar or dissimilar methodology now known or hereafter developed.
The use of general descriptive names, registered names, trademarks, service marks, etc. in this publication does not imply, even in the absence of a specific statement, that such names are exempt from the relevant protective laws and regulations and therefore free for general use.
The publisher, the authors and the editors are safe to assume that the advice and information in this book are believed to be true and accurate at the date of publication. Neither the publisher nor the authors or the editors give a warranty, express or implied, with respect to the material contained herein or for any errors or omissions that may have been made. The publisher remains neutral with regard to jurisdictional claims in published maps and institutional affiliations.

Printed on acid-free paper

This Springer imprint is published by Springer Nature
The registered company is Springer International Publishing AG
The registered company address is: Gewerbestrasse 11, 6330 Cham, Switzerland

Contents

Introductory Remarks from the Editors

Bernhard Brandstätter[1] and Daniel Watzenig[1] on behalf of the Cluster of 4th Generation Electric Vehicles

This book is organized in two volumes (the contents of both volumes are listed at the end of this introduction):

- Volume 1: "Comprehensive Energy Management—Eco Routing & Velocity Profiles"
- Volume 2: "Comprehensive Energy Management—Safe Adaption, Predictive Control and Thermal Management"

Comprehensive Energy Management

Energy management plays a central part in today's vehicles, especially for battery electric vehicles, where a limited number of charging possibilities and time-consuming charging processes lead to range anxiety of the users. This can be considered as an important factor (apart from the increased cost of electrical vehicles compared to conventional ones) that prevents larger number of fully electric vehicles on the road.

Thus, comprehensively treating energy and controlling it is of uttermost importance.

This book provides findings of recent European projects in FP-7 grouped in a cluster named "Cluster of 4th Generation Electric Vehicles", but also gives insight into results from ongoing H2020 projects related to energy management.

Since fuel cell technologies are gaining more attraction again, the last section of the book gives an overview of the state of the art in this field what PEM[2] fuel cells is concerned.

[1]Virtual Vehicle Research Center, Inffeldgasse 21a, Graz, Austria.

[2]Proton exchange membrane

Cluster of 4th Generation Electric Vehicles

The Cluster "4th Generation EV" was set-up in late 2013 by the European projects INCOBAT, iCOMPOSE and eDAS, with the purpose to synchronize on and cojointly promote the R&D topics on electric vehicles. By growing to a total of six projects with the FP7 projects Batteries 2020, IMPROVE and SafeAdapt, the cluster also enlarges its networks and range of influence on the European electric vehicle community (Fig. 1).

The projects within the cluster are focusing on the following goals:

- Batteries 2020+: improve performance, lifetime and total cost of ownership of batteries for EVs
- eDAS: Holistic energy management for 3rd and 4th generation EVs.
- iCOMPOSE: Integrated Control of Multiple-Motor and Multiple-Storage Fully Electric Vehicles.
- INCOBAT: Innovative Cost Efficient Management System for Next Generation High Voltage Batteries.
- IMPROVE: Integration and Management of Performance and Road Efficiency of Electric Vehicle electronics.
- SAFEADAPT: enrich networked embedded systems in e-vehicles.

Uniting more than 40 partners from 12 countries all over Europe, including 7 OEMs, with an overall budget of more than 36 million Euros, the impact of the cluster on the next generation of electric vehicles keeps on growing.

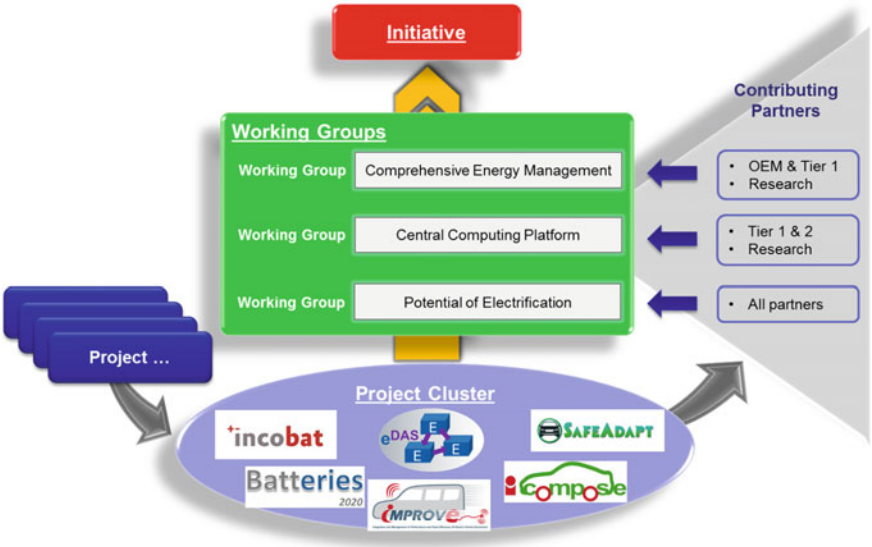

Fig. 1 Cluster of 4th Generation Electric Vehicles

The "4th Generation EV" cluster is organized around the three following working groups:

- Comprehensive energy management
- Central computing platform
- Potential of electrification

Some of the cluster projects will end in 2016 but bridging to H2020 projects has already begun. As an example the H2020 project OPTEMUS can be mentioned, where the comprehensive energy aspect is widened by new technologies like heating panels and energy harvesting technologies with strong focus on thermal comfort sensation inside the cabin (which plays a very important role in overall energy consumption).

Organization of this Book

The chapters of this book are organized in five different groups: ECO driving and ECO routing cover different approaches for optimal speed profiles for a given route (mostly interconnecting with cloud data); model based functional safety and fault-tolerant E/E architectures; advanced control making use of external information (from a cloud) as well; thermal management as a central part for energy optimization and finally some aspects on fuel cells.

These subject areas with their chapters (chapter titles in italic) are listed below:

Volume 1:

- ECO Driving and ECO Routing
  - *Aspects for velocity profile optimization for fleet-operated vehicles*: on-board and off-board optimization including cloud communication
  - *Semi-autonomous driving based on optimized speed profile*: different controllers including model-predictive control
  - *Design of Vehicle Speed Profile for Semi-Autonomous driving: energy consumption optimization for different driving conditions*
  - *Energy-efficient driving in a dynamic environment*: considers energy-optimal velocity profiles in the presence of other traffic participants and overtaking possibility
  - *Model-based Eco-Routing strategy for electric vehicles in large urban networks*: energy consumption model that considers accelerations and road infrastructure

Volume 2:

- Safety Aspects
  Addressing fault-tolerant approaches of automotive energy-efficient E/E architectures and model-based functional safety engineering in
  - *Safe Adaptation for reliable and Energy-Efficient E/E Architectures*
  - *Model-based functional safety engineering*
- Advanced Control
  - *Model predictive control of highly efficient dual mode energy storage systems including DC/DC converter*
  - *Predictive energy management on multi-core systems*: first approach to solve a reference speed tracking problem on a multi-core platform in real time
- Thermal Management
  - *Holistic thermal management strategies for electric vehicles*: including some rudimentary cabin comfort issues
  - *Heat pump air conditioning systems for optimized energy demand of electric vehicles*
- Fuel Cells
  - *Thermal management of PEM fuel cells in electric vehicles*

The aspects within the field of comprehensive energy management are too numerous that all of them could have been addressed in this book (aerodynamics and adaptive control of aerodynamic features could be mentioned in this context as an example). We think, however, that important key enabling elements for optimal energy management taking the environment and context into account have been collected in this book.

We cordially acknowledge all authors and co-authors for their efforts and looking forward to next steps in future projects.

Graz
December 2016

Daniel Watzenig
Bernhard Brandstätter

Chapter 1
Safe Adaptation for Reliable and Energy-Efficient E/E Architectures

Gereon Weiss, Philipp Schleiss, Christian Drabek, Alejandra Ruiz and Ansgar Radermacher

Abstract The upcoming changing mobility paradigms request more and more services and features to be included in future cars. Electric mobility and highly automated driving lead to new requirements and demands on vehicle information and communication (ICT) architectures. For example, in the case of highly-automated driving, future drivers no longer need to monitor and control the vehicle all the time. This calls for new fault-tolerant approaches of automotive E/E architectures. In addition, the electrification of vehicles requires a flexible underlying E/E architecture which facilitates enhanced energy management. Within the EU-funded SafeAdapt project, a new E/E architecture for future vehicles has been developed in which adaptive systems ensure safe, reliable, and cost-effective mobility. The holistic approach provides the necessary foundation for future in-vehicle systems and its evaluation shows the great potential of such reliable and energy-efficient E/E architectures.

Keywords Adaptation · Safety · Reliability · Autonomous driving

1.1 Introduction

Today, the mobility domain is facing tremendous changes including arising changes of how vehicles will be used in the future. One example is the progressing automation of nowadays cars towards intelligent transportation systems. When the driver is not in control of the vehicle all the time [1], the vehicle and its underlying

G. Weiss (✉) · P. Schleiss · C. Drabek
Fraunhofer ESK, Munich, Germany
e-mail: gereon.weiss@esk.fraunhofer.de

A. Ruiz
Tecnalia, Derio, Spain

A. Radermacher
CEA LIST, Palaiseau, France

© The Author(s) 2018

D. Watzenig and B. Brandstätter (eds.), *Comprehensive Energy Management - Safe Adaptation, Predictive Control and Thermal Management*, Automotive Engineering: Simulation and Validation Methods, DOI 10.1007/978-3-319-57445-5_1

system architecture must provide enhanced dependability. In the light of the transition towards software defined cars, the interconnection of presently isolated subsystems plays a major role in implementing new functions in modern vehicles. For instance, modern Advanced Driver Assistance Systems (ADAS) have to reliably read and control diverse periphery, like brake, drive-train, and steering systems as well as other optional sensors, such as cameras and radars. Moreover, the present vigorously pursued vision of autonomous driving [2] prerequisites an even more intertwined vehicle system, in order to integrate required logic and dependable control.

Another emerging trend is the growing market of fully electric vehicles. With the advent of electric drive-trains, the dream of zero emission transportation turns more tangible. However, when trying to transform this vision into reality a multitude of new technologies has to be integrated as well, e.g., wheel-hub drives with recuperation of energy or *Brake-by-Wire* (*BBW*) and *Steer-by-Wire* (*SBW*) systems. For this, well-established mechanic and hydraulic systems will be replaced. The henceforth resulting safety-critical subsystems must now be managed in a way in which safety is ensured and which compensates for failures gracefully.

Initially, mechanical fall-back mechanisms which are able to mitigate the risk of electronic system failures may ease this transition for single functionalities individually. But with the expected increasing number of such functionalities, this co-existence of mechanical and software-based control systems introduces a cost and weight overhead which is not bearable in the long-run for a unit focused cost-driven industry. Considering that high-end automotive *E/E* (*Electric and Electronic*) vehicle-architectures already consist of up to 100 *Electronic Control Units* (*ECUs*) [3], which are interconnected by multiple bus systems and provide up to 3000 atomic software-based functions [4] the implementation of all features required for a *Fully Electric Vehicle* (*FEV*) will undoubtedly complicate and thereby incapacitate current design practices. In order to implement the increasing number of functions in future vehicles by software in a safe and cost-efficient way, a new and substantially revised E/E architecture is needed. Otherwise, the overall product costs will increase due to the required safety enhancements. This will very likely not be acceptable for the addressed mass markets. Such architectures need to manage reliability and energy-efficiency as a system-wide property.

1.2 Challenges of Reliability in Automotive E/E Architectures

In the pursuit of finding a tangible E/E architecture for future vehicles with improved safety characteristics and flexibility, incorporating adaptive concepts pose as a promising opportunity. More precisely, the aspects of adaptivity focusing on flexible system reconfiguration are beneficial to exploit existing system resources in a sophisticated way, e.g., by abolishing completely redundant components.

Other application areas have already faced similar changes. Within the aerospace domain for instance, hot redundant Fly-by-Wire control systems with dissimilar design patterns have already replaced traditional hydraulic and mechanical forms of control, through the advent of so-called Integrated Modular Avionics (IMA) architectures [5]. In turn, this effort towards managing redundancy and fault containment considerably raises complexity and the need for enhanced electronic control. For the aerospace domain this investment is justifiable. Safety-critical functions are required to be as well fully fault-tolerant as also fail-operational and the smaller product quantities facilitate other cost structures.

This simply results from the fact that an aircraft cannot be stopped during a flight in case of failure. However, as soon as automation permeates modern cars and mechanical solutions are substituted by electronic systems, similar requirements arise in the automotive domain. Up to now, the shutting down of failing components constituted a viable solution to ensure a safe state of the vehicle, which is called *fail-silent behaviour*. In contrast, to ensure that an highly-automated vehicle can be stopped safely after a system impairment, a reduced set of most critical functions has to always remain operational, e.g., the steering, driving, and braking. This requires a shift from the previously mentioned fail-silent to *fail-operational behaviour*, which ensures that critical functionality is kept also available in the case of a failure. This approach also increases the overall controllability of the vehicle in hazardous scenarios by offering the driver means to take control of the situation.

A complete adoption of solutions originating from aerospace to the automotive industry is, however, not directly possible or desired due to cost reasons. For instance, there is no need to have dual or triple redundancy or dissimilar systems in the same complex manner. In contrast, the unit-cost driven automotive industry may still profit from the technical solutions found in the aerospace domain, even though implementations in avionics are differing in amount and complexity. Therefore, an approach suitable for automotive E/E systems should copy the principal ideas of redundant systems but optimise the amount of resources required, like the number of ECUs or replicated functions, to attain cost effectiveness, which is in turn crucial for mass market production. While meeting cost constraints, the solution should also ensure high reliability and safety levels. Thus, adaptation of the in-vehicle system to meet reliability and efficiency constraints through adequately organising available resources provides an auspicious approach.

1.3 Safe Adaptation

Taking up the challenge of developing reliable in-vehicle system architectures, the European funded research project *SafeAdapt—Safe Adaptive Software for Fully Electric Vehicles* [6] researches novel architectural concepts for future FEV and autonomous driving. The target is to enhance robustness, availability, and efficiency of in-vehicle systems while preserving the highly-demanding functional safety requirements of anticipated future smart cars. For this, enhanced redundancy

concepts and mechanisms are required to achieve sufficient safety levels, which are also applicable within the automotive sector. SafeAdapt focuses on ensuring enhanced safety based on re-configurability of the software-architecture, including related tools. The main system goal is to provide fail-operational behaviour for safety-critical functionality through a generic mechanism which can be utilised application-independent. The concepts are finally tested and evaluated through diverse demonstrators comprising exemplary pure electric functions like Steer-by-Wire (SBW), ranging from driver-in-the-loop (DiL) simulations over model-car to a full scale e-vehicle prototype.

In detail, the project's main objectives can be broken down into providing:

(1) Novel architecture concepts to enhance robustness, availability, and efficiency of safety-relevant systems while preserving the functional safety in FEVs
(2) Increased safety and availability by the ability to handle complex failures, especially failures where current systems do not degrade gracefully
(3) Reduced bill of material through reducing the number of ECUs by means of generic failure management
(4) Reduced development costs (time-to-market, certification, and testing costs) in future FEVs by providing a generic failure management and software update mechanism
(5) Increasing energy-efficiency in automotive E/E architectures through adaptation.

The objectives are pursued based on use cases of future vehicles and thereby derived requirements. This provides the basis for creating a novel system architecture with generic failure management. In addition, to unleash the full potential of efficiently developing systems with such enhanced architectural features, a novel design methodology and tools, including validation and verification, are researched. At the same time, a generic solution offers potential for reuse by applying the same implementation for different and diverse applications running on top of it.

SafeAdapt incorporates and extends existing approaches while building upon past advances in E/E architecture design. With AUTOSAR an industrial standard for automotive software architectures has been established, allowing ECU-independent software development. SafeAdapt sets out to create a substantially revised blueprint for flexible, but at the same time safe, E/E architectures compliant to this AUTOSAR standard [7]. With ISO26262 [8] an international standard has been published which constitutes a basis for state-of-the-art of automotive functional safety. This is explicitly considered in the developed approach, e.g., by exploiting its concepts for modular safety composition, the so-called *Safety-Element-out-of-Context* (*SEooC*). Through this, a lean integration of the proposed enhanced reliability and flexibility is made possible.

Overall, with the SafeAdapt approach several enhancements are expected. This includes reducing considerably the number of ECUs by combining multiple functions onto generic platforms. Increased safety and availability is aimed by a universal failure handling mechanism which is able to relocate functionality after a

failure of an ECU onto other devices. Moreover, the development costs are expected to be reduced trough simplified E/E-system design, integration, certification, and maintenance efforts. As the mechanism is developed according to ISO 26262, no overhead investment for validation is expected. Improved energy-efficiency is estimated by limiting the number of active devices and communication links. Together with facilitating the abolishment of mechanical fall-back solutions, potentially weight can be reduced and more sophisticated techniques of utilizing system resources are enabled. These characteristics should ease the flexibility to address the diverse use cases which are anticipated for future cars.

1.3.1 Use Cases

For determining requirements on the E/E architectures of future vehicles, several automotive use cases are derived which comprise different scenarios (s. Fig. 1.1). Each scenario is intended to highlight certain key aspects with strong relations to the E/E architecture of future vehicles.

1.3.1.1 Enhanced Failure Management with Fail-Operational Behaviour

This use case includes the failing of vehicle functionality, which may also be safety-critical. This failure has to be handled in an adequate and safe way, so that the control of the car is ensured at any time. One application particularly investigated is the *Steer-by-Wire* (*SBW*) functionality of a modern car, which steers purely

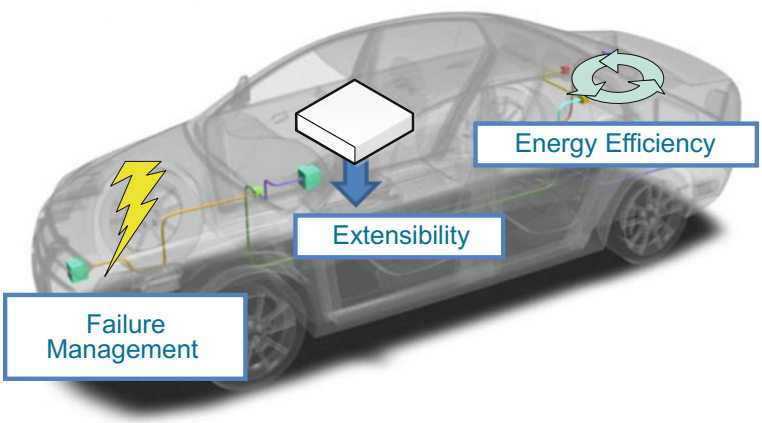

Fig. 1.1 Addressed use cases

electronically without any mechanical backup. An exemplary scenario is that a car is driving on a road and its SBW application experiences a failure. For this failure scenario, a basic SBW application version is available to be executed in a degraded mode, which has to be activated for keeping the control of the vehicle and reaching a safe state. The same need for availability of functionality holds true for other failure situations, e.g., failing of an ECU or disruption of interconnections. Thereby, this use case includes fail-operational behaviour of the underlying E/E architecture which is a blueprint for safeguarding functions which, at least partially, take the driver out of the control loop, e.g., automatic steering.

1.3.1.2 Energy-efficiency

Targeting eco-friendly mobility, energy-efficiency is an omnipresent constraint in today's vehicle development. Nevertheless main vehicle power-consumers are propulsion, heating and air-conditioning, head-lights, or electro-mechanical components, also the E/E architecture is contributing to the overall consumption [9]. This holds also true for common combustion engine system. To meet maximum levels of CO_2 emissions for their whole car fleets, car manufacturers pursue optimizing in-vehicle power consumption [10]. In such scenarios, also marginal savings may already be beneficial to keep numbers below certain limits. Different strategies towards partial networking have been applied in the automotive domain, with the potential of saving up to 25% of a cars' power consumption [11]. The addressed scenarios furthermore extend this approach by considering the shutdown of individual functions and exploiting variable function allocations, so more partial network parts can be involved. This includes enabling a flexible deactivation of not needed functionality in specific contexts while ensuring that critical functionality such as braking remains active. According to [12] the percentage of driving systems in premium vehicles, which may be shut down because of the vehicle or environmental situations, is varying from 10 to 55%. In order to be able to exploit such potentials, the allocation of functionality to networked control units is essential. The more flexible the required functionality can be allocated, the greater parts of the network may be shut down in varying contexts. This includes enabling a flexible deactivation of not needed functionality in specific situations, while ensuring that critical functionality such as braking remains active. A striking example for a potential candidate to be deactivated is the parking assistance during highway driving.

In the case of e-vehicles, energy-savings directly lead to enhanced range. For example, we imagine an e-vehicle driving and detecting a low charge of battery. To maximize the range and being able to reach the navigation target, energy-consuming comfort functionality and unneeded network parts are deactivated while the installed BBW application maximizes regenerative braking. The latter prevents comforting sporty driving; however, this is accepted in exchange for the lower energy-consumption resulting in a longer range of the e-vehicle. Nevertheless, it should be noted that main benefits with respect to energy

consumption are not expected through saved execution of software functionality but from being capable to shut down other power-consuming components because of a flexible and adaptive functional distribution.

1.3.1.3 Plug'n'Play and Extensibility

For taking the demands of higher flexibility and shorter time-to-markets into account, a use case enabling the changing of functionality of a car is considered. An example is a driver who wants to upgrade the vehicle by installing new software. Another example is the adding and removing of components of the vehicle in a plug'n'play fashion. For now, these use cases are foreseen to take place at an official maintenance service provider, while the car is not in operation. This open extensibility and variability poses several challenges to the verification of the whole vehicle system. One of the main barriers for its introduction is a feasible approach to assess that the safety remains after adding the extension. This makes this approach unattractive for standards compliance. In this case, it is important to specify the safety constraints of the overall system beforehand. During the upgrade all safety contracts shall be ensured as well, otherwise the upgrade will not be enforced (cf. [13]). Moreover, the ability to extend and update the vehicle flexibly may also be advantageous with respect to meeting liability claims and vehicle recalls.

These exemplary use cases show requirements of future vehicles and are directly reflected in the developed concepts and overall system architecture.

1.3.2 General Concepts

For embedding system-wide adaptation concepts, the interaction between the hardware and software is crucial. Since the mechanisms should be applicable generically throughout the in-vehicle system, specific assumptions are made (cf. Fig. 1.2). One main anticipated characteristic is that future vehicles provide access to the sensors and actuators without having to rely on specific control units. For this, intelligent sensors and actuators can be addressed directly or via network gateways. In order to ensure that a periphery component fault does not impact the functionality of the entire system, redundancy must be installed. This applies to the individual sensors and actuators, as well as to the existing communication infrastructure. Therefore, at least two communication paths must exist between all communication partners to reliably rectify individual faults.

Since the adaptation has to be planned in a distributed way consistently and deterministically, all main control units must operate based on a common time basis. Therefore, *synchronization* and real-time mechanisms have to be installed within the participating computing platforms. This can, for instance, be enabled via individual or standardized technology, such as time-triggered Ethernet or time-sensitive networking [14].

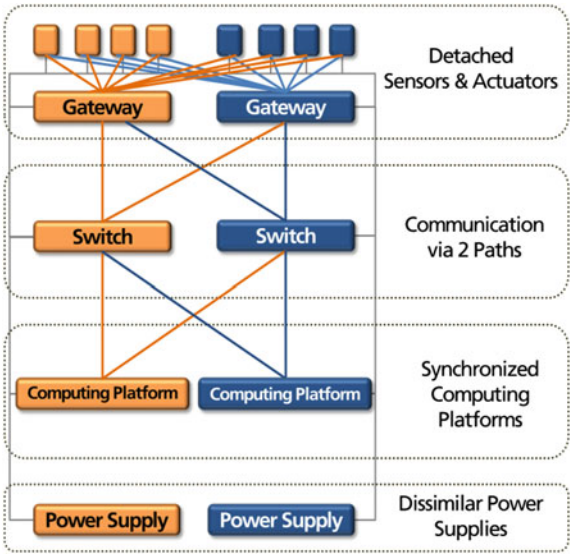

Fig. 1.2 Fundamental architectural requirements of SafeAdapt

In general, the fault tolerance of a component can be increased either through a design that makes it less susceptible to failure or by utilizing multiple components. The first solution is quite complex and costly. Thus, in most cases it is only suitable for single components, if at all. For this reason, fault tolerance is typically provided through redundant components in order to avoid so-called *single-points-of-failure*. When it comes to the E/E architecture, such single-points-of-failure within the process chain of the safety-critical functions must be avoided. This is easily illustrated by the example of the SBW functionality. During the entire process—from the time the steering information is registered until the wheels are positioned—the design must ensure that no single fault impacts the steering behaviour or leads to a complete steering outage. Hence, when defining the system architecture, these individual faults must be excluded for all relevant functions.

Lack of a redundant power supply is a clear example of this issue. Fault tolerant components must be connected to independent power supplies. In other words, a redundant component is useful only if it has access to another power source to keep it operating, in case the primary power supply fails.

Furthermore, the communication architecture is obviously subject to this matter. As it provides the interconnection of all components, it must be implemented in a way that it is capable to compensate for the loss of connectivity. For this reason, two paths must exist between each communication partner in the architecture. In order to implement this approach efficiently, the sensors and actuators must be decoupled from the core computing platforms. Redundant sensors and actuators can be addressed via two separate gateways for instance. They can thus be detached from individual ECUs and be shielded from the direct effects of any ECU fault.

The installed computing platforms execute the corresponding software functions and can provide redundant software functions in case the primary functions fail. If a computing platform with specific software functions fails for instance, another predefined platform can keep the critical functionality available by executing the respective redundant software functions. There are different ways to make these redundant functions available. A main distinguishing factor is how quickly the failed functionality has to be re-established, which is also called *maximal fail-over-time*. For this, different concepts for redundancy are considered with hot- and cold-standby functions. Hot-standby functions are instantly available, in contrast to cold-standby functions which have to be initialized first.

In light of the safety requirements, the system design defines the fail-operational software components and what type of redundancy is necessary to meet these requirements. For the efficient planning of such redundancy and resource allocation in the first place, an optimization algorithm takes into account these requirements and constraints of the software components for creating valid system configurations. An example for a constraint is that a software component should not be allocated together with its backup version on the same computing platform. Instead, it should also run on other computing platforms with different power supplies as explained above. A detailed description of the safety concept underlying the architecture can be found in [15].

1.3.3 Safe Adaptation

In pursuit of easing the design of safety-critical systems, the goal of this approach is to implement a generalised and re-usable process that avoids repetitive and error-prone development aspects. Within the SafeAdapt project, the adaptation management of functionality requiring high availability is targeted as prime candidate for benefiting from this approach. Based on the general architectural concepts, the so-called *Safe Adaptation Platform Core* (*SAPC*) is built as a generic safety mechanism [16]. It incorporates the decisions which configuration is established when a fault occurs. As common practice in safety considerations of static systems, only single faults in the system are considered. The same concept is also exploited to optimize the energy-efficiency. This is realized by the SAPC activating an energy-efficient configuration which is optimized for the driving situation.

By this general principle, the SAPC allows the system to reliably shift functions from a faulty component to a working component and to ensure continuous operation of critical functionality. To enable the installation of the SAPC on diverse platforms, it has initially been designed as an AUTOSAR software component, specified in the AUTOSAR-specific ARXML format [17]. Therefore, the SAPC is introduced as a generic safety mechanism, following the SEooC concept from ISO 26262 [18]. Hence, the SAPC itself can be realized as a platform independent software component. This facilitates the re-utilization of the SAPC implementation, without the need of adapting it to various ECUs with different hardware and of

re-validating its correctness. However, as it provides a basic mechanism on every involved platform, in a production system it would be introduced as a Basic Software Component in the AUTOSAR standard (cf. Fig. 1.3). In order to distinguish between its different tasks, it consists of the components *Fault Filter, Local Fault Manager, Local Database* and *Global Adaptation Manager*. Mainly, the SAPC determines a new local configuration after recognizing the need to adapt, e.g., after an error condition or detection of a too low battery status. In order to realize such generalized redundancy management in a manner that is beneficial to a wide range of safety-critical systems, application software like SBW is classified according to its requirements in case of a failure. Here, the maximal acceptable time to regain control after a critical fault (maximal fail-over time) within the system's infrastructure is a major design factor. Consequently, software applications are classified into *hot- and cold-standby* tasks, depending on their timing and historic data requirements, in order to function correctly. More specifically, hot-standby tasks actively replicate the actions of a primary instance, with the sole difference that its outbound communication is suppressed. In turn, cold-standby tasks are not scheduled during normal operation and only activated in case of a failure. In addition, the *frozen-standby* concept extends cold-standby by storing backup functions in a distributed repository and loading and executing them on demand. It is important to notice that all feasible configurations susceptible to be used in adaptation are specified during the development phases. ISO 26262 follows a deterministic approach for verification activities. Having the possible configurations defined during the development phase ensures safety is still guaranteed after the adaptation has taken place. This approach is considered as a hybrid between static and fully dynamic configurations. It includes that possible configurations are specified beforehand. In addition, it has the capability to autonomously modify the

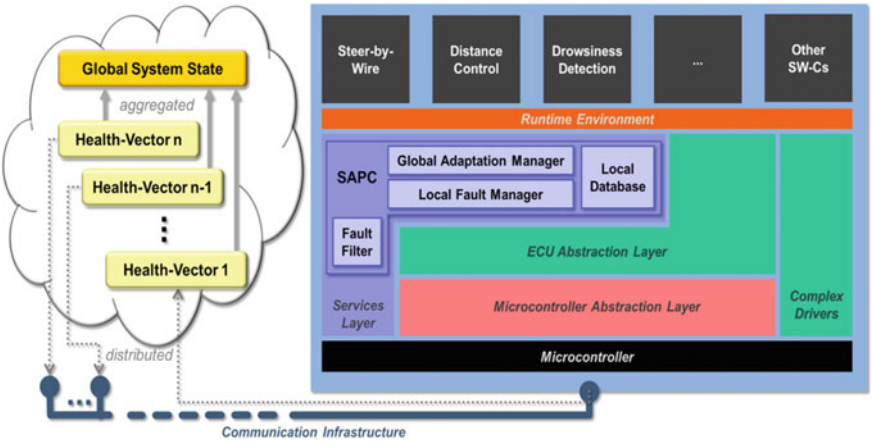

Fig. 1.3 Schematic overview of a computing platform implementing the SAPC

system behaviour at runtime in response to changes in the environment and is in line with the ISO 26262 objectives.

In order to detect failures at runtime, the developed SAPC mechanism relies on a cyclic exchange of extended heart-beat messages—so-called *Health Vectors*. They include the status of each control unit on the granularity of individual software components. These messages are the result of each computing platforms' diagnostic services and convey the platform's capability of executing each hosted application. For finding adequate local configurations, each core computing platform periodically shares with all other platforms the *Health Vectors*. Through the periodic exchange of this status information, each core platform can then derive decentrally the overall global system status. Based on this global system state, the database can then be queried to determine if a local adaptation is required, or if the system is currently in a stable and safe state. Therefore, the developed safety mechanism utilises a platform-independent database concept. Therein, all anticipated failure scenarios are mapped against a dedicated adaptation plan, which is derived during the design of the system. Within such an adaptation plan, each core platform is assigned with a set of tasks that must be activated in order to compensate for the specific fault pattern and to reach a consistent and safe system state again. In detail, such adaptation plans include instructions to activate the communication of software components as well as to schedule and unschedule individual tasks.

Figure 1.4 shows a simple example of a UML state-machine that models the transitions between different configurations. Each state references a configuration which is modelled as a set of instance-specifications (of EAST-ADL design components) which also contain slots for configuration and an allocation to execution resources which in turn are allocated on physical nodes. This way of modelling is inspired by the notion of a *deployment plan* in OMG's CORBA component model (CCM)—even if the component model is based on EAST-ADL and not CCM compliant. This way of modelling is supported by the Papyrus extension for

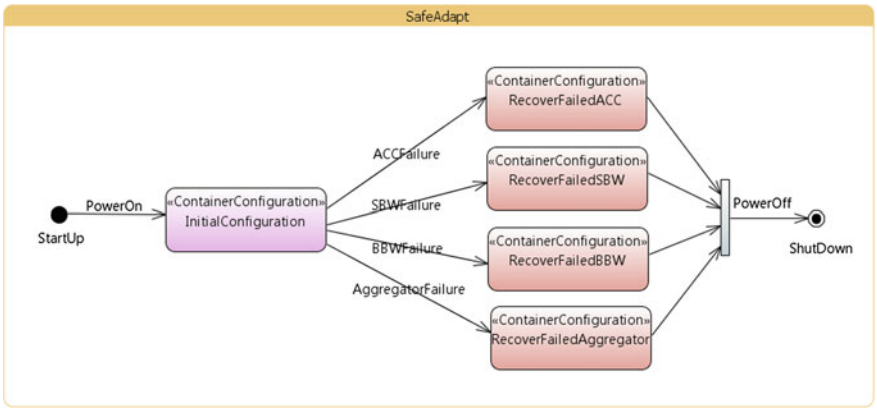

Fig. 1.4 A simple state-machine modelling single failures

software modelling (Papyrus SW designer) in the sense that such deployment plans can be automatically generated from a hierarchical structure with a top-level "system" component, as it is the case for EAST-ADL.

It must be ensured that all computing platforms transition based on the individual plans into a new system state simultaneously, to circumvent inconsistent and unanticipated behaviour. On the modelling level, all required information for this is available via the deployment plans outlined above. On the execution level, all runtime platforms utilise a schedule synchronisation mechanism to guarantee that such reconfiguration scenarios are performed in tight temporal bounds, thus, ensuring the system's determinism with respect to its safety goals. If a core platform fails for example, the other platforms recognize this situation through the missing reception of its Health Vector. In response to this, each platform activates a local configuration predefined for this particular error condition. Because the system maintains redundant real-time communication paths, the fault assumption is that no single error in the communication can cause the disappearance of a Health Vector. Instead, its missing is assumed to be related to the corresponding core platform.

1.3.4 Automated Design Process

For designing the system and being capable to derive the adaptation plans, architectural descriptions in EAST-ADL [19] and AUTOSAR [7] are utilised. Based on this, the SafeAdapt tool chain can be used to generate robust fault-tolerant system configurations, which automatically take into account all of the required characteristics, such as redundant standby versions of critical functions. This automated process makes it possible to generate configurations for every type of error condition, which would be near impossible to carry out manually given the numerous potential scenarios. This also makes it possible to guarantee that only valid system configurations are utilised. That means all requirements, such as the timely execution of functional chains, will be fulfilled. The configurations can then be further used in the system design model or for real applications. This allows developers to generate AUTOSAR ARXML-compliant configurations and source code that can be incorporated into the ECU software directly during development. Together with automatically-generated information that can be used as a basis for the SAPC, system-wide error handling can be implemented. This approach can be used in ECUs with conventional AUTOSAR operating systems, as well as with more powerful real-time operating systems in future adaptive platforms.

In detail, this automated system synthesis process is structured in five steps (see Fig. 1.5). Foremost, the focus is laid on the design of individual driving functionality, such as a Steer-by-Wire system. With current state of the art tooling the communication interfaces can already be modelled and exported into the ARXML exchange format. Moreover, the advance of the AUTOSAR standard's timing extension allows for a fine grained formalisation of a functionality's timing properties and requirements such as End-to-End deadline or the Worst Case Execution

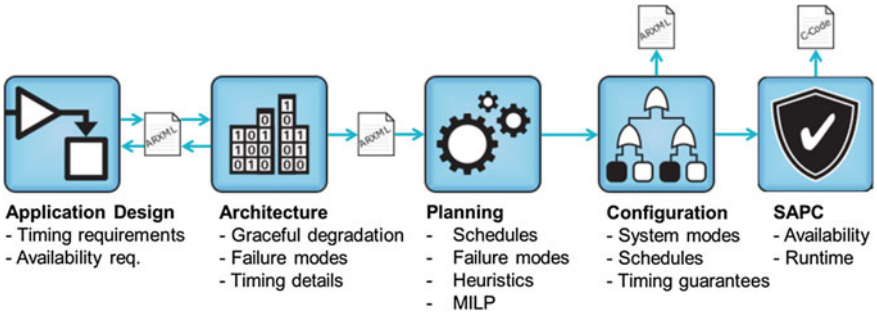

Fig. 1.5 Automated system synthesis

Time (WCET) of a *runnable* on a certain hardware. Despite this extensive expressiveness of the exchange format, it currently still doesn't address availability requirements. Consequently, the exchange format had to be enhanced through vendor-specific extensions in order to be able to formalise availability requirements. Here, each *software component prototype* can be annotated with an application-specific operating mode. For example, a SWC instance may be fully operational or only remain in a cold-standby mode. Based on these application-specific modes, the required availability of individual functionalities can be described. In order to address all failure modes of the system, it is now of interest to declaratively describe which functionality must be available within a certain mode of the entire system. Such a system mode is defined through the available resources in a system, such as ECUs, sensors, or communication links. Based on this extension to the ARXML exchange format, it is now possible to formalise which resources are still available and which SWC instances must remain operational independently for each failure mode.

Based on these individual descriptions of functionalities, a system-wide software architecture is provided. Moreover, all failure modes caused by random hardware faults are aggregated within a system model through the previously described concept of system modes. Based on the information within this system model, it is now possible to automate the further design of the system with respect to integration activities. As such, the ARXML-based system model is transformed into an abstract communication graph annotated with additional timing requirements. This representation is then further translated into a Mixed-Integer Linear Programme (MILP), in order to find a valid assignment of a SWCs to ECUs and MCU cores and a schedule for each runnable within the system under consideration of the availability requirements in each failure mode. Similarly, the communication over buses and networks is also scheduled to ensure all End-to-End timing requirements are met. For this planning process, additional mathematical constraint are required to ensure the correct timing of all SWCs during the transition between two system modes, as for instance observed during the failure of an ECU. The final MILP-representation can now be evaluated by a general purpose solving engine.

After the solving process, the results are reflected back into the ARXML-based system model. In detail, the timing requirements of each runnable and data package are refined through defining during which absolute system-wide time intervals it must execute, in order to ensure the correct functioning of the system. Moreover, a link is created to tie these refined timing requirements to the specific mode of the system. In essence, the configuration of individual ECUs is now severely simplified, as integration aspects, such as ECU timing and communication data packaging, are already predetermined in the system model. For instance, the refined timing requirements may be automatically translated into an AUTOSAR system's schedule table configuration without any manual effort. The configuration of the SAPC component's database is also performed automatically based on the results of the planning process, as the knowledge about which configuration must be activated in a certain system mode has already been formalised in the extended ARXML exchange format.

1.4 Evaluation

In order to demonstrate the applicability and suitability of the concepts, diverse analyses have been carried out and prototypes were implemented realizing the targeted use cases. Therefore, also the system development is specifically supported through software tools for the design and analysis. This allows capturing adaptivity of the software architecture with the modelling language EAST-ADL and developed extensions. Such architecture models can in turn be utilised to validate adaptation properties. For this, methods for simulation with have been realized with different frameworks, e.g., to check the effects of faults and the correctness of the adaptation in reaction through fault-injection. Thus, it could be examined if the system adopts the correct configuration for every specified fault. In order to pre-calculate all needed configurations, an individual planning tool has been developed. It facilitates the development of flexible architectures within current AUTOSAR tool flows. Based on the requirements from the design and results from the safety analysis, valid AUTOSAR configurations are generated which meet all defined system constraints. Also, the information needed for the correct fault handling can be created automatically. This is shown by a model-car which integrates present AUTOSAR-Classic platforms including a SBW application. With the SafeAdapt approach fail-operational behaviour of the safety-critical SBW could be proven.

Moreover, critical scenarios could be evaluated in a safe DiL simulation [20]. Through driver studies, results could be gained with respect to how much time can pass until a failure, like the outage of the steering, must be compensated, so the driver does lose the control of the vehicle. In addition, the simulator could be used to construct a scenario in which adaptation enables a higher energy-efficiency. In this case, non-critical hardware and software functionality which is not needed in the present context can be shut down. The scenario comprises a vehicle exhibiting a low state of charge of the battery which leads to an adaptation of an

energy-optimized system configuration, so the driving destination can still be reached. However, the potential savings are directly depending on the specific architecture. In addition, most energy-consumption may be saved by enabling the shutdown of main power-consuming components through the introduced adaptive allocation mechanism, which may not be possible with static allocations.

To demonstrate the concepts in a real system environment, they are integrated in a full-scale e-vehicle. For this purpose, the e-vehicle was modified with the SafeAdapt E/E architecture and computing platforms interconnected with real-time Ethernet (see exemplary architecture in Fig. 1.6). By this setup, different fail-operational scenarios could be examined. One example is the fail safety of the safety-critical SBW function. The adaptation of the in-vehicle system ensures that different single faults which have been identified in the safety analysis can be compensated. With regard to the SBW, the steering can still be ensured in case the computing platform executing the primary SBW application fails or a relevant communication link is disrupted.

1.4.1 Results

The researched concepts allow for a flexible and reliable E/E architecture as it is required by future automated and electric vehicles. Through the evaluation of the different prototypes, the soundness of the approach could be analysed and proven. For instance, the carried out DiL driver studies [21] have shown that the outage of the SBW in the SafeAdapt architecture has no functional impact on the driver. Only if the duration of a failing steering functionality is greater than 150 ms, the failure is recognized as a qualitative reduction while driving. If it exceeds 250 ms, the failure is considered as safety-critical. The introduced solution is capable through the pre-calculated adaptation plans to manage this failure within reasonable less time.

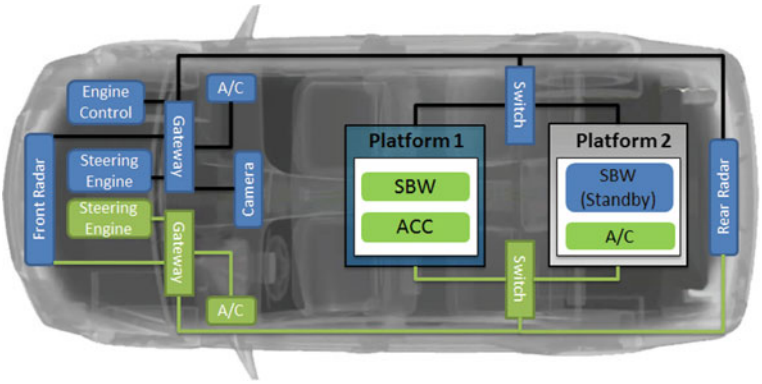

Fig. 1.6 Exemplary E/E architecture including Steer-by-Wire

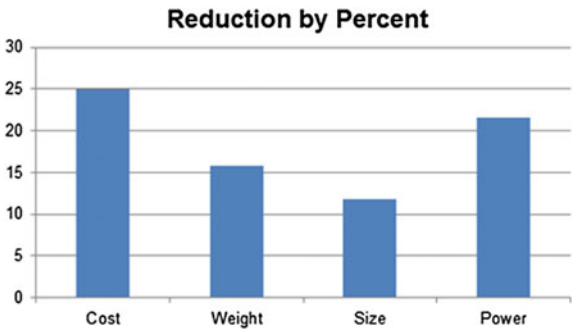

Fig. 1.7 Measurable improvements of the SafeAdapt approach in comparison to a state-of-the art architecture

In sum, the SafeAdapt approach enables a general failure handling mechanism which can be used independently of the individual functions development. This means, not every single safety-critical functionality must be enhanced individually with fail-operational capabilities. Rather, the system-wide available safety mechanism can be exploited in accordance with the ISO26262. Therefore, a deep analysis of the impact of adaptive systems on compliance has been performed and ISO 26262 objectives have been tailored to be applied in the presented approach. Details of the analysis are described in [22]. The latter has been specifically investigated. In detail, it has been analysed how this automotive functional safety standard is applicable to more adaptive vehicle systems.

For comparing the approach with state-of-the-art system architectures, an exemplary vehicle system has been modelled with and without the SafeAdapt concepts [21]. By this example, the resources required for the two different approaches have been calculated. As can be derived from Fig. 1.7, the potential savings which can be achieved following the SafeAdapt approach are promising. However, it must be stated that specific numbers strongly depend on the considered E/E-architecture.

1.5 Discussions and Outlook

The SafeAdapt concepts offer a cost-effective implementation approach of fail-operational behaviour for future automated driving functions. Responding to this paradigm change requires modifications to current E/E architectures in any case. The challenge of a change to the E/E architectures which have been growing over the years is not new to vehicle manufacturers. The focus often revolves around the need for a disruption as opposed to an evolution of existing approaches. While there may be no general answer to this question at the moment, the integration of high-performance, centralized computing platforms and the decoupling of the sensors and actuators is already apparent. Up to now, semi-automated driver assistance systems have been the key driver for this trend. In general, new vehicle manufacturers have an advantage in flexibility since they are less restricted when it

comes to new developments. However, established OEMs boast a know-how edge when implementing safety-critical mass products.

The point in time at which intelligent fail-operational concepts are introduced in series vehicles depends primarily on the extent to which the number of highly-automated driving functions grows. For individual functions, as well as for smaller highly-automated driving test fleets, simple fail-operational concepts with redundant hardware are frequently being employed. However, once highly-automated driving has to be implemented for multiple functions and series vehicles, an overall fail-operational behaviour concept becomes inevitable. Companies that adopt this early, while moving from proprietary solutions to a generic concept, will experience an initial technology boost and enjoy a competitive advantage in the development of future driving functions. In light of increasing competition through innovative business models spurred through new vehicle functions, particular attention should be paid to this issue. Over the long term, an in-vehicle system characteristic that is imperceptible to the user, like the E/E architecture, does not serve as a distinguishing feature. For this reason, a uniform solution and standardization is favourable in this case as it minimizes the development costs for fail-operational behaviour over time. With the presented concepts such a solution is already readily available.

1.6 Conclusion

Electric mobility and automated driving pose new challenges on the in-vehicle systems. As mechanical parts are vanishing and software functions with high availability demands will be integrated in future automated vehicles, the requirements on the underlying E/E architecture intensify. Therefore, novel concepts are required which enable reliable and energy-efficient solutions. By exploiting adaptation in the form of reconfiguration of the software system, the SafeAdapt approach provides a promising solution. With a generic safety mechanism the concepts allow to provide a system-wide fail-operational behaviour of safety-critical functions. Moreover, the adaptation can be used to provide a flexible management of the available in-vehicle systems' resources leading to an enhanced energy-efficiency. The approach has been implemented and evaluated in several demonstrators highlighting the benefits of such safe adaptation. As the number of safety-critical functions with high availability demands steadily increases in modern cars, the SafeAdapt concepts comprising a generic safety mechanism offer great potential for future in-vehicle E/E systems.

Acknowledgements The research leading to these results has partially received funding from the European Union Seventh Framework Programme ([FP7/2007–2013] [FP7/2007–2011]) under grant agreement n°608945, project SafeAdapt—Safe Adaptive Software for Fully Electric Vehicles.

References

1. Gold C, Damböck D, Lorenz L, Bengler K (2013) "Take over!" How long does it take to get the driver back into the loop? Proc Hum Factors Ergon Soc Annu Meet 57:1938–1942
2. Aeberhard M et al (2015) Experience, results and lessons learned from automated driving on Germany's highways. IEEE Intell Transp Syst Mag 7:42–57
3. Fürst S (2010) Challenges in the design of automotive software. In: Proceedings of design, automation, and test in Europe (Date)
4. Pretschner A, Broy M, Kruger IH, Stauner T (2007) Software engineering for automotive systems: a roadmap. In: Future of software engineering (FOSE '07)
5. Bieber P, Noulard E, Pagetti C, Planche T, Vialard F (2009) Design of future reconfigurable IMA platforms. In: Special issue on the 2nd international workshop on adaptive and reconfigurable embedded systems (APRES'09)
6. SafeAdapt. Safe adaptive software for fully electric vehicles. (Online). HYPERLINK http://www.safeadapt.eu. Last Accessed on 15 July 2016
7. AUTOSAR. Automotive open system architecture. (Online) HYPERLINK http://www.autosar.org. Last Accessed on 15 July 2016
8. ISO/IEC 26262 (2011) Road vehicles—functional safety, Part 1–10
9. Barthels A, Fröschl J, Michel H-U (2012) An architecture for power management in automotive systems. In: Architecture of Computing Systems—ARCS
10. Schmutzler C, Simons M, Becker J (2012) On demand dependent deactivation of automotive ECUs. In: Proceedings of the conference on design, automation and test in Europe (Date '12)
11. Balbierer N, Waas T, Meyer J, Jakob M, Seitz J (2013) Multinet—a wake-up protocol for multicast network groups. In: Proceedings of the eleventh workshop on intelligent solutions in embedded systems (WISES 2013)
12. Schmutzler C (2012) Hardwaregestützte Energieoptimierung von Elektrik/Elektronik-Architekturen durch adaptive Abschaltung von verteilten, eingebetteten Systemen. KIT Scientific Publishing, Karlsruhe, Germany
13. Amorim T, Ruiz A, Dropmann C, Schneider D (2015) Multidirectional modular conditional safety certificates. In: Safecomp workshops, Delft, pp 357–368
14. Institute of Electrical and Electronics Engineers. Time-sensitive networking task group. (Online) HYPERLINK http://www.ieee802.org/1/pages/tsn.html. Last Accessed on 15 July 2016
15. Ruiz A, Juez G, Schleiss P, Weiss G (2015) A safe generic adaptation mechanism for smart cars. In: IEEE 26th international symposium on software reliability engineering (ISSRE 2015)
16. SafeAdapt (2015) D3.1 concept for enforcing safe adaptation during runtime. Project Deliverable
17. Voget S (2010) AUTOSAR and the automotive tool chain. In: Proceedings of the conference on design, automation and test in Europe (Date '10), pp 259–262
18. Ruiz A, Melzi A, Kelly T (2015) Systematic application of ISO 26262 on a SEooC: support by applying a systematic reuse approach. In: Design, automation & test in Europe conference & exhibition (Date '15), pp 393–396
19. Cuenot P et al (2008) Developing automotive products using the EAST-ADL2: an AUTOSAR compliant architecture description language. In: Ingénieurs de l'Automobile (Automobile Engineers), vol 2, no 793
20. Pena A, Iglesias I, Valera JJ, Martin A (2012) Development and validation of Dynacar RT software, a new integrated solution for design of electric and hybrid vehicles. In: Technical article on integrated solutions for new vehicles designing, (EVS26)
21. SafeAdapt (2016) D5.3 evaluation results of the specified use cases and scenarios. In: Project deliverable
22. SafeAdapt (2015) D3.3 specification of ISO 26262 safety goal for self-adaptation scenarios. In: Project deliverable

Chapter 2
Model-Based Functional Safety Engineering

Dariusz Szymanski, Matthias Scharrer, Georg Macher, Eric Armengaud and Holger Schmidt

Abstract This chapter presents some aspects of model-based way of working applied in the EU funding projects called iCOMPOSE [1] and INCOBAT [2]. The presented results from INCOBAT project focus on basic structure that serves to organize/handle the technical complexity of the system under development. This approach was supported by the use case of INCOBAT battery system. The presented result from iCOMPOSE project focus on SysML model-based approach applied during the safety engineering development process and software integration of Integrated Comprehensive Energy Management System (iCEM). Some extensions to SysML profile are proposed and presented in this chapter and some findings on the data processing capabilities are discussed. The software development and integration of iCEM's embedded software required also a dedicated toolchain which was established and deployed taking into account constraints typical for automotive domain like safety criticality, real-time applications, various communications interfaces, variety of tools involved in the development process.

Keywords Software development toolchain · Functional safety · SysML · Model-based · Automotive domain

D. Szymanski (✉)
Flanders Make, Lommel, Belgium
e-mail: dariusz.szymanski@flandersmake.be

M. Scharrer
VIRTUAL VEHICLE Research Center, Graz, Austria
e-mail: Matthias.Scharrer@v2c2.at

G. Macher · E. Armengaud
AVL, Graz, Austria

H. Schmidt
Infineon, Augsburg, Germany

© The Author(s) 2018

D. Watzenig and B. Brandstätter (eds.), *Comprehensive Energy Management - Safe Adaptation, Predictive Control and Thermal Management*, Automotive Engineering: Simulation and Validation Methods, DOI 10.1007/978-3-319-57445-5_2

2.1 Introduction

Modern automotive systems require high computational power due to complicated algorithms and are often of safety critical nature. This safety criticality imposes additional constrains on the embedded software itself as well as on its development process including the integration phase. While the requirements for safety-critical software development are well defined in part 6 of ISO–26262 standard [3], the efficient execution of the process can still be a challenge. SysML modelling promises to solve this problem of consistent and evolutionary description of the item including required traceability. However SysML profile is not capable of providing a full support for the safety engineering process. Some extensions to SysML profile towards functional safety engineering are possible and enhanced interfaces to supporting toolchains are required. The new concept of augmented Fault Tree Analyses (aFTA) performed with the help of SysML is presented in subchapter 3 of this paper, while the integration toolchain for software development supporting the SysML profile is presented in subchap. 5. The concept of Global System Structure providing support in correct structuring of complex systems is presented in subchap. 1.

2.2 The INCOBAT System Modelling Approach

In context of the automotive domain it is very common to have some basic structure that serves to organize and handle the technical complexity of the system under development. Within AVL Global System Structure (GSS) has been defined and an aligned "Level Structure" for requirements, specifications, design, and integration steps & testing has been set up. This GSS level structure is depicted in Fig. 2.1 and also used in the INCOBAT project.

The purpose of the level approach is to have a classification framework to assign requirements/designs to the level they belong to. On the individual level, the requirements/designs are the basis to derive further requirements/designs to the next down-stream level. In other words: the requirements/designs are developed following a top-down cascading approach where on every level the requirements/designs will get more detailed. Nevertheless, if the project specifics and scope require, certain levels may be omitted.

Level 0—Vehicle—The vehicle structure element hierarchy and vehicle level solely represents a possible use-case for the battery management system and helps to serve as a common knowledge base for the project partner.

On this level specific environmental constraints can be govern and this most abstract layer helps to serve as a common knowledge base for the project partner to determine the sources and sinks for information of the BMS and the electronic and mechanical interaction partners. Due to the fact, that the INCOBAT project is focusing on a generic battery system applicable for manifold applications and

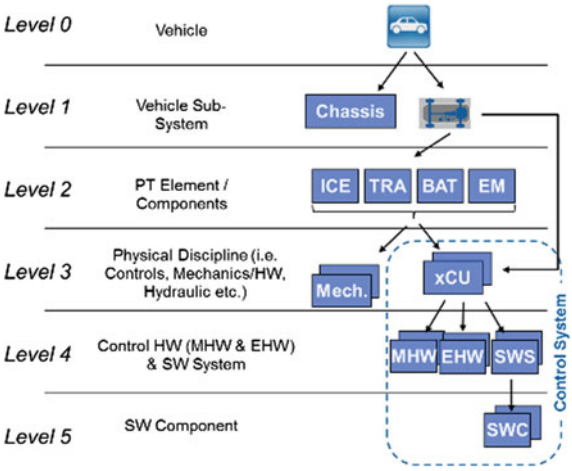

Fig. 2.1 AVL global system structure (GSS) and level structure (abbreviations are explained further in the text)

vehicles no assumptions, requirements, or design specifications are done on this level for the vehicle or vehicle's powertrain.

Level 1—Vehicle Sub-system—On this level again a generic electric powertrain structure is assumed. This structure mainly consists of a combustion engine (ICE), transmission (TRA), energy storage (BAT), and an electro-motor (EM). Nevertheless, some assumption and requirements for the powertrain and electrical drive have to be done on this layer.

As the INCOBAT battery system is developed according to the safety element out of context (SEooC) approach of part 10 of ISO–26262 [4], some fundamental assumptions are stated for the SEooC development. Assumption examples for the INCOBAT battery are e.g.: 'A_04 recuperative braking is not the only brake system within the car' and 'A_14 e-motor is freewheeling in case of powertrain failure or battery disconnection'.

Level 2—Powertrain Element (PT)/Component—On this layer the item definition for the INCOBAT battery system is done. According to clause 5.4.2 of part 3 of ISO–26262 [5] 'the boundary of the item, its interfaces, and the assumptions concerning its interaction with other items and elements, shall be defined …'. Therefore, the INCOBAT battery item and its interfaces to the environment are defined and a Hazard Analysis and Risk Assessment (HARA) has been performed on this level.

The objective of the HARA is to identify and categorize the hazards that malfunctions in the item can trigger. Furthermore, to formulate the safety goals related to the prevention or mitigation of the hazardous events, in order to avoid unreasonable risk.

Safety goals (SG) and their assigned ASIL are determined by a systematic evaluation of hazardous events. This analysis is based on the item's functional behavior and determines the ASIL for the system by considering the estimation of the impact factors severity, probability of exposure, and controllability of the hazardous events.

'SG5: Prevent from electric shock' with an assigned ASIL D is here an example. On this level the functional safety concept (FSC) is composed by functional safety requirements (FSR), such as: 'FSR_07: The safe state which shall be reached is disconnection of HV contactors.' And 'FSR_13: BMS shall control the energization/de-energization of the HV boardnet by control of the contact relays'.

This FSC is related to the INCOBAT battery system and its sub-components. Hereby, also the mechanical system must be taken into considerations, thus also a separation of mechanical and electronic control system is done on this level.

Level 3—Physical Domain/Control System—This layer constitutes the most concrete layer of system development and solely focuses on electrical and electronical components (HW and SW). Therefore the structure elements of the main and satellite modules compose of hardware and software elements.

On this abstraction level the FSC is evolved to a technical safety concept (TSC) and functional requirements are engineered, such as: 'Req 346102: BMS shall control HV+ relay for proper energization and de-energization of HV boardnet when requested by vehicle control unit' and 'Req 346197: BMS shall control HV precharge relay for proper energization (ramp-up) of HV boardnet when requested by vehicle control unit'.

Level 4—HW/SW System—This abstraction level is not included in classical system development approaches but defines the start of parallel software and hardware architecture design. This abstraction level is therefore mostly only present in special purpose SW development tools or HW design tools rather than SysML based system development tools. With the INCOBAT modeling approach this tool breach and semantic gap can be bridged and SW architecture definition can be represented by the model-based development tool.

Already at this level (and further on for Level 5) the limitation of using SysML approach has been experienced. Hence, the high level of details and the specific vocabulary makes the use of Domain Specific Languages (DSL) more appropriate. The challenge is thus to transfer and synchronize the information between a general purpose language (such as SysML) to different DSL. To support this the elements on this level are represented using the INCOBAT model approach and meta-model.

At this level the mapping of HW to SW interfaces (HSI) [6] can be modeled. This supports the explicit definition and configurations required to support correct implementation of, e.g., HV relay signals.

Furthermore, SW architectures and specific HW blocks can be designed.

2.3 iCOMPOSE Model-Based Functional Safety Engineering

The starting point of functional safety engineering process according to ISO–26262 is Concept Phase (see Fig. 2.2).

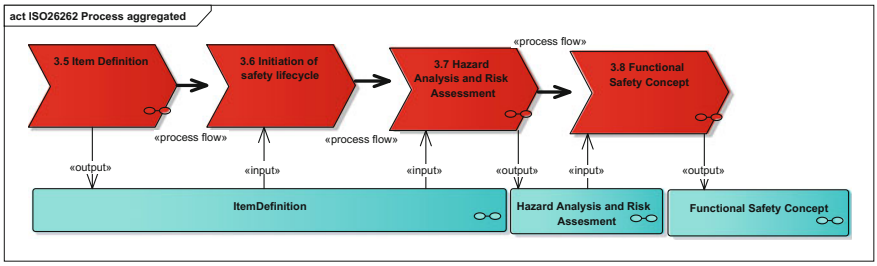

Fig. 2.2 Process model of ISO 26262 concept phase of safety engineering lifecycle in business process modelling notation (BPMN)

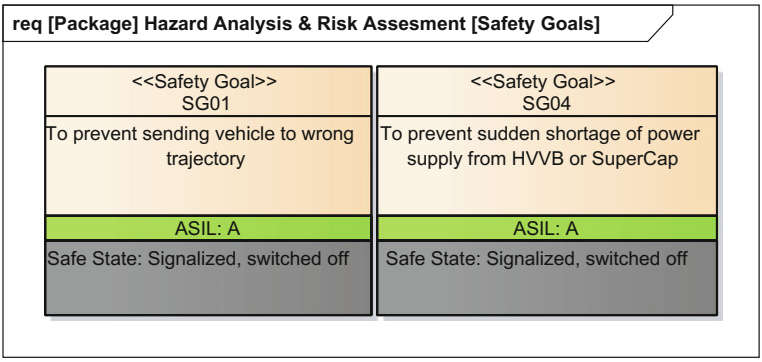

Fig. 2.3 Safety goals of iCEM in case of road usage

During this phase functional, operational and environmental requirements were collected, the boundaries of Integrated Comprehensive Energy Management System (iCEM) together with its preliminary architecture were identified. iCEM's architecture was modelled with the help of block definition diagrams. Safety Goals (SG) were identified with the help of HARA and they were captured in the SysML model with the help of dedicated extension [7] (see Fig. 2.3).

According to clause 8.4.2.3 of part 3 of ISO–26262 [5] Functional Safety Requirements (FSR) derivation can be supported with Hazard and Operability Study, Failure Mode and Effect Analysis, Fault Tree Analysis (FTA). In the presented approach FTA constitutes the basis for FSR derivation and it is included in SysML model and augmented in this sense that it also shows relations of undesired event to previously identified shortfall states, SGs, software units and basic events (UE). The concept of augmented FTA (aFTA) requires mixed elements coming from various SysML diagrams to be present as a specific view in a single diagram (see Fig. 2.4).

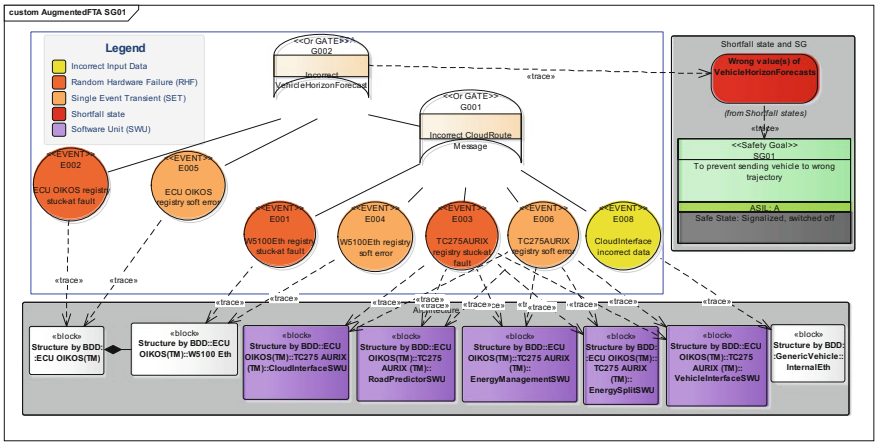

Fig. 2.4 Augmented fault tree for SG01

Activities which describe the functionality of basic safety mechanism preventing from violation of SGs were designed after identification of UEs with the help of top-down approach using System Use Cases (SUCs). The specific feature of these SUCs is that SGs are actors and all SUCs have unique identifiers (see Fig. 2.5). Finally aFTA together with system use cases constitute demanded rationale for FSRs.

During the System Design phase of ISO–26262, SUCs defined with the help of aFTA are further detailed. This enabled an identification of activities which describe the response of the iCEM and other elements to stimuli that can lead to violation of SGs as depicted in Fig. 2.6.

Finally the activities were decomposed into the Technical Safety Requirements (TSR) and rationale was provided for each derived TSR. The presented structure of TSRs (see Fig. 2.7) reflects the scope of clause 6.4.2.2 of part 4 of ISO–26262 [6]. Furthermore, the numbering scheme applied to TSRs also matches the labeling applied to lists in the clause 6.4.2.2.

The specific coloring schemes applied in the diagrams provide not only better readability of the diagrams but also they cover some important pieces of information which can be seen in the legend included in Fig. 2.7. Also the frames were used as the way to cluster important information. The frame with grey background shows elements already present in the model which are re-used in given diagram. In this way the evolution of safety design can be captured. Finally, the Preliminary Architecture was further detailed resulting in System Design architecture. This architecture takes into account measures to control random hardware failures provided by native safety mechanism of AURIX controller [8, 9].

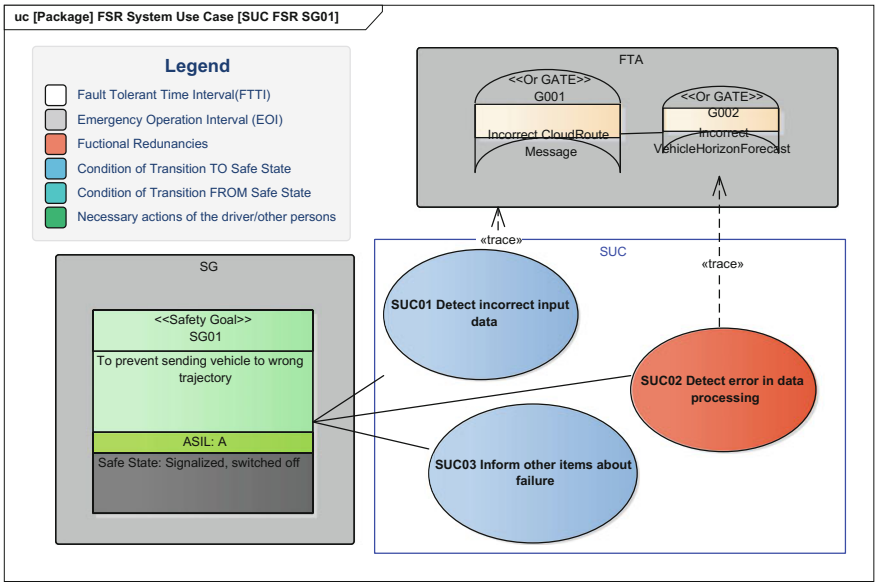

Fig. 2.5 FSR derivation with the help of system use cases

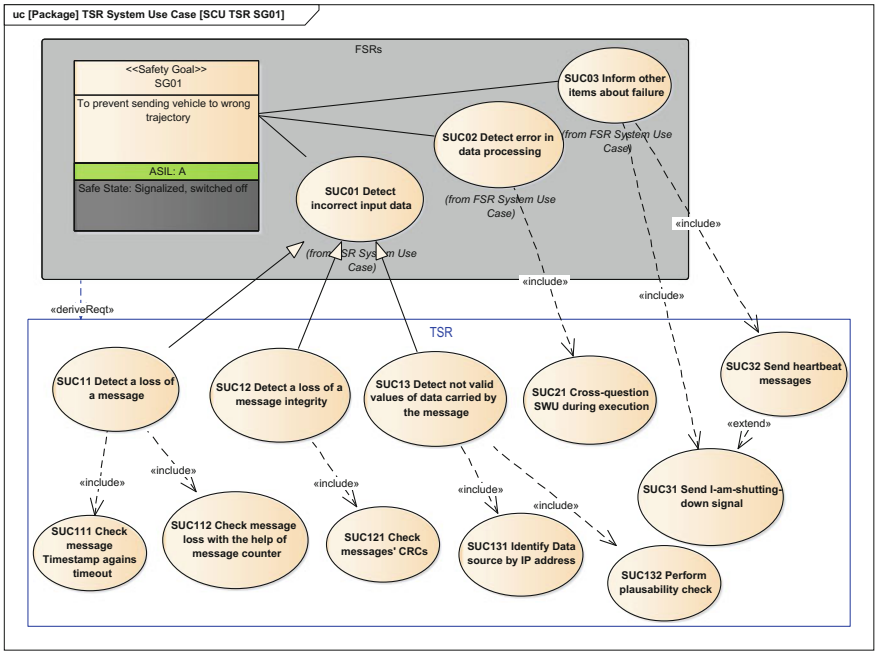

Fig. 2.6 TSR derivation with the help of system use cases

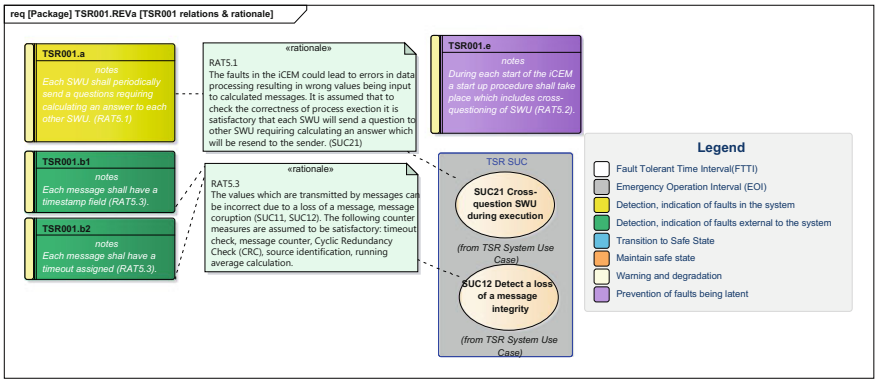

Fig. 2.7 Technical safety requirements representation

2.4 Aspects of Traceability

The applied approach assures achieving traceability between all important artefacts of the development process, however it requires creating various relations between different types of SyML modelling elements: requirements to requirements, use cases to uses cases, blocks to use cases, SGs to use cases, SGs to states, OR as well as AND gates of aFTA to states, aFTA gates to aFTA events, aFTA events to blocks, aFTA gates to use cases, requirements to blocks, requirements to signals, requirements to rationale, rationale to SUCs, blocks to blocks, SGs to blocks. Where, SGs, OR as well as AND gates and events of FTA are non-standard extensions of SysML profile.

It was noticed that due to complicated structure of relations the best results in performing traceability can be achieved by direct querying SQL database running in the background of the SysML modelling tool, which in this case was Enterprise Architect.

2.5 Software Development and Integration Toolchain

The main idea of the software development scenario within the iCOMPOSE project was to set up a consistent toolchain from requirements to deployed code with code generation at the earliest stage possible. The elaborated toolchain is based on models of different levels of abstractions and it is offering consistency from Functional Safety Concept up to software development and software testing. Figure 2.8 shows the proposed and implemented workflow.

Functional software development started already in the concept phase described in Sect. 2.3. The preliminary architecture was identified along with drafting state machines that described the iCEM's behaviour. This information was detailed

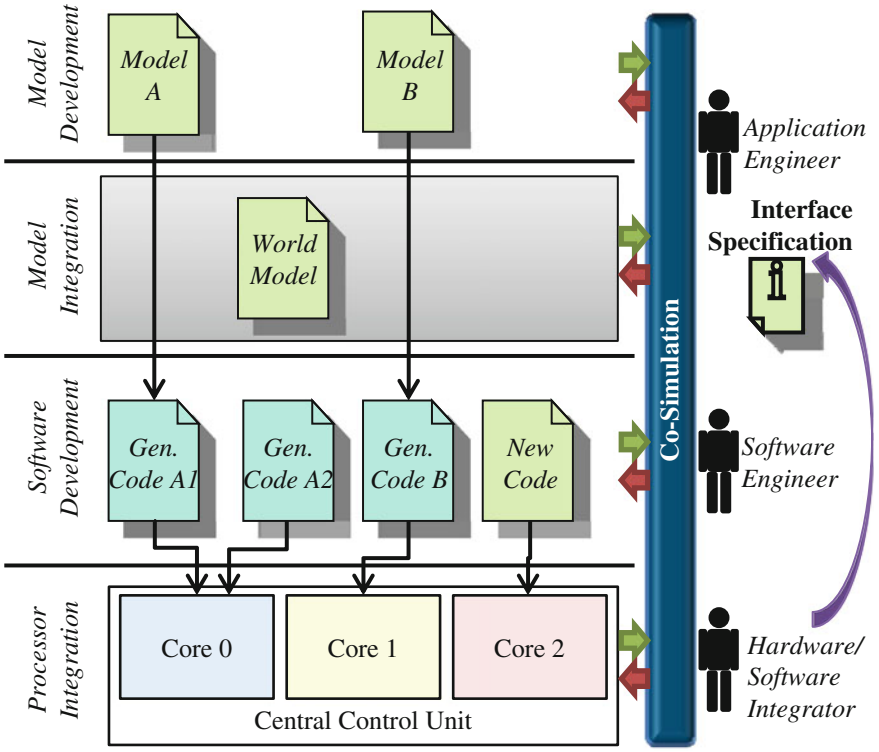

Fig. 2.8 Proposed software development and integration workflow

further during System Design Phase by drafting class diagrams and improving the state machine behaviour.

The major contribution to the toolchain achieved in Enterprise Architect is the automatic generation of MATLAB[1] script code implementing and thus making further use of the state machine behaviour and class structure as designed earlier. A new *Enterprise Architect Code Template* was implemented for MATLAB consisting of:

- classes, including
  - attributes,
  - methods,
  - actions, i.e., branches, loops, calls, and assignments, and
  - behaviours, as well as

[1]MATLAB 2016b, https://www.mathworks.com/products/matlab/.

- state machine fragments of type “legacy”, i.e., previous to release 11.0,
  - states
  - transitions, and
  - triggers.

The generated state machines serve as a code stub to the iCEM’s framework for subsequent software development, reducing the effort as well as sources for errors with respect to re-implementing the designed software in the target programming language.

Since all functions to be integrated into the iCEM’s software are based on MATLAB and Simulink, Mathworks Embedded Coder together with MATLAB Coder and Simulink Coder were employed to generate C-code from Simulink diagrams targeting at embedded devices. This generated C-code is particularly well suited for use in real-time applications. Figure 2.8 depicts the proposed software development and integration workflow. Development stages are separated by horizontal black lines and labelled at the left. Items under development are depicted schematically on every stage and linked to corresponding items on the next development stage. Pictograms of humans and labels show the roles in the development process at the right. All stages are connected vertically via a common “co-simulation” that may interact with a combination of models at any stage. The arrow on the right indicates a stronger interaction between the Hardware/Software Integrator up to the Application Engineer level by providing the interface specification to the higher level.

For many real-time projects it is essential to communicate with target hardware via hardware interfaces. Hardware interfaces from Software in Simulink are typically source or sink blocks. In this project, device drivers for two interfaces were developed targeting the iCEM application:

- Controller Area Network (CAN) and
- Universal Asynchronous Receiver Transmitter (UART), better known as RS232 or serial port.

The device drivers were developed using the Legacy Code Tool in MATLAB. This tool automatically generates a block for custom code.

Figure 2.9 shows a Simulink diagram with a CAN receive and two CAN transmit devices already linked to a subsystem block that represents a generic model. Both block types handle common CAN message settings, such as offset, factor, start bit and stop bit of each input signal. This configuration is similar to the dbc format of VECTOR tools.[2]

In contrast to the bus-based CAN communication, data transmission through UART is designed to be a very flexible and generic point-to-point connection, but in this case, the UART device drivers were implemented to encapsulate data in a

[2]CANdb++, http://vector.com/vi_candb_en.html. The dbc format provides a quasi-standard for specifying CAN messages and included signals in terms of frequency and data format.

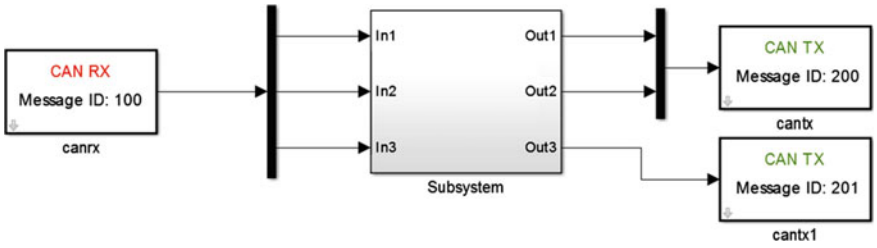

Fig. 2.9 CAN device drivers in a Simulink diagram

similar fashion to the CAN-protocol, as both implementations were designed to communicate with a vehicle controller.

Since these functions are hardware specific, it is necessary to ensure that the functionality of the devices is only used in combination with the target hardware. During simulation on the development platform, i.e., the development desktop computer, the devices blocks (sinks and sources) have no functionality, yielding constant input. However, on the target platform the blocks result in code fragments that implement the desired functionality.

On top of the device drivers described above, another major contribution to the toolchain achieved in MATLAB is the automatic generation of a Simulink model stub. Since the description of the communication via the CAN bus is described commonly in dbc format, a tool was developed that translates a dbc file into a Simulink model featuring inbound messages (emitted by other bus subscribers) as sources and outbound messages (to be emitted by the device implementing the model) as sinks. Thus there exists the possibility to include a communication specification—as shown in Fig. 2.8—provided by the Hardware/Software-Integrator directly into the models by the Application or Software Engineer in a less error-prone fashion.

All models in the iCOMPOSE project have been developed in MATLAB and Simulink, yet it makes sense to use co-simulation for disconnecting components from another. It is thus possible to establish a clear interface, reduce model complexity and enable the easy replacement of individual parts by newer versions or variants. In co-simulation, an overall system is divided into several component models that can be modeled in their original, (possibly) different simulation tools or versions ("multi-tool"). During computation each component is provided its respective solver ("multi-method"). The solver used may also be customized with different time-steps ("multi-rate").

The gradual integration of real components into the co-simulation environment at hardware/software integration level enables the testing of the iCEM, as well as several of its controlled components, in a virtual environment before they are used in the entire system and interacting with the products. For example, every modification to one function of the iCEM's software is tested within a restricted environment designed to test this particular function on the target hardware by replacing its stimuli (sensor data) by results of a simulation and return the control commands in the simulation.

The correct co-simulation on model, model integration and software level of the digital prototype ultimately enables analyzes that may be difficult or impossible to carry out on physical prototypes, such as parameter sweeps and testing close to or out of valid bounds.

2.6 Conclusion

Systems engineering is a key aspect to coordinate the different development and generate a level of common understanding between engineering experts. The challenges are to gather and to manage the information efficiently and to generate an added value related to the generation and maintenance of this knowledge.

In the context of the INCOBAT project a method for the integration of system and SW models was developed. This approach consists on the refinement of a modeling profile and on the implementation of tool bridges toward SW development frameworks.

The SysML model based approach presented in the context of iCOMPOSE project, showed to be useful. However using standard SysML profile looks to be not fully sufficient for the purpose of functional safety engineering, and what's more, requirements on traceability between artefacts created during the development process are highly demanding. The fulfillment of the demanding requirements imposed on the traceability can be tool dependent.

Furthermore, based on the SysML model a toolchain was developed to generate code for MATLAB from class diagrams and state machines. To enable communication between models in generated code on the target platform CAN and UART interface blocks were devised for Simulink. These interface blocks may be automatically generated from a VECTOR-dbc file based CAN-specification, thus easing the specification exchange between Hardware/Software-Integrators and Application and Software engineers. The integration of developed toolchain with higher level conceptual models was achieved.

Finally, we provided a brief outline of the testing environment using co-simulation as a fundamental tool for testing at every development stage.

Acknowledgements The research work of the authors has been funded by the European Commission within the projects Integrated Control of Multiple-Motor and Multiple-Storage Fully Electric Vehicles (iCOMPOSE) and INCOBAT under the European Union's Seventh Framework Programme (FP7/2007–2013) under grant agreement №. 608897 and №. 608898.

VIRTUAL VEHICLE Research Center is funded within the COMET—Competence Centers for Excellent Technologies—programme by the Austrian Federal Ministry for Transport, Innovation and Technology (BMVIT), the Federal Ministry of Science, Research and Economy (BMWFW), the Austrian Research Promotion Agency (FFG), the province of Styria and the Styrian Business Promotion Agency (SFG). The COMET programme is administrated by FFG.

References

1. http://www.i-compose.eu/iCompose/
2. http://incobat-project.eu/
3. ISO–26262 Road vehicles—functional safety, Part 6: product development at the software level
4. ISO–26262 Road vehicles—functional safety, Part 10: guideline on ISO 26262
5. ISO–26262 Road vehicles—functional safety, Part 3: concept phase
6. ISO–26262 Road vehicles—functional safety, Part 4: product development at the system level
7. Szymanski D, Dexters B, Descas Y, Van Vlimmeren M (2014) Model based and scalable functional safety engineering methodology for on- and off-highway vehicles, FISITA 2014—Maastricht (NL)
8. TriCore AURIX family 32-Bit AURIX safety manual, AP32224, Infineon
9. AURIX TC27x 32-Bit single-chip microcontroller, user's manual

Chapter 3
Model Predictive Control of Highly Efficient Dual Mode Energy Storage Systems Including DC/DC Converter

Ralf Bartholomäus, Thomas Lehmann and Uwe Schneider

Abstract Combining lithium-ion batteries with supercapacitors within the storage systems of electric and hybrid vehicles is a way to fulfil the demand for both a high energy content and a high power level. In addition, it is possible to avoid power peaks within the lithium-ion batteries, which leads to a significantly increased lifetime. In order to fully exploit this potential, it is necessary to achieve optimal control of the power distribution between the two storage components. For this purpose, a predictive control strategy is developed that uses a short-term prediction of the vehicle's expected power demand to calculate the current setpoint for the supercapacitors in real-time. In order to accurately follow that setpoint a highly dynamic DC/DC converter is developed.

Keywords Electric and hybrid vehicles · Predictive energy management · DC/DC converter

3.1 Design of the Dual Mode Energy Storage System

Modern electric vehicles are usually equipped with lithium-ion batteries as their storage systems. Compared to supercapacitors, this type of storage unit has a higher energy density, which allows for a higher vehicle range. On the other hand, its power density is comparably low due to the internal resistance, so that in case of high power demands, excessive heating of the lithium-ion batteries and, in consequence, a significant reduction in lifecycle would result [1].

An obvious approach to reducing power peaks without impairing the acceleration and recuperation characteristics of a vehicle is to combine the lithium-ion batteries with a supercapacitor storage unit, which only has a low energy density

R. Bartholomäus (✉) · T. Lehmann · U. Schneider
Fraunhofer Institute for Transportation and Infrastructure Systems IVI, Dresden, Germany
e-mail: ralf.bartholomaeus@ivi.fraunhofer.de

© The Author(s) 2018

D. Watzenig and B. Brandstätter (eds.), *Comprehensive Energy Management - Safe Adaptation, Predictive Control and Thermal Management*, Automotive Engineering: Simulation and Validation Methods, DOI 10.1007/978-3-319-57445-5_3

but a high power density and a long lifetime. The high power density is a consequence of the low internal resistance of supercapacitor cells, which is typically ten times smaller than that of lithium ion battery cells used in electric vehicles.

In the iCOMPOSE project the battery electric drivetrain of a Lotus Evora 414E sports car was supplemented with a supercapacitor storage in order to avoid the aforementioned dynamic stress of the battery. Among different topologies [2] the structure depicted in Fig. 3.1 has been selected since the existing drive train should be left unchanged as a fallback. The resulting Dual Mode Energy Storage System (DMES) consists of a lithium-ion battery (14.9 kWh, nominal power 120 kW) covering the vehicle's base load and the newly integrated supercapacitor storage unit for power peaks (0.16 kWh, peak power 200 kW). In contrast to lithium-ion batteries, supercapacitors progress through a wide voltage range during the charging and discharging processes, which makes it necessary to connect them to the intermediate circuit via a DC/DC converter. The DC/DC converter needs to handle not only the high power, but also the high power dynamics arising in that application, which is one of the main challenges in the iCOMPOSE project.

The aim of the DMES controller is to manage both the current and the state of charge of the supercapacitors so that the lithium-ion battery experiences as little power fluctuation as possible. The best results are achieved using a predictive control strategy based on the prediction $\hat{p}$ of the power demand p. The power demand p of the electric motor and the auxiliary systems is estimated by the block "Power Predictor" in Fig. 3.1 using map data, position information and current traffic information. Within the "Model Predictive Controller" component, the predicted power demand $\hat{p}$ and the state of charge calculated from the supercapacitors' voltage u_c are used to calculate the optimal current for the supercapacitors, which is

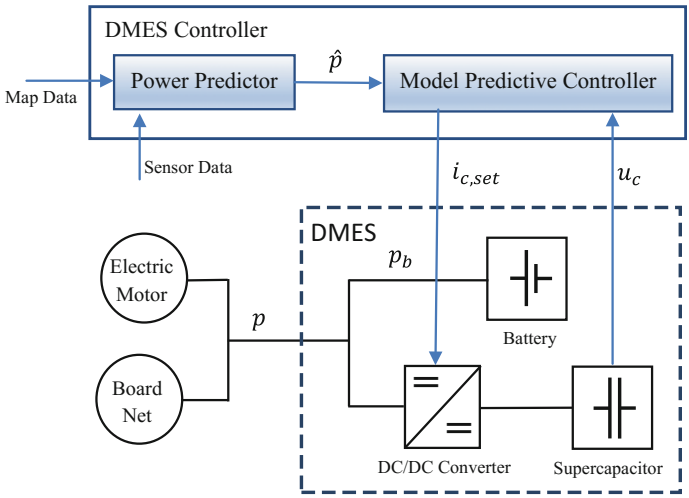

Fig. 3.1 Sketch of proposed board net configuration

used subsequently as the current setpoint for the DC/DC converter. Since this optimization task has to be executed in real time, the formulation and numeric solution of the control problem is another challenge of the iCOMPOSE project.

This Chapter is structured as follows: Sect. 3.2 will describe the control algorithm implemented in the DMES controller. Because model-predictive controllers have the potential for high control quality but are also very complex, Sect. 3.2.1. will start by presenting a semi-predictive approach that is easy to implement. Section 3.2.2 will describe the predictive DMES controller presented in Fig. 3.1, and Sect. 3.2.3 will give a comparative assessment of the two controllers.

For an optimal smoothing of the supercapacitors' power demand, the time lag between the DMES controller's calculation of the current setpoint for the DC/DC converter and the setting of the actual value by the DC/DC converter must be as small as possible. For this purpose, Sect. 3.3 will present a DC/DC hardware and software architecture that features a high-speed current setpoint behavior. Section 3.4 will summarize the results.

3.2 Control Strategy

3.2.1 Basic Control Algorithm

In order to appropriately evaluate the features of the predictive controller developed in Sect. 3.2.2, a reference algorithm will be introduced in the following section. Because non-predictive control strategies, e.g., load-following control and SOC-based control [3], usually do not yield satisfactory results for dual storage systems, the reference algorithm includes a simple prediction of the traction power. This prediction is derived from the vehicle speed. The aim is to control the state of charge of the supercapacitors so that the sum of the vehicle's kinetic energy (i.e., the maximum amount of energy that can be fed to the supercapacitors during braking to a speed of zero) and the energy stored in the supercapacitors remains constant at all times. Under these circumstances, the power peaks occurring during braking and acceleration can be absorbed and provided entirely by the supercapacitors. Because supercapacitors in vehicles will most likely only have a small storage capacity due to reasons of space and weight, the desired smoothing of power peaks can only partly be realized.

For this scenario of insufficiently sized supercapacitor, the green curve in Fig. 3.2 shows the speed-dependent maximum state of charge. If this value is greater than zero, it ensures that the supercapacitors will be able to absorb the entire kinetic energy recuperated in case of braking to a standstill. Accordingly, the red curve indicates the minimum state of charge needed to ensure that acceleration to maximum speed can be realized using only the energy stored in the supercapacitors. The blue curve shows one option of making a compromise between the two contradictory demands.

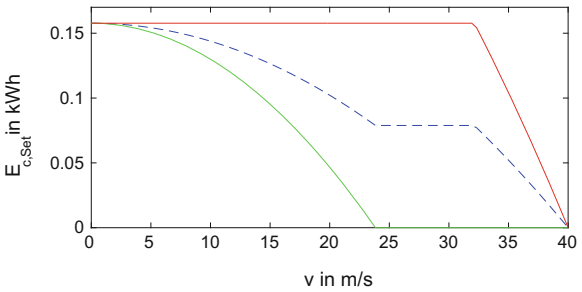

Fig. 3.2 Setpoint for the speed-dependent energy content $E_{c,set}$ of the supercapacitor unit based on different criteria: $\bar{E}_c = max\{0, E_{c,max} - \frac{m}{2}v^2\}$ for maximum recuperation of braking energy (*green*), $\underline{E}_c = min\{E_{c,max}, \frac{m}{2}(v_{max}^2 - v^2)\}$ for maximum acceleration (*red*), and $E_{c,set} := \frac{1}{2}(\underline{E}_c + \bar{E}_c)$ as a compromise between the two cases (*blue*); where $m = 2000\,\text{kg}$, $v_{max} = 40\,\frac{\text{m}}{\text{s}}$, $E_{c,max} = 0.158\,\text{kWh}$

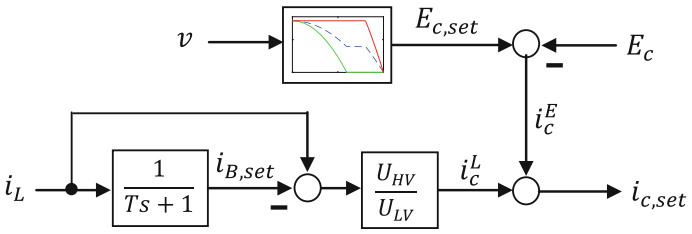

Fig. 3.3 Layout of the basic controller

Figure 3.3 shows how the current setpoint $i_{c,set}$ for the DC/DC converter is derived from an superposition of the two components i_c^E and i_c^L. Comparison of the setpoint value $E_{c,set}$ for the supercapacitors' energy density with the actual value E_c yields the current setpoint i_c^E necessary for reaching the respective state of charge setpoint $E_{c,set}$ corresponding to the different speeds. The difference between the battery current setpoint $i_{B,set}$ (which can be derived by smoothing the load current i_L with time constant T typically smaller than 1 s) and the load current is the current needed to absorb power peaks on the HV side of the DC/DC converter. This current is converted to the capacitor current i_c^L via the DC/DC voltage ratio.

3.2.2 *Predictive Control Algorithm*

Model predictive control seems to be superior to e.g., rule-base control in HEV as well as in energy storage applications. Nevertheless there is still room for improvement. DMES systems of similar [4] or equal [5, 6] structure to the one shown in Fig. 3.1 are often linearized before applying MPC algorithms in order to

ensure real-time ability of the controller. However, there are nonlinearities in the model, e.g., the efficiency map of the DC/DC converter or the relation between electrical power and current due to varying supercapacitor voltage, which cannot be neglected without decreasing the control performance. When using dynamic programming (DP) the model of the DMES is no longer restricted to be linear, but in those cases DP is often only applied to calculate a global optimal reference for evaluating the performance of MPC for linearized models [5]. In [7] not only a reference but a control law is calculated by DP, however, it is supposed that the power demand over the time horizon is fully know in advance [7], which is an unrealistic assumption.

The predictive controller developed during the iCOMPOSE project uses information about the SOC of the supercapacitors and a prediction of the power demand over a short time horizon in order to minimize stress on the battery. As the performance objective, the sum of squares of the power provided by the battery during the prediction horizon is used

$$\|p_b\|_2 = \|\hat{p} - p_c\|_2 \rightarrow \min$$

This criterion reflects the expectation that minimization of peaks in battery power leads to an increased battery lifetime [1].

The prediction horizon for the power demand $\hat{p}$ has a length of 10 s, which is reasonable for non-autonomous vehicles. It is divided into four time periods $T_1 = 0\,s \ldots 1\,s$, $T_2 = 1\,s \ldots 3\,s$, $T_3 = 3\,s \ldots 6\,s$, $T_4 = 6\,s \ldots 10\,s$, the corresponding average values of the power demand are denoted by p_1, p_2, p_3, p_4. The idea behind the introduction of non-equidistant discretization is to address the increasing forecast uncertainty associated with larger prediction ranges. In addition, a discretization of the state variable, i.e., the open circuit voltage U_0 of the supercapacitor, and a discretization of the supercapacitor current i_c as the control variable is performed which implies that only a finite number of control strategies remain to be considered in the optimization.

Based on a commonly used RC model of the supercapacitor (e.g., [6]), the efficiency map of the DC/DC converter and constraints on the supercapacitor voltage and DC/DC current, the DP algorithm calculates the optimal feedback control law $i_{c,set} = i_c^*(p_1, p_2, p_3, p_4, U_0)$, which is a nonlinear map that is implemented by linear interpolation in a five-dimensional lookup table. In practice, the open circuit voltage U_0 can be calculated using the measured supercapacitor voltage u_c and the value of the internal resistance.

The calculation of the feedback control law is executed offline, as it is typical for explicit model predictive control. Since the controller simply solves an interpolation task taking the input data U_0 and $\hat{p}$ as arguments and providing the setpoint $i_{c,set}$ (see Fig. 3.1), the real time ability of the control algorithm is ensured.

Figure 3.4 shows the control law restricted to the (p_1, U_0) space. If U_0 is close to the lower bound of 50 V, the supercapacitor only accepts charging currents (i.e., $p_1 > 0$). For the higher values of U_0, discharging currents can occur up to its maximum value of −1000 A.

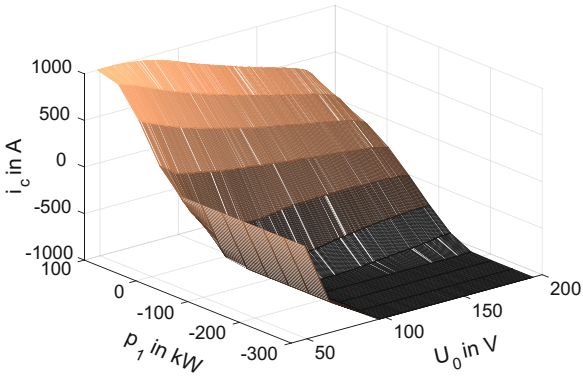

Fig. 3.4 Illustration of the lookup table $(\boldsymbol{p}_1, \boldsymbol{U}_0) \rightarrow \boldsymbol{i_c}$ (values of $\boldsymbol{p}_2, \boldsymbol{p}_3 \boldsymbol{p}_4$ are fixed to zero)

3.2.3 *Evaluation of the Control Strategies*

The design objective of the predictive controller is to avoid the occurrence of high battery power levels, or battery current levels respectively, in order to maximize the battery's lifetime. Therefore, a histogram of the battery current is an adequate measure for evaluating the benefit resulting from the DMES system. In Fig. 3.5, the battery current of the Hethel Test Track[1] is presented for different storage configurations and DMES controllers. The following scenarios can be observed (from top to bottom).

- In pure battery operation that is without an integrated supercapacitor storage system there are significant discharging peaks of up to 800 A.
- The DMES system equipped with the predictive controller yields a strong reduction of large discharging currents as well as charge currents during recuperation.
- The DMES system equipped with the basic controller shows a similar performance as the predictive controller. Since it was expected that the predictive controller would perform better than any controller without knowledge about the future progression of power demand, the hypothesis is that the quality of the prediction might be insufficient.
- In order to quantify which performance from a predictive controller with ideal predictions is feasible, a predictive controller with full information about the future is evaluated [5]. In this case, the complete power progression is available the controller in advance. This approach results in the minimal value of the objective function $\|p_b\|_2$ that is achievable with the DMES system. Since the width of the resulting battery current distribution function is considerably

[1] http://www.lotuscars.com/racing/hethel-test-track.

smaller than that for the predictive controller with a prediction horizon of 10 s, the conjecture about the insufficient quality of power prediction, which was formulated above, is plausible. As a conclusion for a better system performance, measures for enlarging the prediction horizon should be investigated.

Not only the performance, but also the complexity of the basic controller and the predictive controller with a prediction horizon of 10 s are comparable. However, one should bear in mind that the predictive controller is, in general, more flexible in handling constraints (bounds on the supercapacitor current and voltage) than the basic controller (with a feedback controller that is essentially designed for a linear system behavior of the supercapacitor).

3.3 DC/DC Converter

High currents and the resulting temperature peaks are the main reason for batteries ageing ahead of time. The chosen dual storage architecture can effectively minimize high current peaks in the battery by re-directing large currents to the supercapacitor instead. But because of the different voltage levels, the capacitor cannot be connected directly to the DC link. By converting the currents between the DC link and the supercapacitor, the DC/DC converter plays a key role and has to be very fast in order to cope with fluctuating loads that occur during drive cycles. If the converter is not fast enough, the currents would still put stress on the battery. Within the iCOMPOSE project, the DC/DC converter had to deal with power peaks of up to 200 kW. At a voltage level of approximately 200 V, this leads to currents of up to 1000 A.

The DC/DC converter was based on an existing device from Prisma Ecotech GmbH in St. Peter, Germany. This converter was equipped with a re-designed controller board for more computing power to handle the advanced control algorithms. Moreover, a completely new DC/DC converter control software was developed and implemented to enable use of MPC strategies and highly dynamic control.

3.3.1 Hardware Requirements

The project requirements resulted in the final hardware component structure shown in Fig. 3.6. Note that only one bridge on the low voltage (LV) side is depicted for reasons of clarity. The real converter has two bridges that are driven in phase shift in order to minimize voltage ripples at the output. Each bridge consists of three parallel strings with their own IGBT switches S1 and S2, their own choking coil L and one output capacity C_{LV}. Each switch is built from 13 single IGBTs that all work in parallel. This enables the DC/DC converter to provide the desired 1000 A.

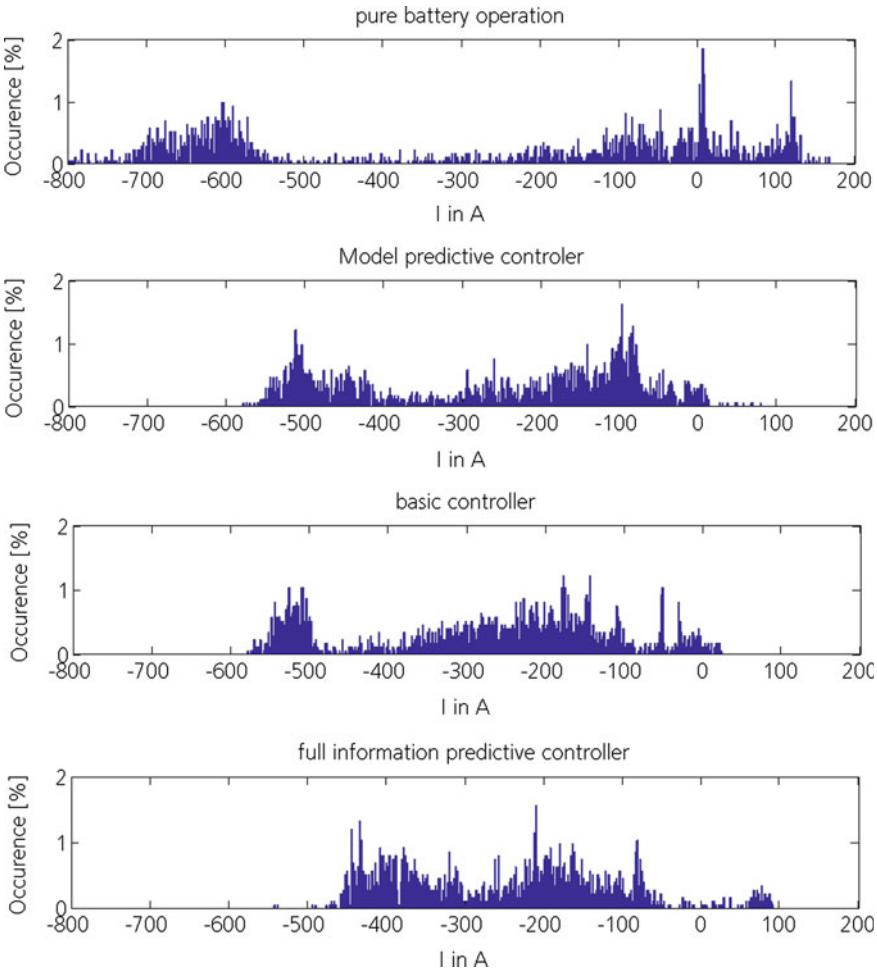

Fig. 3.5 Histogram of battery current for different power splits

3.3.2 Controller Design

PID controllers are probably the most common control algorithms used in actual DC/DC firmware. These algorithms have a number of advantages, such as simple equations which can be computed very fast. But PID controllers also show serious disadvantages, such as the fact that they are designed only for a certain operating point. This means that the controller is not going to work well at quickly shifting operating points that often occur in electrically driven vehicles. Therefore, separate controllers are frequently implemented for $U_{LV}, U_{HV}, I_{LV}, I_{HV}$ and the switching between these control algorithms needs special handling to avoid unsteadiness and oscillation.

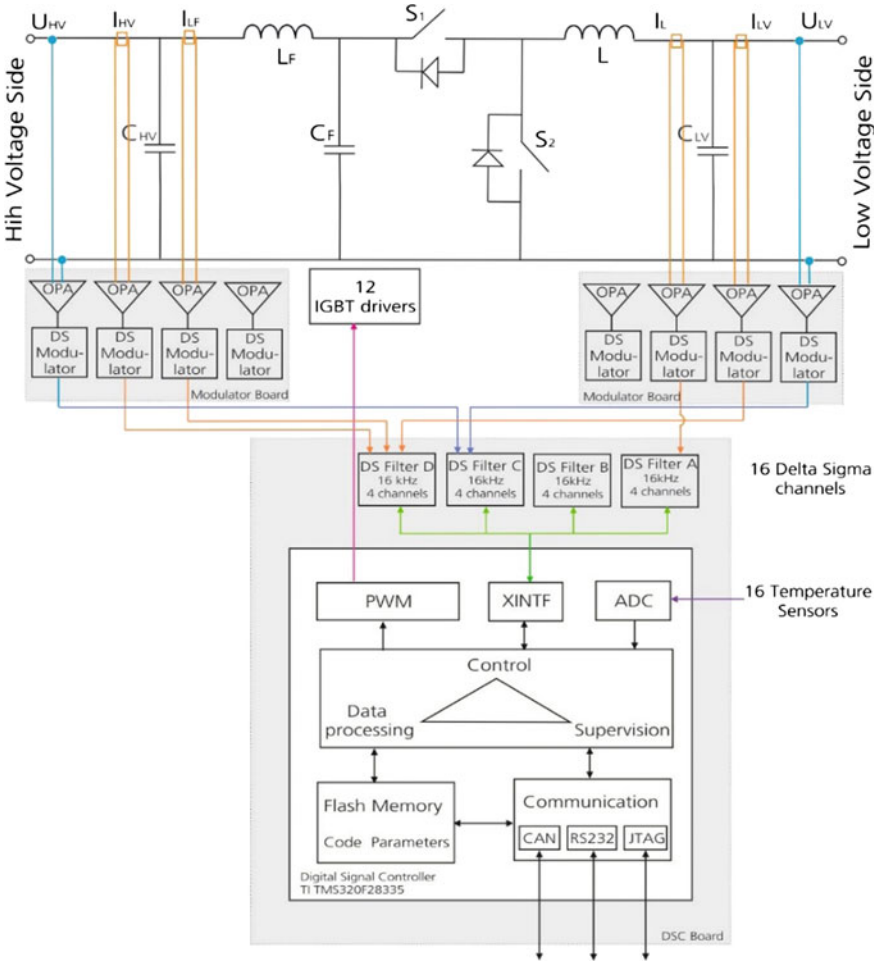

Fig. 3.6 DC/DC converter, component overview for one LV-bridge

The aim for the newly developed controller was to design a control strategy that does not have the disadvantages of PID controllers while still requiring reasonable additional computation power and time. The implemented control strategy uses a nonlinear, model-based control algorithm to compute the duty cycle of the switches. One significant advantage compared to other known control strategies is that there is only one control algorithm for computing I_{LV} that also considers all other set-points and limits. It is not necessary anymore to switch between several completely independent controllers.

The implemented current controller needs an instantaneous measurement of the current, i.e., it calculates and sets a new duty cycle d_k within every microcontroller clock cycle T, which is 60 µs. During each of these clock cycles, a new duty cycle for the subsequent interval k is calculated based on the setpoint for I_{LV}, the measurement values for I_{LV}, U_{LV}, U_{HV} and the duty cycle d_{k-1} that was active during the previous clock interval $k-1$. The duty cycle d_k is chosen so that that during the next duty cycle d_{k+1}, the steady state duty will be reached.

All further explanations assume that the DC/DC converter is working in buck mode as an example. Figure 3.7 shows that the expected current during one microcontroller cycle has a rising section and a falling section. The current rises while the IGBT switch S1 is closed. When S1 is opened again, the current decreases for the rest of the cycle time. The current flow commutates through the diode D2 of switch S2. The controller's measurement board can only measure the mean value of the current over one microcontroller cycle period T. But the real curve shape can be recalculated using a number of model assumptions, measurement values and component parameters such as the inductance L.

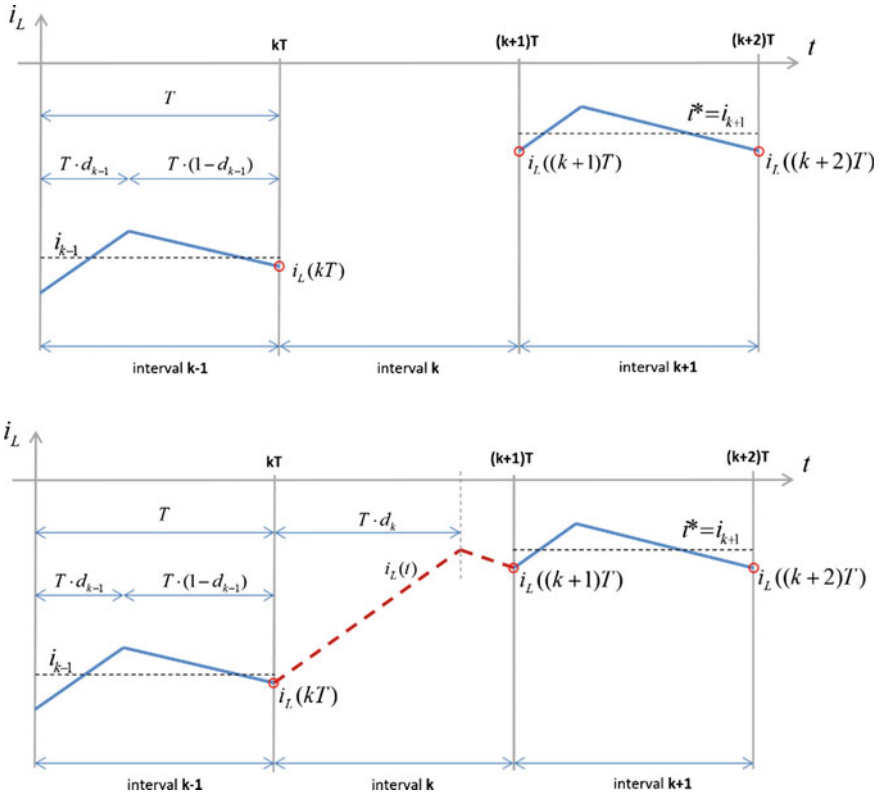

Fig. 3.7 Computation of the duty cycle d_k

3.3.3 Implementation on Test Bench

In order to validate the behavior of the DC/DC converter, the components of the DMES system where implemented on a test bench (Fig. 3.8). The electric drive train of the vehicle was simulated by a bidirectional electronic load. According to Fig. 3.1, the DC/DC converter was connected to the supercapacitors on the LV side and to the electronic load and the battery on the HV side. The DMES controller was implemented on a vehicle controller board.

The Hethel drive cycle was used to generate the setpoint for the electronic load and the DMES controller provides the current setpoint for the converter. As shown in Fig. 3.9, the setpoint is accurately met. A rapid current change from −800 to 700 A can be seen at the left side of the diagram in Fig. 3.9. Even in that case, the actual values (mIL) follow the setpoint values (sIL) so closely that the setpoint curve is almost not visible anymore. The actual values are printed over within the diagram.

Setpoints of drive cycles do not show real steps, because accelerating and braking a mass has a smooth ramp character. There are expected current changes at a maximum of 2 A/ms when looking at the Hethel drive cycle. The converter is able to change currents at approximately 100 A/ms. Thus, the converter can handle all required power and current setpoint changes that a drive cycle demands.

The behavior of the current control algorithm can be seen in Fig. 3.10. The setpoint jumps to 800 A (green line) and the actual current value (red line) follows very fast and without overshooting or any oscillation. The first 2 ms of "dead time" result from the time remaining from a 10 ms communication cycle period lasting until the setpoint value is sent to the DC/DC converter again. At that time, the transient response starts and takes approximately 10 ms. This is an outstanding performance and states the advantages of the nonlinear, model-based control strategy.

In general terms, the DC/DC converter as a unit consisting of both hardware and software components, including the new control algorithm in particular, shows a

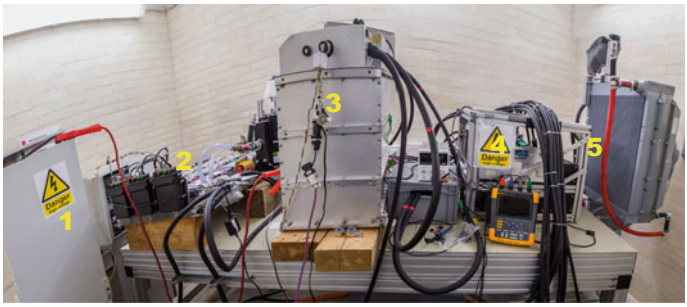

Fig. 3.8 DMES on the test bench: **1** connection to power load, **2** Supercap, **3** Lotus battery, **4** DC/DC converter, **5** cooling system

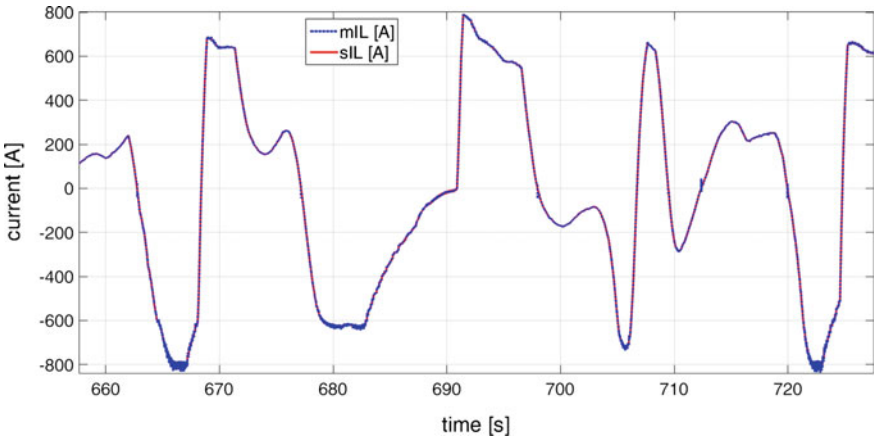

Fig. 3.9 DC/DC current, part of Hethel drive cycle

Fig. 3.10 Setpoint jumps to 800 A (*green*), actual value follows (*red*)

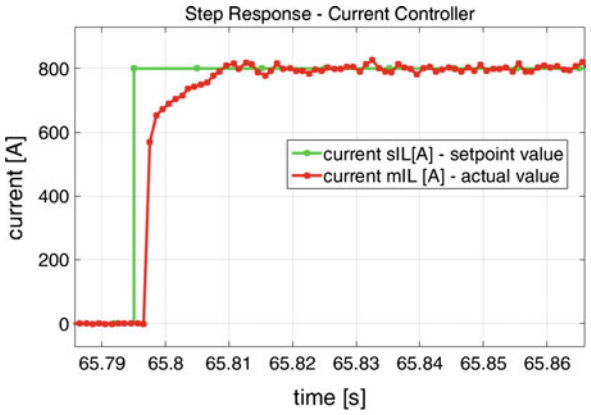

very good performance. The switch to the new and powerful Texas Instruments microprocessor made it possible to implement an alternative, slightly more CPU-intensive control strategy. Because of the high accuracy of the clock-synchronous captured, actual measurement values, an impressing overall accuracy of the controller is reached. The nonlinear control algorithm developed at the Fraunhofer IVI is not only working independently from the operating point, but it also reaches the fastest possible transition times, as they are only limited by the physical characteristics of the hardware used, e.g., the choking coil.

During various test cycles, the controller showed its advantages compared to the formerly used PID control algorithm. Transition times, oscillations and overshooting effects were all be minimized significantly.

As a summary it can be said that the DC/DC converter with its corresponding control strategy fulfils the requirements and is a good choice for DMES application scenarios.

3.4 Conclusion

A powerful DMES system including a predictive control strategy and a re-designed DC/DC converter were developed that fully exploit the advantages of the hybrid energy system. The validation of the system was carried out on a test bench based on measurement data recorded for this purpose on the Hethel Test Track.

Detailed evaluation of the DMES characteristics was done in simulation (Fig. 3.11). Compared to using a configuration without supercapacitors, the following can be stated.

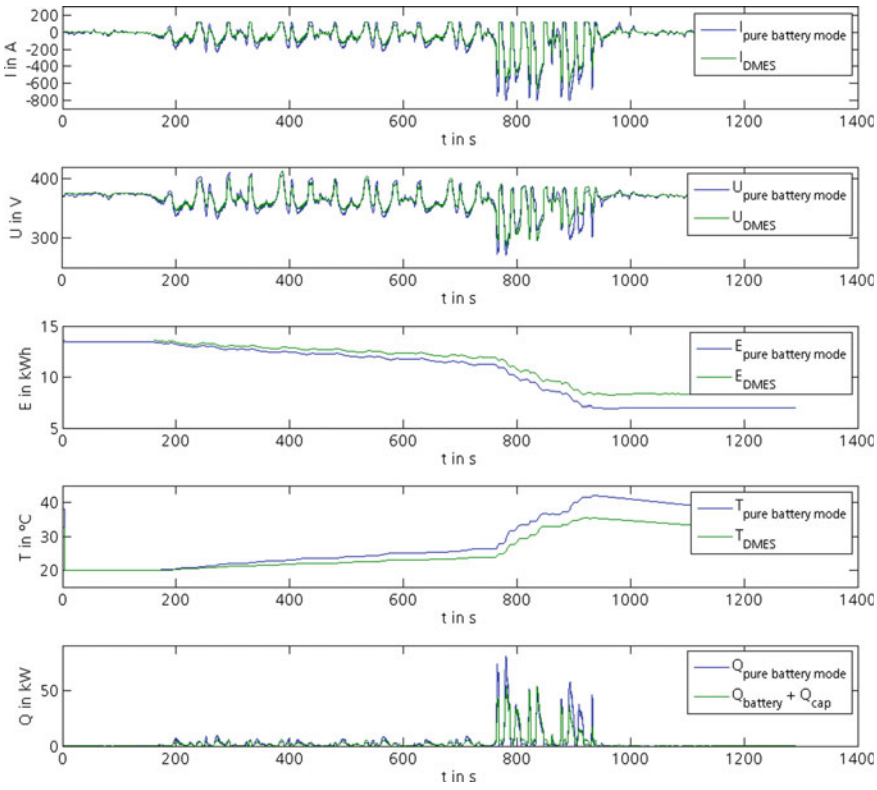

Fig. 3.11 Battery simulation for pure battery mode and for predictive controller

- The dynamic stress of the lithium-ion battery is reduced. Since the controller prevents the system from high temperatures and high current peaks, the lifecycle of the battery can be increased significantly.
- The recuperation potential can be increased. Using the Hethel drive cycle, this is a significant effect. The energy savings are at about 9%.
- The waste heat can be reduced. This is due to the significant lower ohmic resistance of the supercapacitors compared to lithium-ion cells. The result is an increase of the charging/discharging power efficiency of up to 16%. Another positive impact is a reduced demand for the HVAC system. The energy consumption savings derived from this synergy are at least 1%.
- The range of the vehicle can be extended by up to 10%, due to the reasons explained above.

References

1. Wanga J et al (2011) Cycle-life model for graphite-LiFePO4 cells. J Power Sources 196:3942–3948
2. Cao J, Emadi A (2012) A new battery/ultracapacitor hybrid energy storage system for electric, hybrid, and plug-in hybrid electric vehicles. Trans Power Electron 27(1)
3. Bartholomäus R, Klingner M (2010) Prädiktives Energiemanagement in Hybridfahrzeugen. 1st commercial vehicle technology symposium Kaiserslautern. In: Berns K (Hrsg) Aachen, Shaker 2010, S 95–108, ISBN 978-3-8322-9040-5
4. Hredzak B, Agelidis VG, Demetriades G (2015) Application of explicit model predictive control to a hybrid battery-ultracapacitor power source. J Power Sources 277:84–94
5. Santucci A, Sorniotti A, Lekakou C (2014) Power split strategies for hybrid energy storage systems for vehicular applications. J Power Sources 258:395–407
6. Song Z et al (2014) Energy management strategies comparison for electric vehicles with hybrid energy storage system. App Energy 134:321–331
7. Ansarey M et al (2014) Optimal energy management in a dual-storage fuel-cell hybrid vehicle using multi-dimensional dynamic programming. J Power Sources 250:359–371

Chapter 4
Predictive Energy Management on Multi-core Systems

Stephanie Grubmüller, Matthias K. Scharrer, Beate Herbst, Allan Tengg, Holger Schmidt and Daniel Watzenig

Abstract To meet climate agreements, electric vehicles will become very important in the next few years. One class of electric vehicles are Fully Electric Vehicles (FEVs) which are purely powered by electric energy. At the moment the driving range of FEVs is very limited compared to vehicles driven by internal combustion engines. To contribute to increasing the driving range, a comprehensive energy management and enhanced control algorithms like the Model Predictive Controller (MPC) are introduced. The MPC presented in this book chapter is a first approach of solving a reference speed tracking problem on a multi-core platform in real-time. First a high performance off-board system generates an energy and time optimal reference speed profile. This optimization problem is solved by a dynamic programming approach with respect to speed limits, track profile and cloud-sourced data. Afterwards, the reference speed profile is provided to a MPC that is implemented on the vehicle's on-board system. When utilizing a multi-core computing platform, the on-board system provides information about current speed, position and the driver's torque demand, which is made available by the MPC. To enable the concept of a comprehensive energy management, a revised information and communications technology reference architecture is presented, as well as an overview about the available hardware and toolchain is given.

Keywords Model predictive control · Reference tracking · Dynamic programming · Multi-core platform · Cloud-sourced data · Toolchain · Co-simulation

S. Grubmüller (✉) · M.K. Scharrer · B. Herbst · A. Tengg · D. Watzenig
VIRTUAL VEHICLE Research Center, Inffeldgasse 21a, 8010 Graz, Austria
e-mail: stephanie.grubmueller@v2c2.at

H. Schmidt
Infineon Technologies AG, R&D Funding Projects, 81726 Munich, Germany
e-mail: holger.schmidt2@infineon.com

© The Author(s) 2018

D. Watzenig and B. Brandstätter (eds.), *Comprehensive Energy Management - Safe Adaptation, Predictive Control and Thermal Management*, Automotive Engineering: Simulation and Validation Methods, DOI 10.1007/978-3-319-57445-5_4

4.1 Introduction

Fully Electric Vehicles (FEVs) are considered a key solution in ensuring sustainable mobility. Recent reports [1–3] suggest that the global market share of emerging electrified passenger vehicles (plug-in hybrid and fully electric vehicles) is going to significantly increase until 2020—from the current 1 up to 10%; and may reach up to 40% by 2040. However, to achieve these growth rates, electric vehicle technology has to advance to match the customer expectations set by current conventional passenger cars powered by internal combustion engines. Successful FEVs have to provide, among other properties, a combination of adequate driving range (approx. 150 km [4]), good driveability and handling performance at an acceptable price.

In particular, the driving range problem is addressed from two sides: (i) by increasing the amount of available energy and (ii) by reducing the energy usage. The first point is tackled through extensive ongoing research in electric energy storage technology (batteries and supercapacitors) done by current projects SuperLib,[1] Estrelia,[2] SMART-LIC,[3] AUTOSUPERCAP.[4] These projects are supported by the 7th Framework Programme (FP7) which funded European research and technological development from 2007 until 2013.

In terms of car energy usage, manufacturers and suppliers spend a lot of time and effort on developing highly efficient components such as novel electric motors, inverters and steering systems. Yet, as the individual vehicle components and, more importantly, the corresponding controllers are developed in a part-specific piecemeal fashion, the integration and interaction of all building blocks in the FEV for optimising energy efficiency is still a major challenge for manufacturers. Furthermore, considering the quickly growing number of information and communications technology functions in the FEV, it is crucial that the integration of systems must not lead to more complexity, but even more simplicity [5]. Thus, a completely revised information and communications technology reference architecture is required. This much needed step change in FEV system integration is addressed in iCOMPOSE[5] by developing and demonstrating a comprehensive energy management system, including infrastructure integration. The benefits of this approach are highlighted by recent studies that identify great energy saving potential through the adoption of integrated comprehensive energy management systems to optimally coordinate the energy flows in the FEV [6–9].

[1] http://www.superlib.eu/.

[2] http://www.estrelia.eu/.

[3] https://sites.google.com/site/smartliceu/.

[4] http://cordis.europa.eu/result/rcn/164347_en.html.

[5] http://www.i-compose.eu.

The vehicle dynamics and energy management are integrated to have a comprehensive management of the energy and power flows within the FEV. The integrated controller, which represents the main project result, is considered future-proof, as it incorporates the interface with the information from satellite navigation systems, the internet and possibly radars and cameras installed on the vehicle, in order to be immediately usable in the case of vehicles equipped with forms of semi-autonomous and autonomous driving.

In the overall vehicle context, the potential of the existing mechatronic systems regarding energy efficiency is still limited by the traditional control architecture based on stand-alone controllers. The integration of the energy and thermal management, the driveability controller, the vehicle dynamics controller and the controllers of the ancillaries into a single supervisory controller based on control allocation and model predictive control techniques, allows significant performance benefits in energy efficiency, active safety, driveability, comfort and fun-to-drive [9]. The integrated control system is implemented on the multi-core control hardware platform (TriCore™ AURIX™) specifically developed by Infineon[6] for high performance automotive control applications.

Furthermore, the controller benefits from the integration of 'cloud-sourced' information, like vehicle position information from satellite navigation systems, weather conditions, traffic information and mapping information, for the enhanced estimation and prediction of the vehicle states, within a cooperative vehicle-road infrastructure. A first analysis of this subject has been carried out in the FP7 project OpEneR [10]. The simulation and control software developed in that project, enables to represent several realistic traffic situations, analyses the interaction of traffic objects and recommends to the driver an optimal route selection considering the vehicle energy consumption characteristics, real-time traffic situation around the road network and road topology.

The cloud-sourced information enables energy management based on predictive control techniques, e.g. for computing the optimal power split between the battery and supercapacitor in the case of dual mode energy storage systems, and determining the optimal torque demand profile and the motor actuation in the case of autonomous driving, including consideration of cornering conditions.

The focus of this book chapter is on the MPC approach which enables the demonstrator's velocity tracking of an energy optimized speed profile along a test rack including cloud-sourced data. Section 3.2 describes the problem arising with evolutionarily derived controller architectures and the demonstration setting to conceptually proof the new architecture. Section 3.3 discusses the implemented architecture, focussing on the semi-autonomous driving control application. The hardware architecture, as developed and used in iCOMPOSE, is briefly outlined in Sect. 3.4. Section 3.5 depicts the software integration as well as the controller logic.

[6] https://www.infineon.com/.

4.2 Problem Description

Current vehicle control architectures derive from the evolution of the control functions. The first controllers have been introduced for the fuel injection control of internal combustion engines and progressively included more advanced functionalities such as driveability control. Popular examples for driver assistance systems are the Anti-lock Braking Systems (ABS, Bosch, 1978) and the overall vehicle stability control functionality (Electronic Stability Program of Bosch, 1995). In recent years, a multiplication of the control functions has been experienced due to the introduction of new actively controlled vehicle systems such as electric power steering and active steering systems, active and semi-active suspension systems, electronically controlled differentials and advanced Heating, Ventilation and Air-Conditioning (HVAC) systems. Additionally, Adaptive Cruise Control (ACC) systems are progressively evolving towards forms of semi-autonomous driving.

The continuous addition of new control functions has resulted in vehicle electronic architectures (Fig. 4.1) characterised by a multitude of control units linked by communication buses such as the well-known Controller Area Network (CAN) and FlexRay. Traditionally, each of the controllers are designed separately by different Tier 1 suppliers or different divisions within the same company, with the resulting requirement of significantly time consuming, expensive and resource intensive calibration procedures and the risk of contradictory control actions. Typically, the complexity of this approach leads to a sub-optimal performance of the overall system. Moreover, despite the large bank of academic literature dealing with advanced model-based optimal controllers, actual implemented automotive controllers are often simple rule- or look-up-table-based, or characterised by very simple feedback control structures (e.g. PID controllers, such as those adopted in anti-jerk controllers for internal combustion engine drivetrains [11]). Due to the state-of-practice, the actual signals adopted for each control function are often limited to the ones that have been traditionally used and do not incorporate signals that are already commonly available on modern vehicles, yet would improve the

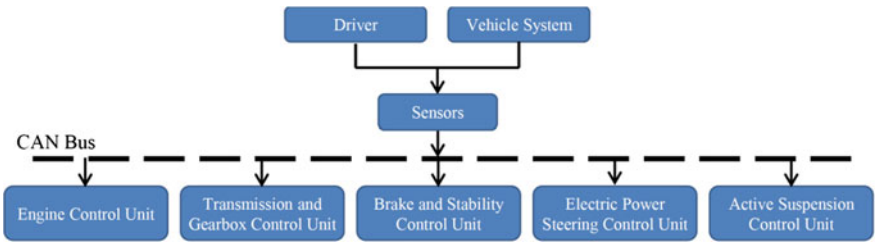

Fig. 4.1 Typical control system architecture of an internal combustion engine driven vehicle

controller performance. This fundamental issue is addressed by the development of the integrated control structure for comprehensive energy management and vehicle dynamics control.

In addition, electro-mobility provides the opportunity of redefining the vehicle control system architecture. Possible FEV control system architectures have been proposed in the literature (e.g. in [12]) but none of them simultaneously accounts for: (i) the continuous generation of a reference yaw moment and an overall wheel torque through a wheel torque distribution defined according to energy efficiency criteria; and (ii) the integration of a comprehensive energy management system with ACC, autonomous/semi-autonomous driving and cloud-sourced information.

The proposed integrated comprehensive energy management (iCEM) system introduced by the iCOMPOSE project has access to the satellite navigation information, the environmental, and traffic information and the driving record from the information cloud. This cloud-sourced data is coupled with the information from maps commonly used by navigation systems. With the model-based approach, the states of the overall vehicle and all its relevant subsystems regarding energy efficiency can be plausibly estimated. The optimal driving route and load profile can then be determined by taking into account all the relevant vehicle subsystems. With assistance of predictive controllers, the iCEM can also adapt itself to the changing environmental/traffic conditions. With the AURIX^{TM} platform developed by the iCOMPOSE consortium partner Infineon, highly comprehensive and accurate algorithms can be implemented for the on-board application of the iCEM.

The new information and communications technology forced an expansion of the architecture. A new layer of state estimators and state predictors was defined for the organization of the cloud-sourced information and the derivation of the optimal mission profiles.

One main objective is to provide software and hardware for the Central Control Unit (CCU) of a prototype FEV with multi-propulsion system and a demonstrative FEV based Hardware-in-the-Loop system with dual mode energy storage. Both prototypes include the iCEM.

As mentioned above, there is a substantial separation between the different control functions in the current generation of FEVs. From the implementation point of view, the control hardware for the different control functions consists of dedicated and separated electronic control units. The potential for higher safety, better performance and cost saving is strongly limited by this distributed computing approach. For this reason, one target is to develop the hardware and software of the CCU for applications with high safety standard and applications requiring high computing performance, and for integration of control functions from different domains into a single supervisory controller.

Fig. 4.2 iCOMPOSE demonstrator vehicles

For testing, in iCOMPOSE three demonstrators are available: (i) The Škoda[7] Rapid Spaceback, (ii) the Range Rover[8] Evoque and (iii) the Lotus[9] Evora 414E based Hardware-in-the-Loop rig.

Škoda provided the vehicle demonstrator Škoda Rapid Spaceback that is a prototype of a FEV. The second vehicle demonstrator is an electric Range Rover Evoque, a demonstrator with four electric drivetrains which was developed within the FP7 project E-VECTOORC.[10] The Evoque is used for the testing and demonstration of the integration of the energy management system developed in iCOMPOSE with the torque-vectoring-based vehicle dynamics controller of E-VECTOORC. The third use case under consideration is a Hardware-in-the-Loop system based on selected components of the Lotus Evora 414E which is a plug-in hybrid electric vehicle with a range extender and independent rear wheel drive. The Hardware-in-the-Loop system is applied for virtual testing to investigate the performance of the dual mode energy storage system and the comprehensive energy management concept based on real measurements.

Figure 4.2 highlights all demonstrators.

For each demonstrator vehicle, different test tracks have been defined. Skoda uses public urban roads and highways near Mlada Boleslav in Czech Republic. Lotus utilized their proving ground at Hethel and a public test track in Millbrooks. The Evoque has been tested on two tracks at Ford Lommel Proving Ground.[11] This chapter considers one test track shown in red in Fig. 4.3.

4.3 Approach

To show the flexibility of the control architecture, a semi-autonomous driving mode is in the scope of iCOMPOSE implemented. In that mode the driver controls the steering wheel angle, but the wheel torque demand is controlled by the CCU. In this

[7] http://www.skoda-auto.com/.

[8] http://www.jaguarlandrover.com.

[9] http://www.lotuscars.com/.

[10] http://www.e-vectoorc.eu/.

[11] https://www.fordlpg.com/en/index.htm.

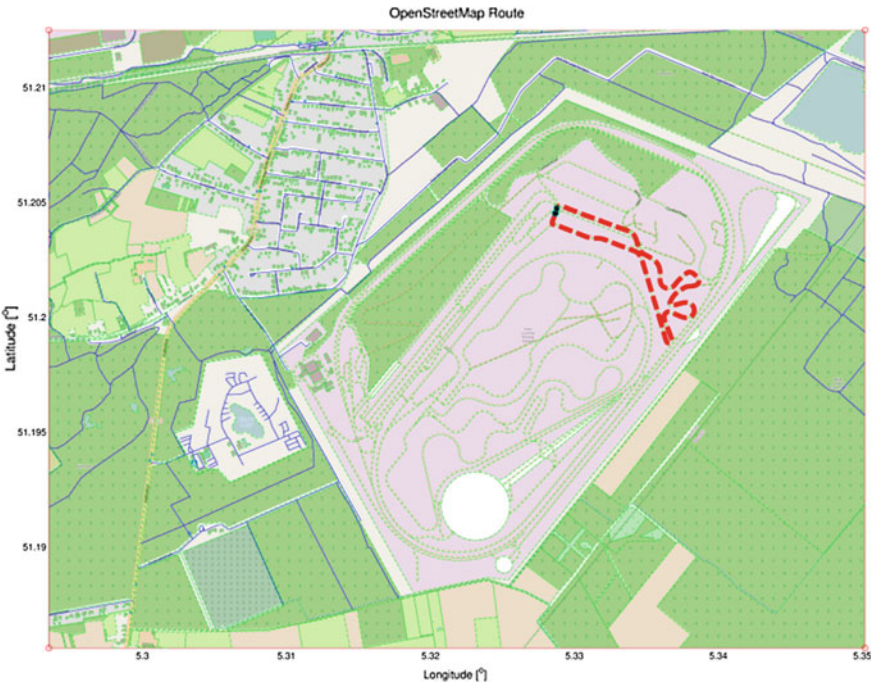

Fig. 4.3 Lommel test track in OpenStreetMap (www.openstreetmap.org)

condition, a high performance off-board system computes the reference vehicle speed profile in advance. This system estimates the reference speed profile for the journey, which represents the best compromise between speed, time and efficiency, and considering the speed limits of the roads. The driver indicates his/her final destination at the beginning of the journey and the off-board system generates a speed profile according to an initial off-line optimization algorithm, which is to be revised on-line during the journey. The reference speed profile is the solution of a global optimization problem (theoretically solvable through dynamic programming, in practice computationally very demanding). The reference profile is followed by a predictive controller which runs on the on-board system within the vehicle. The controller solves a reference tracking problem using a real-time MPC approach and current cloud-sourced data. Figure 4.4 shows the technical concept of iCEM and the predictive controller. The Information Harvesting Layer processes and provides on-board and off-board data. In this context, data sources and networks within the vehicle are part of the on-board system. Data obtained from sources outside the vehicle are defined as off-board data. Additionally, the exact vehicle's position is computed by a state estimator.

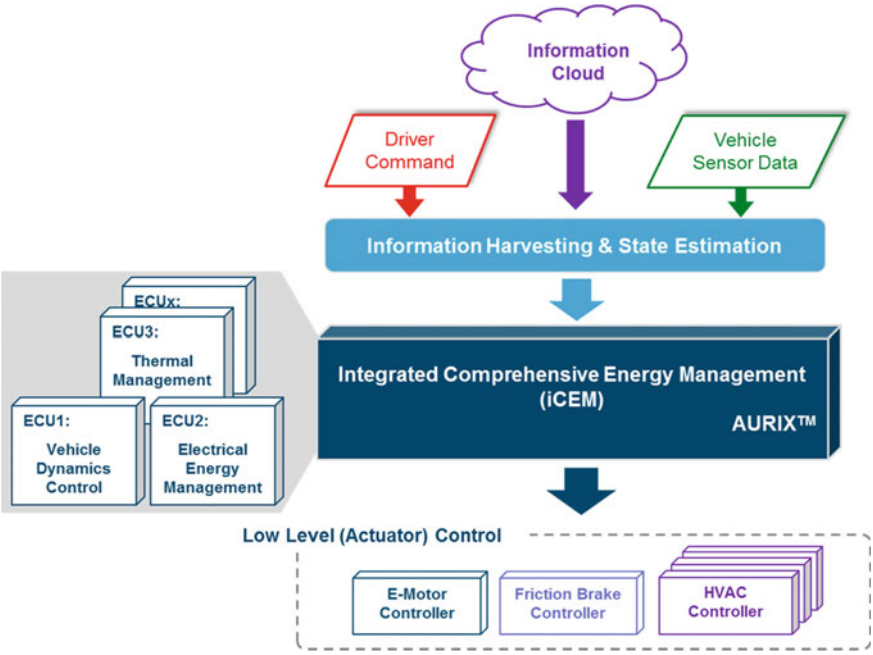

Fig. 4.4 Technical concept of iCEM

A possibility to obtain the required large amount of information for the development of novel functionalities of the FEV, such as comprehensive energy management and semi-autonomous driving, is to use cloud-sourced data. Recently, telematics services for passenger vehicles that fall outside the safety and security scope have taken off in Europe. All major original equipment manufacturers, like Audi, BMW, Mazda, Mercedes-Benz, Renault, Toyota and Volkswagen, offer connectivity for infotainment purposes including weather information, Facebook, Google services etc. It can be expected that modern wireless communication technology will be available to the new generation of vehicles in the near future. Regarding the work done in this book chapter, cloud-sourced information directly affects the comprehensive energy management of the FEV (i.e., the control reference for the actuators) and is also adopted for the generation of the speed profile for vehicle semi-autonomous driving. Figure 4.5 shows the information sources which influence the vehicle parameters. These sources define the so-called information cloud.

From the controller perspective, the cloud provides all information from sensors and networks to the iCEM, i.e. weather and traffic services from internet/Intelligent Transport Systems (ITS), navigational information from internet/navigation systems and sensor information accessible on the car bus. Each data source is possibly connected to the vehicle via a different bus system.

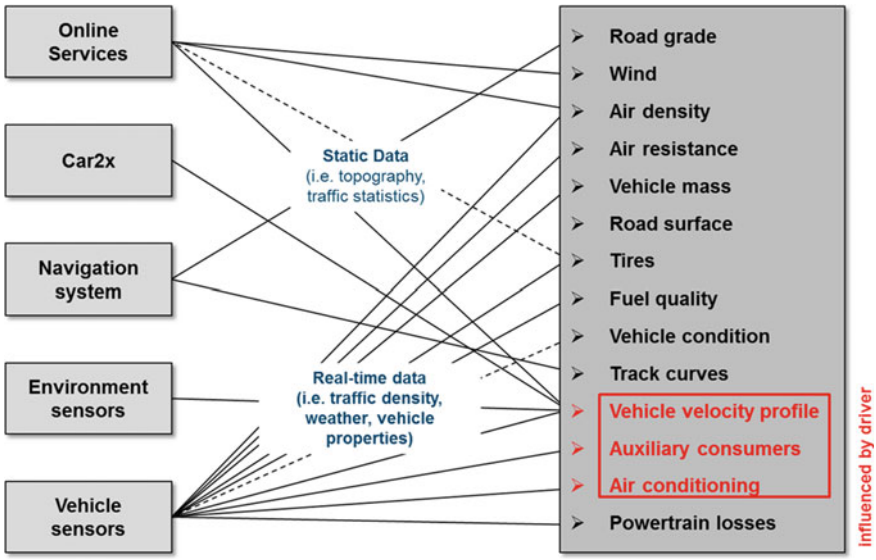

Fig. 4.5 Information sources of influencing parameters

Cloud-sourced data is provided via the off-board system.

Data provided by the off-board system include all information from cloud sources and off-line processing. Cloud-sourced data is defined as web-based (navigational and weather) and ITS-based data, whereas off-line processed data contains all pre-journey computed information, like the reference speed profile which is computed using an optimization approach.

For the optimization of the velocity for the whole track the Dynamic Programming algorithm using Matrix operations (DPM), implemented by Swiss Federal Institute of Technology Zurich [13], has been used. The goal is an optimal velocity profile that minimizes the energy consumption of a vehicle over the whole track with respect to all speed limits.

For simulations of MPC of hybrid electric vehicles dynamic programming is successfully used which was developed by Olle Sundström and Lino Guzzella [13]. The algorithm controls the energy management (balance battery and combustion engine). For this work, the dynamic programming approach is used to generate the optimal reference speed considering the optimal balance of the dual mode energy storage system for a given distance profile (velocity, acceleration and inclination) in respect to speed and vehicle constraints. The DPM generates a grid containing all possible solution states resolved over distance and the desired resolution of the state space. Caused by a very large grid, the computation of an accurate speed profile is very demanding with respect to processing power and memory.

In general the optimization problem is formulated as:

$$\begin{aligned} &\min_{\mu(s)} J(\mu(s)) \\ &s.t. \\ &\dot{x}(s) = f(x(s), \mu(s), s) \\ &x(0) = x_0 \\ &x(s_e) \in \left[x_{e,\min}, x_{e,\max}\right] \\ &x(s) \in X(s) \subset \Re^n \\ &\mu(s) \in M(s) \subset \Re^n \end{aligned} \tag{4.1}$$

where $f(\cdot)$ represents the longitudinal vehicle model,μ represents the change of the vehicle's speed between two time steps and is the model input,x gives information about the bounded model states and $J(\cdot)$ is the optimization objective function. The states are the velocity of the vehicle and the state of charge of the used energy storage system(s). The boundaries of the velocity are given by the government as official speed limits, by the current traffic flow and by the curvature of each path segment.

A major criterion within the modelling task is the possibility of a smooth application of the models within the iCEM functionality which basically represents an optimization task. These problem statements lead to the choice of a quasi-static system modelling approach in a backward-facing model (velocity towards driving forces and power) [14, 15] and is considered in the DPM approach. For a specific vehicle velocity demand and gradient of the road the necessary propulsion force can be derived. The modelling of the listed components following the approach described:

- Translational vehicle dynamics
- Transmission
- Electric motor/generator
- Battery
- Super capacitor if implemented.

In order to achieve an advantageous situation for the optimization task of the iCEM the system is considered in terms of distance and not (as usual) in terms of time.

Depending on the optimization goal chosen, the algorithm yields a different reference profile. Figure 4.6 shows a time optimal reference profile for the Lommel test track, considering a maximum lateral acceleration of 3 m/s^2 and (artificial) regulatory speed limits, versus an unconstrained human test drive.

The on-board system contains all vehicle on-board data sources and the predictive controller software. Data sources within the vehicle are for example the Global Positioning System (GPS), the Six Degrees of Freedom, the wheel velocity etc.

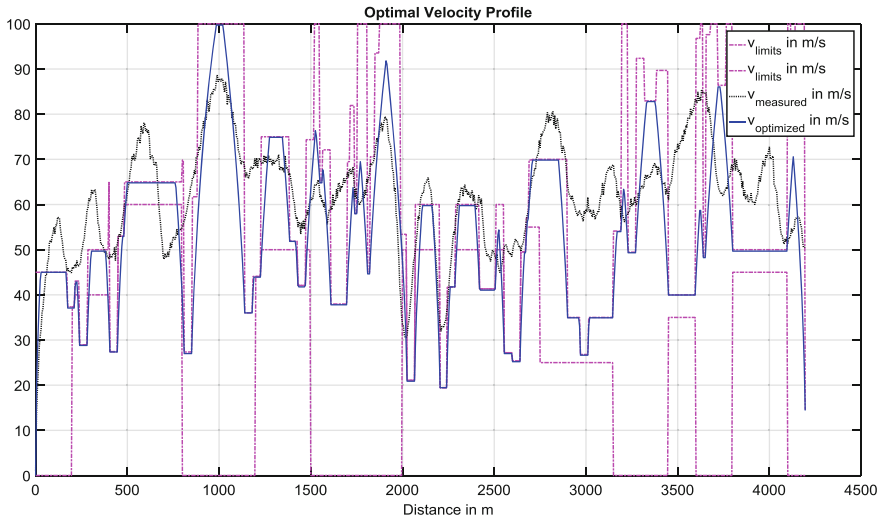

Fig. 4.6 Velocity profile Lommel track

To gather and apply information from the off-board system a cloud interface has been implemented. It provides reference values for the controllers, as route, distance, velocity, and additionally weather and ITS data in appropriate formatting.

To track the reference speed profile generated by the off-board system a MPC approach is used which provides the speed and torque demand to the energy management system. In summary, this speed profile is a function of the information deriving from the cloud, the mapping of the road (i.e., including the speed limits information), the on-board state estimation or data sources, like compass, wheel speed, GPS etc.

A big issue is the real-time capability of the predictive controller in each time step. The reference tracking must meet real-time constraints to be runnable on the AURIX^{TM} platform. That includes the performance of the optimization algorithm and the structure of the control problem, as well as the size of the MPC horizon. Furthermore, the overall memory consumption was too large for an embedded microcontroller. Consequently, the DPM approach is very time as well as memory consuming and is not applicable on the AURIX^{TM} platform, only on the off-board system calculating the reference speed profile. In [16] a solution of a real-time optimization problem is given, using the Toolkit for Automatic Control and Dynamic Optimization (ACADO Toolkit) [17, 18]. It offers a software environment and algorithm collection for automatic control and dynamic optimization, especially for MPC. It is implemented in C++, provides a MATLAB interface and is designed to generate code applicable on an embedded computing platform.

First, the controller has been implemented in MATLAB for the Evoque demonstrator and a test track on Flander's Make Lommel proving ground. For developing code runnable on hardware, the code generation tool provided by the

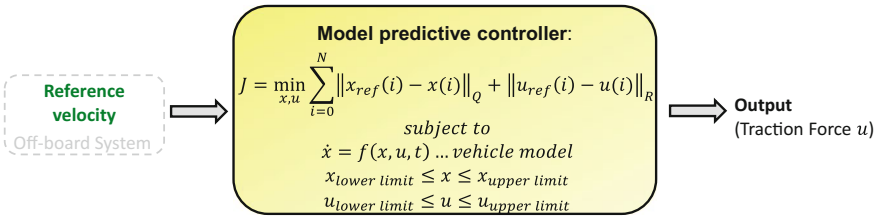

Fig. 4.7 Global optimization goal reference tracking

ACADO Toolkit shows great potential for deploying a real-time MPC on the AURIX™ platform. Hence, this toolkit has been chosen for the development of the on-board MPC.

The global objective of the reference tracking algorithm is given in Fig. 4.7. The goal is to minimize the error between reference state $x_{ref}(t)$ as well as the reference control input $u_{ref}(t)$ and current state $x(t)$ and control input $u(t)$ in each time step within the horizon N regarding speed limits as well as vehicle constraints. The states are defined as $x(t) = [v(t), s(t)]$ and the control inputs $u(t) = [T_m(t), T_b(t)]$. The output of the algorithm is the vehicle's needed traction force $T_m(t)$, and breaking force $T_b(t)$ or also called control inputs. The state $v(t)$ defines the velocity of the vehicle in meter per second and $s(t)$ the driven distance in meter. The reference trajectory is provided by the cloud. The matrices Q and R are weighting matrices. The structure of a weighting matric is similar to the unit matrix, but with possible diagonal entries unequal to one. The entries of the diagonal of each weighting matrix define the weight of each error compared to the reference in each step during the optimization. For velocity tracking, the entry responsible for the speed is higher than for the control inputs. Referring to the implementation, the matrices Q and R are combined into one weighting matrix W.

For developing the control algorithm we consider a simple non-linear longitudinal vehicle model:

$$\dot{v} = \frac{T_m g_r \eta_{tr,EM}}{m\, r_w} - \frac{1}{2m} \rho c_d A_f v^2 - c_r g - g sin(\alpha) - \frac{T_b g_r}{m r_w \eta_{tr,EG}}$$

$$\dot{s} = v$$

A simplified model compared to the DPM approach to reduce the computation time, which is needed for real-time embedded computing.

The constant parameters g_r, r_w, m, ρ, c_d, A_f, c_r, g represent the gear ratio, wheel radius, vehicle mass, air density, aerodynamic drag coefficient, vehicle surface, rolling resistance and the gravity of earth, respectively. The electric motor and generator transmission efficiencies $\eta_{tr,EM}, \eta_{tr,EG}$ are considered as constant. The inclination of the road α may vary online while the vehicle is moving. This information is treated as online data in the ACADO Toolkit. The controller receives

the data online during the journey from the navigation system. The velocity v and position s are the differential states. The drive moment T_m and break moment T_b are the outputs of the controller and also known as control signals $u(t)$.

One big advantage of this approach is that state and control constraints may vary over time during runtime.

Using the tracking algorithm implemented in ACADO, states and controller outputs track a reference trajectory of the velocity, the driven distance, the drive moment and break moment provided by the off-board system. Since the focus is on speed tracking and the entries of matrix $W$are carefully chosen, the error between reference control signals and computed ones hardly affect the optimization goal. In contrast to the DPM approach, the reference speed profile needs to be resolved over the time.

A first MATLAB simulation result for an energy saving driving mode is given in Fig. 4.8. Dashed blue lines indicate the reference speed and torques. Solid red lines show the results of the MPC. The speed profile produced by the MPC algorithm perfectly matches the reference value, as opposed to the computed torques. The deviations are explicable by the usage of the simpler vehicle model in the MPC algorithm.

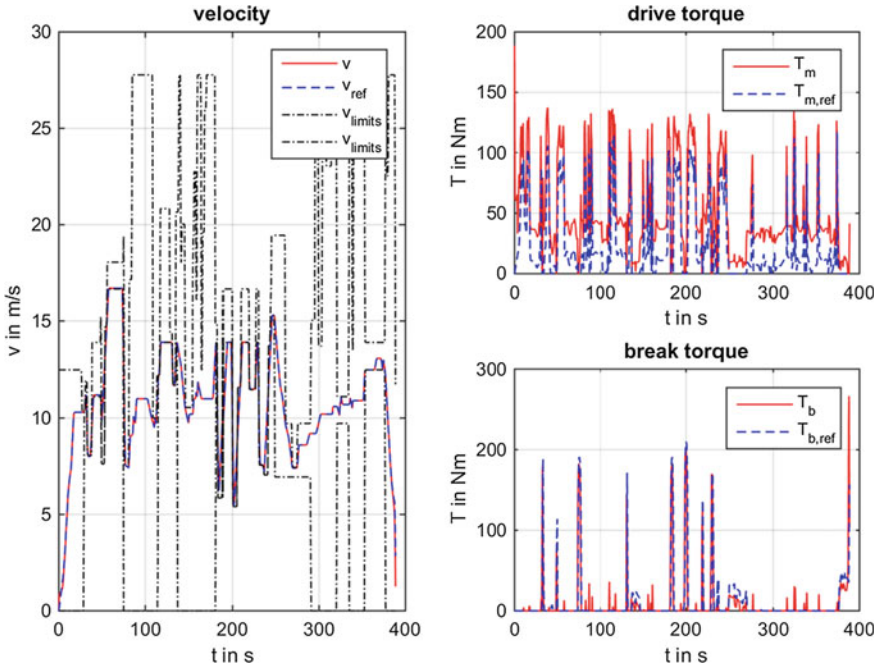

Fig. 4.8 Results from MPC speed tracking

4.4 iCEM Central Control Unit

In the scope of the iCOMPOSE project an integrated control structure (see Fig. 4.4) has been introduced for comprehensive energy management and vehicle dynamics control. It demands for a CCU as an extension to the established concept of single domain controllers such as motor control, battery management or HVAC control. The concept of such an integrated control structure is shown in Fig. 4.9.

Due to real-time and safety requirements certain functions of this kind of supervisory controller should reside in the vehicle. It is of importance to prove the feasibility of using an automotive CCU for this purpose. A major challenge is the high performance required by the integrated energy management in terms of compute power, memory and communication bandwidth. The feasibility analysis resulted in an approach of coordinated software and hardware measures.

Equipping the iCEM CCU with one TC299TX prototype of the Infineon AURIX^{TM} multicore microcontroller family has been rated to meet the needs of the iCEM. This automotive microcontroller provides 3 cores running at 300 MHz, 2776 kB RAM and various powerful communication interfaces such as CAN-FD (fully compatible to traditional CAN) and FlexRay for connections to the vehicle network. Its Ethernet connection is used to represent the connection to the cloud.

The controller is designed to be ISO26262 compliant, provides a dedicated safety management unit and supports safety requirements up to ASIL-D. An embedded programmable hardware security module (HSM) is available to address security requirements such as for example secure communication.

Furthermore, the iCEM CCU provides a Bluetooth interface for connections to mobile devices and a BroadR-Reach interface (“automotive Ethernet”) for early

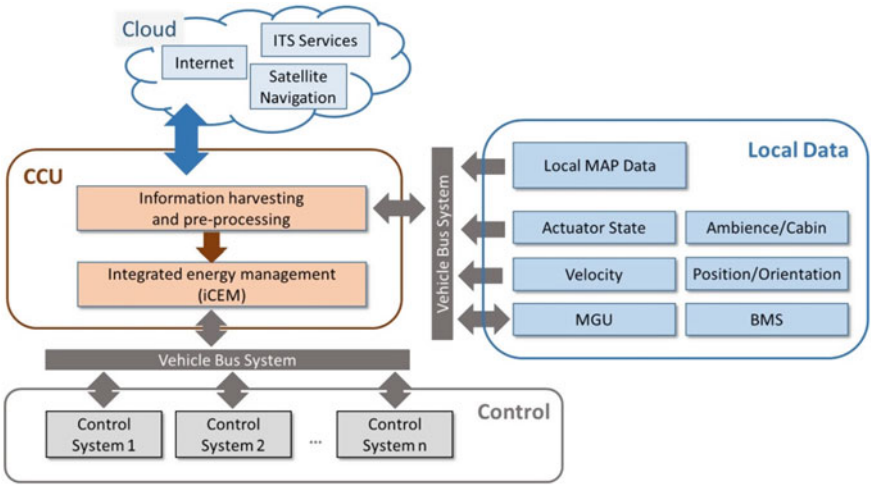

Fig. 4.9 Concept of FEV control structure with central control unit

technology exploration. For the development of the iCEM CCU synergies were used with the CCUs of the INCOBAT[12] and EDAS[13] project which constitute a project cluster together with ICOMPOSE. One example for this is the re-use of the power supply concept based on the Infineon safety power supply ASIC prototype. A shutdown of the CCU in critical situations can be implemented on this basis.

Figure 4.10 shows the prototype of the iCEM CCU which is not designed for smallest size but for technology exploration. The AURIX™ is located almost in the centre of the PCB surrounded by the various communication interfaces. The empty area on the top right is dedicated to a BroadR-Reach extension board.

4.5 Software Implementation

Meeting cost and integration requirements, the development environment is required to be a low-cost solution with the possibilities to integrate software components from other partners—see also chapter "*Holistic thermal management strategies for EVs*" for a description of the HVAC system and chapter "*Model based functional safety engineering*" for a brief outline of the code and interface generation framework.

The fundamental configuration of the software development comprises a set of Makefile generation rules, optimised GNU C libraries and settings embedded into the HighTec compiler toolchain [19]. The Free-RTOS operating system (OS) [20] has been ported and adapted to the AURIX™ TC27x and TC29x families as a basis for the integration and runtime management of the integrated applications. FreeRTOS is a widely used real-time operating system professionally developed by Real Time Engineers Ltd. that supports 35 architectures and is freely available under GNU General Public License. It is targeted to do the OS configuration, including the definition of tasks, queues and share of resources automatically within the framework.

Inter-Core communication is implemented as a dedicated task on each core, accessing the Local Memory Unit's storage via the Shared Resource Interconnection Crossbar. This function is accessible to higher level code via specific interface code in MATLAB deployed during the code generation step.

The implementation of the TCP/IP stack used for communication with the off-board system is adopted from the open source package "*lwIP*", developed by Adam Dunkels at the Swedish Institute of Computer Science [21].

As a quasi-industry standard, the CAN bus messages are specified using VECTOR Informatik's CANdb format [22]. The generated dbc-files are translated into dedicated interface blocks for further use in MATLAB® script and

[12] http://www.incobat-project.eu/.

[13] http://edas-ev.eu/.

Fig. 4.10 iCEM CCU Prototype

SIMULINK. The interface blocks are implemented via custom driver code utilizing the AURIX™ hardware modules (MultiCAN and the asynchronous serial interface).

On the highest level of abstraction, the system architecture has been designed in SparxSystem's Enterprise Architect [23]. Further detailing included the design of a state machine for describing the system's states, transitions and behavioural description. As described in chapter "*Model based functional safety engineering*", a new code generation language template was implemented and subsequently used for implementing the state machine in MATLAB® script. After implementing the states and adding interface code for lower level implementation, C-Code has been generated for the final step in the software development toolchain.

Figure 4.11 shows the development process schematically in a tool centred view.

The MPC application based on the ACADO Toolkit uses the qpOASES (quadratic programming Online Active SEt Strategy) algorithm for solving the optimization problem [24]. Replacing the ACADO Toolkit's packaged C++ implementation of qpOASES by embedded-qpOASES enabled the deployment of the solver on the AURIX™ platform. Several files provided by the code generation tool used by the interface to MATLAB® had to be adapted, such as setting eqpOASES' single precision flag and adapting the weighting matrix W to guarantee a successful run. As a remarkable result, the MPC is usable on the AURIX™ platform.

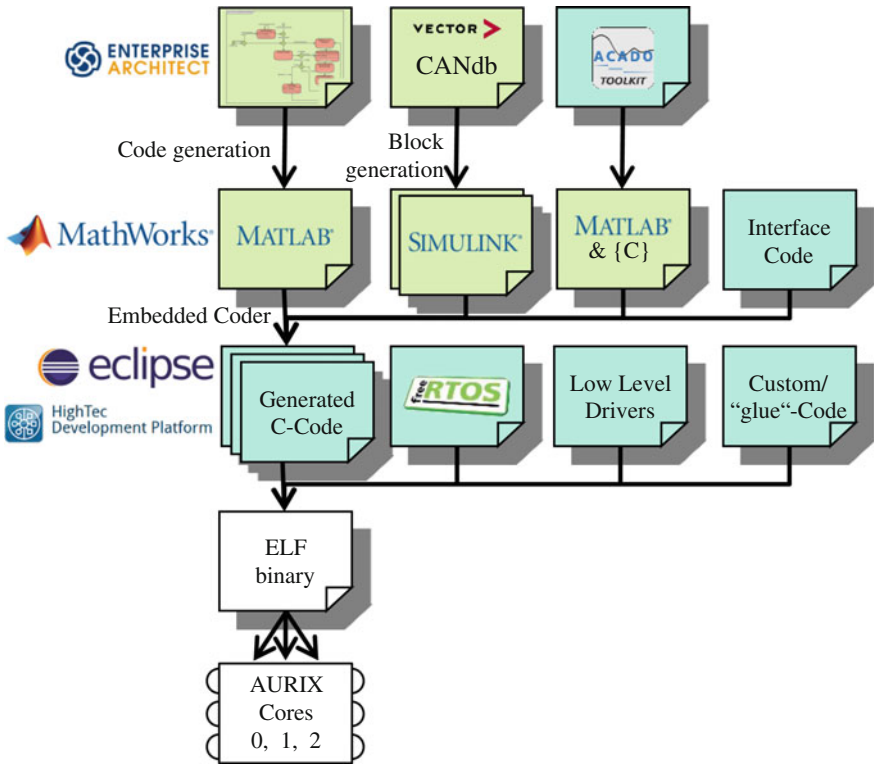

Fig. 4.11 iCOMPOSE software development framework

For testing, a simplified vehicle model has been generated in MATLAB® SIMULINK and subsequently coupled with the MPC running on the AURIX™ via the Independent CO-Simulation (ICOS[14]) framework developed by VIRTUAL VEHICLE. This is depicted in Fig. 4.12. CAN communication was established for sending packets between the two models. The MPC cycle time was set to 500 ms due to runtime requirements. Since information exchange rates were set to 100 ms cycle time, data interpolation implemented a first-order-hold to provide useful data. The horizon for the MPC is set to 20 sampling points. That is a window of 10 s in the future. Figure 4.13 shows the significantly good results of this setup.

Ripples around the optimal solution can be observed, which result from the interpolation and communication of the control inputs between two consecutive MPC calculations. The solution provided by the MPC shows deviations from the reference value due to the usage of single precision data types, the limited MPC horizon and precision truncated communication, as well as the simplified vehicle model.

[14] http://www.v2c2.at/icos/.

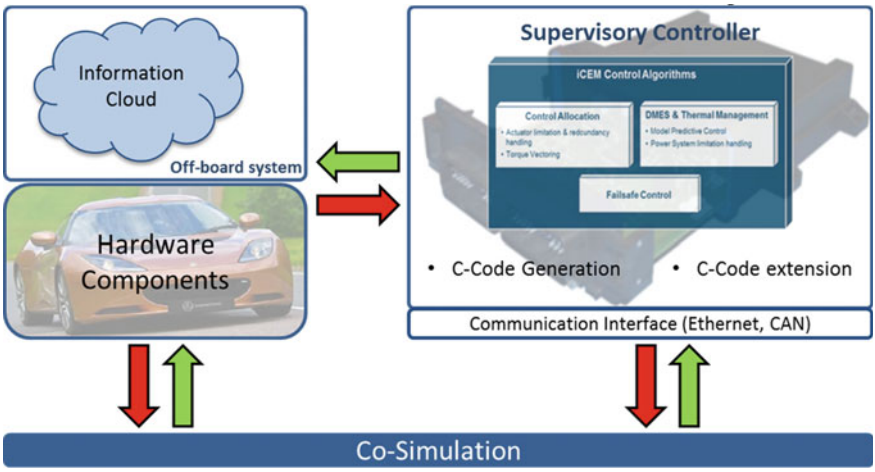

Fig. 4.12 Test environment

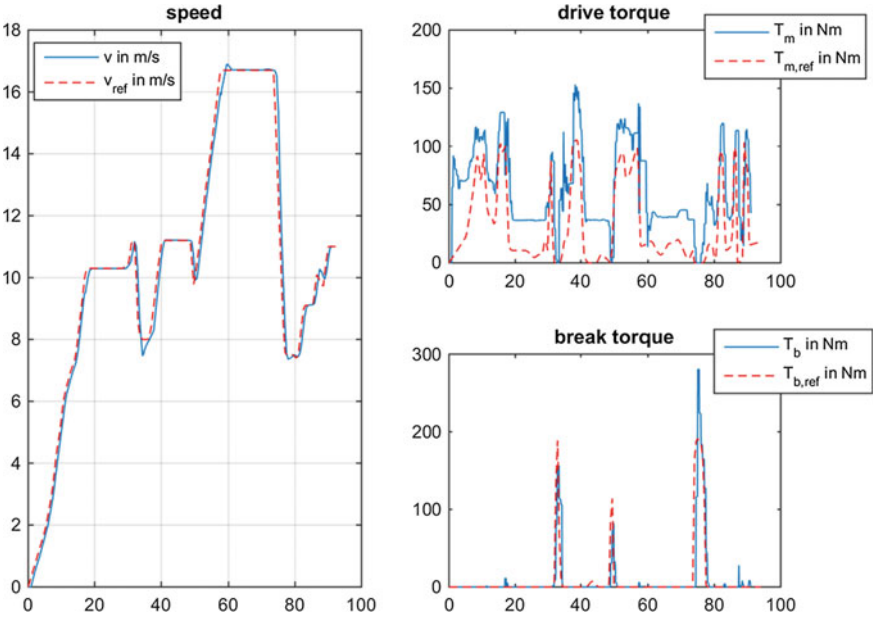

Fig. 4.13 Co-simulation results including MATLAB model and AURIX™ platform coupled over CAN

4.6 Conclusion

This book chapter summarizes results of research activities in the field of comprehensive energy management. In particular, it presents a revised information and communication architecture, the structure of the deployed multi-core platform, the implemented toolchain and a first approach of a real-time MPC running on the multi-core platform.

For performance demanding algorithms, like the one generating the reference speed profile, an off-board system is installed which provides its results to the information cloud. The reference profiles in combination with map and ITS data are part of the information cloud. Since the iCEM running on the CCU apply cloud-sourced data, an information harvesting layer and state predictors are introduced. The layer processes data in a way to be utilizable by the iCEM at the on-board system. That new architecture provides the basis for a real-time capable MPC.

The design of the CCU is based on the project's requirements of iCOMPOSE. The CCU is an automotive embedded platform and provides 3 cores, a CAN-FD/FlexRay/Bluetooth/BroadR-Reach interface and it is ISO26262 compliant. In addition, a toolchain is presented which enables the conversion of MATLAB® SIMULINK Simulink code and C code into machine code runnable on the AURIX™ CCU.

One remarkable result achieved by the work described within this book chapter is the MPC approach runnable on the AURIX™ platform. The algorithm tracks an optimal speed trajectory with respect to speed limits. This trajectory is provided by an off-board system. To design a predictive controller, the ACADO toolkit is deployed. This toolkit contains optimization solvers provided by the qpOASES package. By integration of the embedded qpOASES and setting certain real-time flags, it is possible to run algorithms designed by the ACADO toolkit on embedded platforms. This work gives an insight of a first implementation of an MPC using the mentioned packages on an automotive qualified multi-core platform. The results show good potential for further research in this direction and give positive feedback for similar platforms like the AURIX™. Further steps in this project are the implementation of the communication with the off-board system, an integration of a localization algorithm and the implementation on demonstrator vehicles.

Acknowledgements The research work of the authors has been partially funded by the European Commission within the project Integrated Control of Multiple-Motor and Multiple-Storage Fully Electric Vehicles (iCOMPOSE) under the Seventh Framework Programme grant agreement №. 608897.

The authors acknowledge the financial support of the COMET K2—Competence Centres for Excellent Technologies Programme of the Austrian Federal Ministry for Transport, Innovation and Technology (BMVIT), the Austrian Federal Ministry of Science, Research and Economy (BMWFW), the Austrian Research Promotion Agency (FFG), the Province of Styria and the Styrian Business Promotion Agency (SFG).

References

1. Mock P (2015) European vehicle market statistics. The International Council on Clean transportation: Pocketbook 2015/16
2. Technology Roadmaps: Electric and plug-in hybrid electric vehicles (EV/PHEV): available at https://www.iea.org/publications/freepublications/publication/EV_PHEV_Roadmap.pdf, 2011. Accessed 11 Aug 2016
3. Global EV Outlook 2016: Beyond one million electric cars: available at https://www.iea.org/publications/freepublications/publication/Global_EV_Outlook_2016.pdf. Accessed 20 Sept 2016
4. Pearre NS, Kempton W, Guensler RL, Elango VV (2011) Electric vehicles: how much range is required for a day's driving? Trans Res Part C Emerg Technol 19(6):1171–1184
5. Briec E, Mazal C, Meyer G, Müller B (2012) European roadmap electrification of road transport. 2nd edn, June 2012: available at http://www.ertrac.org/uploads/documentsearch/id31/electrification_roadmap_june2012_62.pdf. Accessed 23 Apr 2017
6. Omar N et al (2012) Electrical double-layer capacitors in hybrid topologies—assessment and evaluation of their performance. Energies 5:4533–4568
7. Chen Y, Wang J (2012) A branch-and-bound algorithm for energy-efficient control allocation with applications to planar motion control of electric ground vehicles. The 2012 American control conference, Montréal, Canada, 27–28 June 2012
8. Mutoh N et al (2006) Driving characteristics of an electric vehicle system with independently driven front and rear wheels. IEEE Trans Ind Electron 53(3):803–813
9. De Novellis L et al (2014) Wheel torque distribution criteria for electric vehicles with torque-vectoring differentials. IEEE Trans Veh Technol 63(4):1593–1602
10. Steinmann J et al (2012) Deliverable 2.3: report documenting vehicle specification, topology and simulation results. Also running vehicle delivery, Deliverable 2.3, OpEneR consortium
11. List H, Schoeggl P (1988) Objective evaluation of vehicle driveability, SAE 980204
12. Ringdorfer M et al (2010) Vehicle dynamics controller concept for electric vehicles, AVEC10
13. Sundstrom O, Guzzella L (2009) A generic dynamic programming Matlab function, Control Applications, (CCA) & Intelligent Control, (ISIC), 2009 IEEE, pp 1625,1630, 8–10 July 2009
14. Guzella L, Amstutz A (2005) The QSS toolbox manual, measurement and control laboratory. Swiss Federal Institute of Technology Zurich, Zurich
15. Guzzella L, Sciarretta A (2005) Vehicle propulsion systems, introduction to modeling and optimization. Springer, Berlin, Heidelberg, ISBN 3540251952
16. Verschueren R et al (2014) Towards time-optimal race car driving using nonlinear MPC in real-time, 53rd IEEE conference on decision and control, Los Angeles, CA, pp 2505–2510
17. Ariens D et al (2011) ACADO for Matlab User's Manual, available at http://www.acadotoolkit.org, 2011. Accessed 11 Aug 2016
18. Houska B et al (2011) ACADO Toolkit—an open source framework for automatic control and dynamic optimization. Optimal Control Appl Methods 32(3):298–312
19. HighTec EDV-Systeme GmbH: TriCore Development Platform. Available at http://www.hightec-rt.com/en/downloads/product-information.html, 2012. Accessed 17 Aug 2016
20. The FreeRTOS™ project website. http://www.freertos.org. Accessed 17 Aug 2016
21. Dunkels A (2001) Design and implementation of the lwIP TCP/IP Stack, Swedish Institute of Computer Science, Kista
22. Vector Informatik GmbH: CANdb++ manual. Available at http://vector.com/vi_downloadcenter_de.html, 2010. Accessed 17 Aug 2016
23. Sparx Systems: Enterprise Architect. http://www.sparxsystems.com/. Accessed 17 Aug 2016
24. Ferreau HJ et al (2014) qpOASES: a parametric active-set algorithm for quadratic programming. Math Prog Comput 6:327–363

Chapter 5
Holistic Thermal Management Strategies for Electric Vehicles

Matthias Hütter, Wolfgang König and Stefan Kuitunen

Abstract Thermal management systems in vehicles ensure the demand-based supply and extraction of the heating and cooling energy that is needed to fulfil the specific requirements of components regarding their operating temperatures and to guarantee thermal convenience inside the cabin. Due to the limited energy capacity of fully electric vehicles, the energy efficiency of thermal management systems is a key factor for the sustainability of electromobility. In order to improve the efficiency of the overall system through a holistic approach, it is necessary to use the existing heat sources and lower the primary energy demand. The thermal management system that is currently being developed within the EU-funded iCOMPOSE project follows this approach. The most important element of the project is a centralized multicore computing unit in which the vehicle's essential control functions are implemented, these functions being traction control and power split between battery and supercapacitors in addition to thermal management. The obvious aim, therefore, is the development and implementation of a resource-conserving model predictive controller for all thermal functionalities. On the basis of a specially developed library of cooling and air-conditioning components, a simulation environment for the development and testing of the controller was built. In the process, three different system configurations were explicitly analyzed using a LOTUS Evora 414E in order to reference the controller in compliance with current development trends. The following article introduces the overall project concept before discussing the development of the component models in detail. Afterwards, the simulation of the three reference systems using the example of one of these systems will be described. The development and testing process for the model predictive controller will follow. The article concludes with a summary of the results and an outlook on existing optimization opportunities.

M. Hütter (✉) · W. König
AVL List GMBH, Hans-List-Platz 1, 8020 Graz, Austria
e-mail: matthias.huetter@avl.com

S. Kuitunen
Fraunhofer Institute for Transportation and Infrastructure Systems IVI,
Zeunerstraße 38, 01069 Dresden, Germany

© The Author(s) 2018

D. Watzenig and B. Brandstätter (eds.), *Comprehensive Energy Management - Safe Adaptation, Predictive Control and Thermal Management*, Automotive Engineering: Simulation and Validation Methods, DOI 10.1007/978-3-319-57445-5_5

Keywords Thermal management system · Model predictive control · MPC · HVAC

5.1 Introduction

Full electric vehicles showing an increased challenge in terms of the Vehicle Thermal Management System (VTMS) to cover two main parts. First an increased challenge in power efficient operating strategies for the cooling system of the powertrain as well for the HVAC (Heating Ventilation and Air Conditioning) system of the passenger cabin to reduce the impact on reduction of autonomic range. Additionally the VTMS has to consider the small optimal temperature range of the high voltage traction battery.

Based on these boundary conditions a holistic approach for the development and for the operating strategy of the VTMS controller is required. This demand could be satisfied by model based development to optimize the usage of available heat sinks and sources and to implement model predictive control algorithm which allow to consider the thermal request of the components as well in future based on given driving profiles.

Therefore the article deals with all aspects of the VTMS control development based on the Lotus Evora 414E:

- Setup of VTMS concepts with VTMS model library to defined the most appropriate topology for specific vehicle requirements
- Layout of holistic thermal manager to cover all thermal requirements of the powertrain and the passenger cabin
- Introduction of model predictive approaches to minimize energy consumption of the VTMS based on defined driving profiles
- Comparison of model predictive and conventional control approaches for battery cooling.

5.2 Component Library for VTMS Simulation

In a first step a modular simulation library was built up in MATLAB/Simulink to be able to assemble and simulate different thermal systems. Figure 5.1 gives a summary of all developed components. The simulation is generally based on characteristic maps, chemical media data, mass-and energy balances. The “in” and “out” connectors refer always to mass fluxes of air or liquid including their state variables such as temperature, pressure, moisture and mass flow. Within the different components the change of the state variables is determined, e.g. the temperature of a water mass flow going through a PTC-heater (heat source) will rise, while at the same time the PTC-heater will cause a pressure drop. Additionally the heat capacities of relevant components (heat source, heat exchanger and cabin) and their influence on the thermal inertia of the thermal system are taken into account.

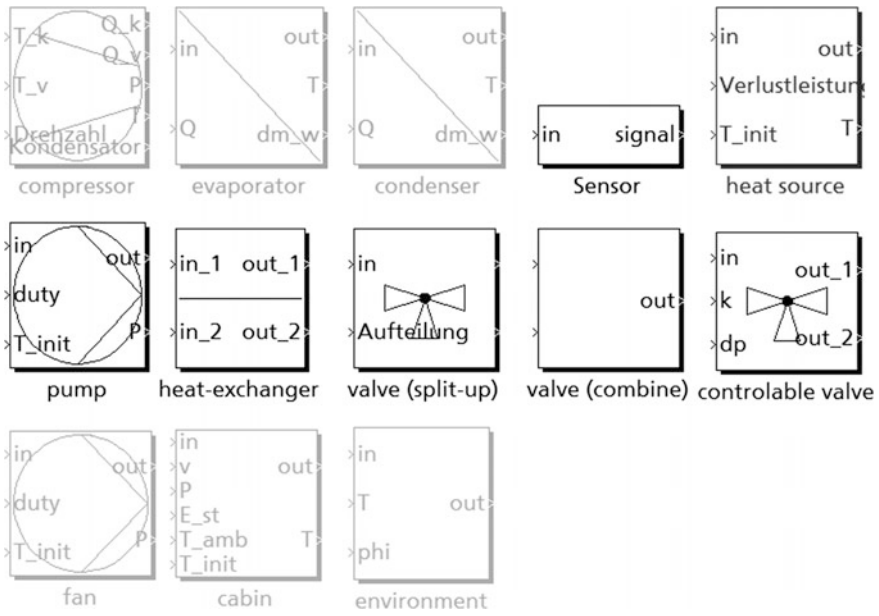

Fig. 5.1 Modular HVAC simulation library

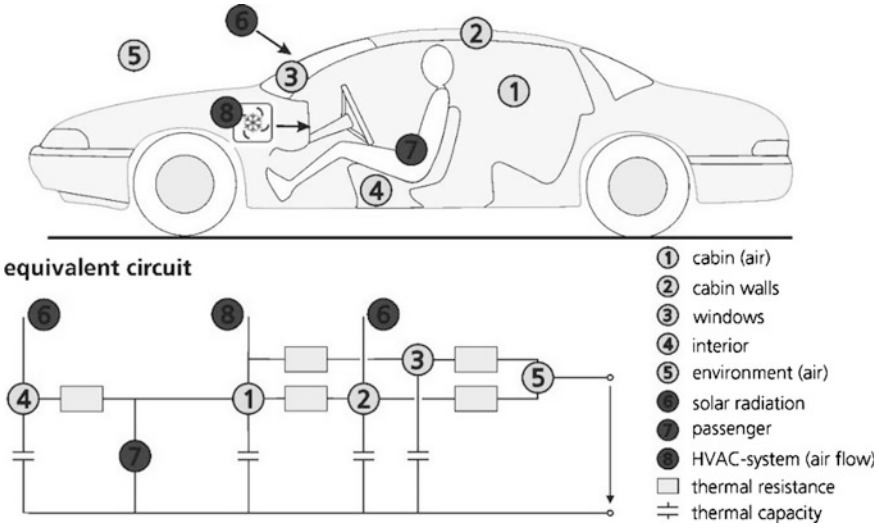

Fig. 5.2 Cabin model scheme

Figure 5.2 displays the scheme of the cabin and the corresponding equivalent circuit. The equivalent circuit illustrates the different heat capacities (air, cabin walls, windows, interior, environment) and the heat sources (solar radiation,

passenger, HVAC system) and the relations between them in the form of thermal resistances. The implementation in Simulink is based on the resulting energy balances.

5.3 HVAC-System Model

Based on the component library three different HVAC system models (1—conventional, 2—with waste recovery, 3—with heat pump) for the Lotus Evora have been realized in Simulink. During the course of the project HVAC system 2 has been selected for the development of the model predictive thermal management. The corresponding layout scheme of the cooling and refrigerant circuit is displayed in Fig. 5.3a. The heating of the battery and the cabin is conducted by dedicated PTC-heaters. Additionally the waste heat of the power electronics can be utilized with the help of a heat-exchanger (CH) to support the cabin heating.

The two evaporators can be used as well in single as in parallel mode. In this way the cabin and the battery can be cooled not only with ambient air but also independent from each other with the vehicles refrigerant circuit. Through the utilization of valves and a second pump, the coolant circuit can be split up into two separate circuits, so that the battery can be cooled (refrigerant circuit) and heated (PTC-heater) independently from the power electronics. However the cooling of the battery with ambient air requires its integration into the power electronic cooling circuit.

Figure 5.3b shows the realization of the HVAC system model with waste heat recovery in Simulink including the cooling circuits for the battery and the power electronics and the AC system of the cabin. Furthermore the system model features a dynamic characteristic curve for the main fan, which considers the combined influence of the vehicle speed and the fan revolution speed on the air flow rate, which ensures the removal of heat at the condenser and the heat-exchanger.

The HVAC system model can be integrated into the vehicle model due the included interface. Because a standalone mode was required during the development phase of the HVAC system model all controllable components can optional be controlled by internal PT1 based controllers.

The components and system model have been iteratively parameterized and validated by taking into account reference data for transient heating and cooling scenarios. Afterwards functional simulation tests have been conducted for the system models by utilizing the internal controls and different model configurations to consider the various heating and cooling options for the battery, power electronics and the cabin. The prepared system model will be further used as starting point for the development of the model predictive thermal management.

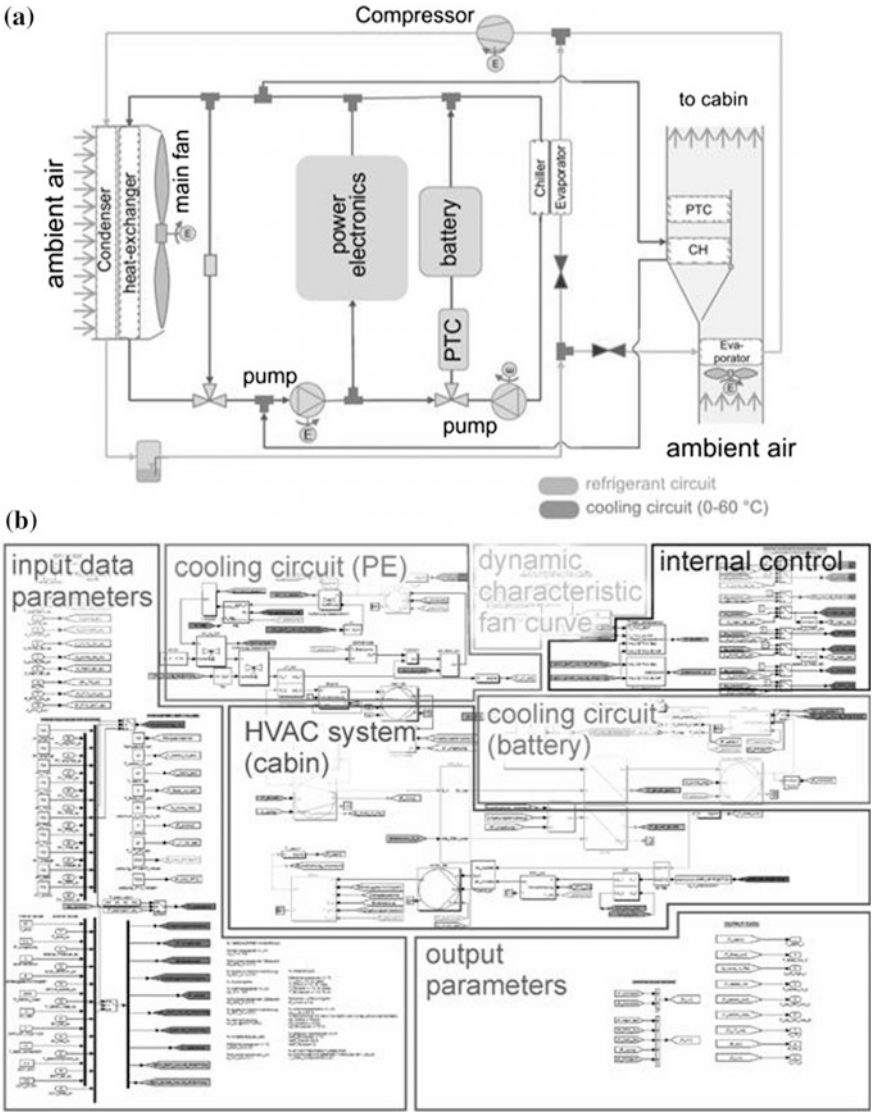

Fig. 5.3 Scheme HVAC system model 2 with waste heat recovery (**a**) and corresponding Simulink model (**b**)

5.4 Thermal Management

The main objective for the thermal management is to ensure that all components are operating within optimal temperature limits. In case of the power electronics as the e-motor, inverter and capacitors, the thermal management has to ensure that the

component temperature does not exceed a certain limit. In case of the battery a lower limit must be considered as well, since the internal resistance of the battery increases significantly at low temperature which leads to a reduction of available electrical capacity and power. Additionally the battery cell might be damaged significantly while being charged at low temperatures due to lithium plating effects. A holistic thermal management has to consider the thermal request of the cabin as well.

The second objective of the thermal management is to keep the demand of power for auxiliaries as low as possible. Therefore, a well-structured approach for the control layout is required to ensure that auxiliaries with low energy consumption reach the limits before a component with a higher energy demand is activated.

5.5 Thermal Management Controller

The input of the "Thermal Management Controller" (Fig. 5.4) includes predictive data from the cloud and measurement data from the car. Based on this data a thermal request is generated in the "Thermal Request Generator". That can be a cooling as well a heating request. With this request, the "Thermal Mode Selection" activates a defined thermal mode for each cooling circuit. The "Component Controller" includes controller for each component, which were used to define the final output for the actuators as pumps, fans for every thermal mode.

5.5.1 Thermal Request Generator

In the "Thermal Request Generator", the physical or virtual inputs are used to evaluate the thermal requirement for each circuit. Figure 5.5 shows the definition of the thermal requirements for the power-electronics (electric motor, inverter, DCDC, capacitors), the battery and the HVAC system. The less critical power electronics have only two different cooling requests (low or high cooling) since this

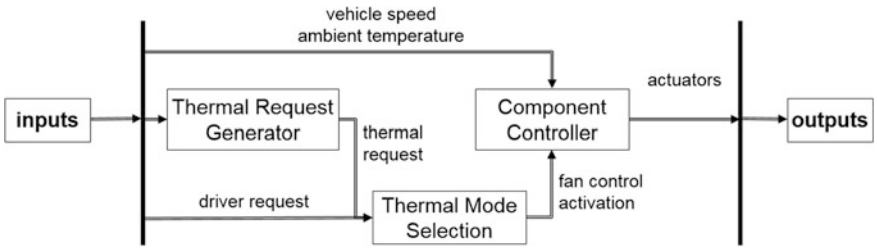

Fig. 5.4 Architecture of the thermal management controller [1]

EC thermal request	Low PE cooling request	High PE cooling request
Condition	PET<80°C±2K	Default

Battery thermal request	Battery warm-up request	No battery cooling request	Low battery cooling request	High battery cooling request
Condition	CellT_min<2°C±2K AND CellT_max<20°C±2K	CellT_max<30°C±2K	CellT_max<40°C±2K	Default

HVAC thermal request	Cabin cooling request	Cabin dehumidification request	Cabin heating request
Condition	CabinT>20°C±2K	CabinT>15°C±2K AND AmbT > 20°C±2K	Default

Fig. 5.5 Thermal request generator for the electric components (EC), the battery and the HVAC system

components do not require any heating. The battery is much more critical regarding the optimal temperature level. Therefore more thermal request states are used. For the HVAC system three different request states are defined, since the cabin requires heating, dehumidification of air and cooling.

5.5.2 *Thermal Mode Selection*

The next step is the definition of the thermal function within the "Thermal Mode Selection" using information of thermal request of each circuit.

The next step is the definition of the thermal function within the thermal mode selector using information of thermal request of each circuit. Figure 5.6 shows the thermal modes of the power electronics and for the battery. The specific mode will be defined based on information of the thermal request generator.

5.5.3 *Component Controller*

The last part of the thermal controller is the "Component Controller". In this part controllers for all components are defined for each thermal function and can contain a simple constant value, a map based controller or even a model based control functionality (Fig. 5.7).

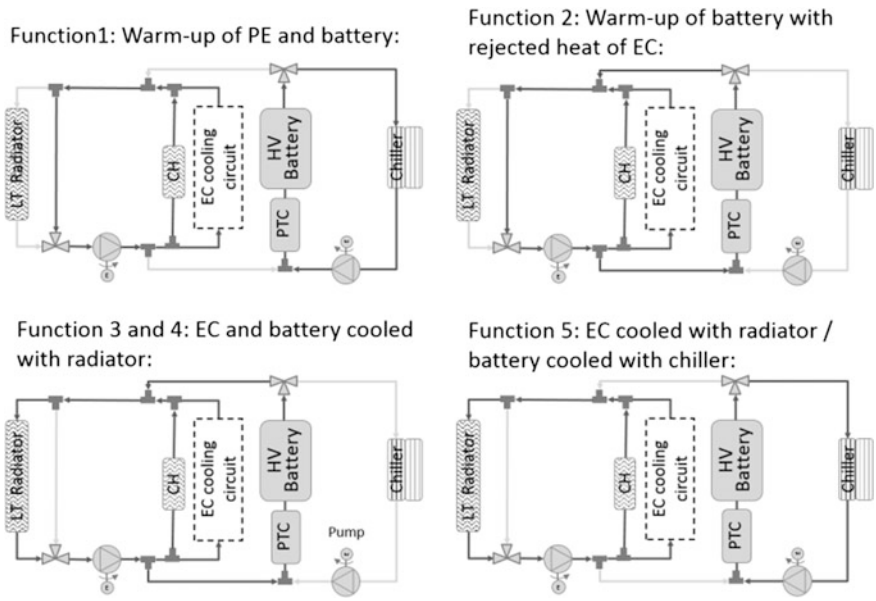

Fig. 5.6 Thermal function for cooling system of electric components and of the battery

	Function 1 Warm-up of PE and battery	**Function 2** Warm-up of battery with rejected heat of PE	**Function 3** PE and battery cooled with radiator, fan off	**Function 4** PE and battery cooled with radiator, fan on	**Function 5** PE cooled with radiator Battery cooled with chiller
n_LT_ECP	10%	100%	controllable	100%	controllable
n_bat_ECP	100%	off	off	off	100%
SOV_chiller	closed	closed	closed	closed	opened
SV_bat	A-AB	B-AB	B-AB	B-AB	A-AB
n_comp_bat	0%	0%	0%	0%	controllable
n_fan_LT	off	off	off	controllable	controllable
PTC_bat	controllable	off	off	off	off

Fig. 5.7 Component controller setting for thermal functions for PE and battery

5.6 Predictive Calculation

For the battery a model based approach will be used to get the battery temperature as a function of time to predict the warm up based on the information of the driving cycle. Figure 5.8 shows a simplified model of the cooling mode: “Cooling via LT radiator”.

Based on the simplified physical model a continuous state model with following shape can be generated.

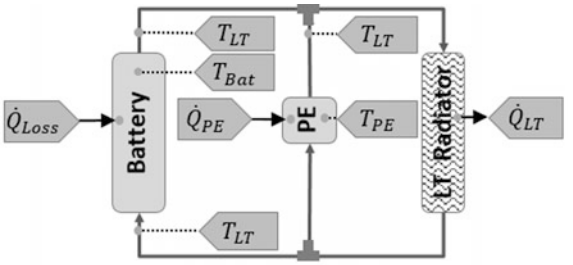

Fig. 5.8 Simplified cooling system of battery for thermal concept with waste heat recovery to calculate the warm up of the battery as function of the battery power

$$\dot{T}_{Bat} = \frac{\dot{Q}_{loss}}{C_B} - \frac{\mathrm{k}A_B(T_{Bat} - T_{LT})}{C_B}$$

$$\dot{T}_{PE} = \frac{\dot{Q}_{PE}}{C_{PE}} - \frac{\mathrm{k}A_{PE}(T_{PE} - T_{LT})}{C_{PE}}$$

$$\dot{T}_{LT} = \frac{\mathrm{k}A_B(T_{Bat} - T_{LT})}{C_{LT}} + \frac{\mathrm{k}A_{PE}(T_{PE} - T_{LT})}{C_{LT}} - \frac{\dot{Q}_{LT}}{C_{LT}}$$

$$\dot{Q}_{LT} = f(\dot{m}_a, T_a, \dot{m}_c, T_c)$$

$$\dot{\boldsymbol{x}}(t) = \boldsymbol{A}\boldsymbol{x}(t) + \boldsymbol{B}\boldsymbol{u}(t)$$

where $\dot{\boldsymbol{x}}(t)$ represents the derivative of the state vector and $\boldsymbol{u}(t)$ the required input for the model. The matrix $\boldsymbol{A}$ and $\boldsymbol{B}$ contain constant parameter as the heat transfer coefficients and the thermal capacities.

The cooling with radiator can be described with following linear system of differential equation. To predict the battery and the chiller temperature, the evaporation temperature of the AC system and the rejected heat of the battery is required for the entire predicted horizon.

$$\dot{\boldsymbol{x}}(t) = \begin{bmatrix} -\frac{kA_B}{C_B} & 0 & \frac{kA_B}{C_B} \\ 0 & \frac{kA_{PE}}{C_{PE}} & \frac{kA_{PE}}{C_{PE}} \\ \frac{kA_B}{C_{LT}} & \frac{kA_{PE}}{C_{LT}} & -\frac{(kA_B + kA_{PE})}{C_{LT}} \end{bmatrix} \begin{bmatrix} T_{Bat} \\ T_{PE} \\ T_{LT} \end{bmatrix} + \begin{bmatrix} \frac{1}{C_B} & 0 & 0 \\ 0 & \frac{1}{C_{PE}} & 0 \\ 0 & 0 & \frac{1}{C_{LT}} \end{bmatrix} \begin{bmatrix} \dot{Q}_{loss} \\ \dot{Q}_{PE} \\ \dot{Q}_{LT} \end{bmatrix}$$

To predict the temperature of the battery, the power electronics and the LT radiator, the rejected heat of the battery, the rejected heat of the power electronics (inverter and e-motor) and the rejected heat of the LT radiator is required.

5.6.1 Evaluation of the Predictive Calculation

To evaluate the predictive calculation, the predictive temperature was compared with the battery temperature based on the continuous-time vehicle model. As seen

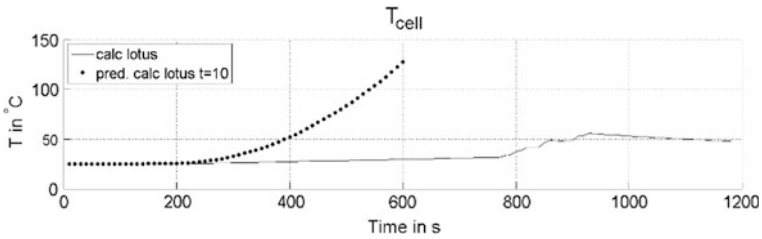

Fig. 5.9 Temperature and prediction at t = 10 s

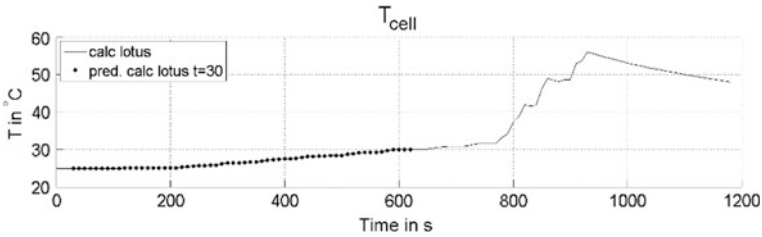

Fig. 5.10 Temperature and prediction at t = 30 s

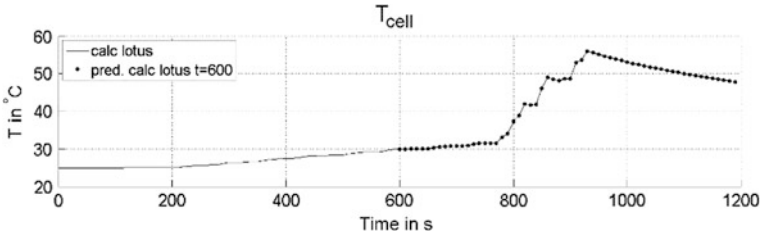

Fig. 5.11 Temperature and prediction at t = 30 s

in Fig. 5.9, the predictive battery temperature shows a strong deviation from the actual course, based on the continuous-time vehicle model, after the first time step (t = 10 s).

Already after 3 time steps, (t = 30 s) (Fig. 5.10) the predicted temperature fits well to the results generated with the physical battery model.

Figure 5.11 shows that the predictive calculation then corresponds well with the continuous-time simulation model to the end of the test cycle.

5.7 Realization in MATLAB/Simulink

The thermal management controller is implemented in MATLAB/Simulink (Fig. 5.12) and extended by the "Input Control" block (Fig. 5.13). There, the battery temperature is predicted according to the selected prediction horizon of 10 min and passed to the "Thermal Mode Selection".

The predictive calculations carried out as described in Sect. 5.6 Predictive Calculation. The need for the calculation of heat loss performance of the battery and the power electronics is supplied by the control unit. The thermal dissipation loss of the LT radiator is calculated with a lookup table. For this purpose, the ambient temperature and the vehicle speed over the entire prediction horizon is needed.

5.7.1 Comparison Predictive Control and Conventional Control Using Lotus Cycle

The threshold value for the conventional control was set to 30 °C and compared to the model predictive control. Since the MPC switches earlier from Function 4 to Function 5 in this case, the maximum battery temperature is lower than that of the

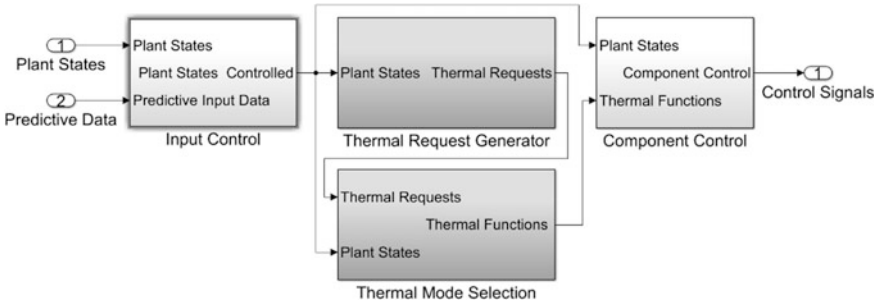

Fig. 5.12 Thermal management controller in MATLAB/Simulink

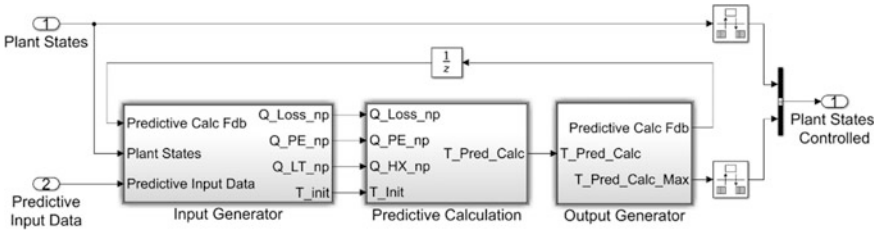

Fig. 5.13 Input control with predictive calculation

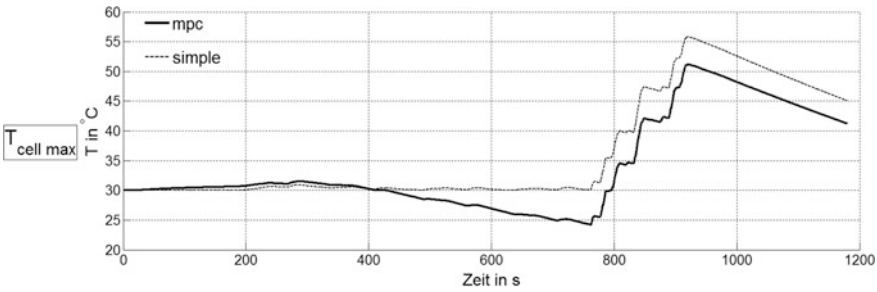

Fig. 5.14 Maximum cell temperature, Lotus cycle, MPC, simple control 30 °C

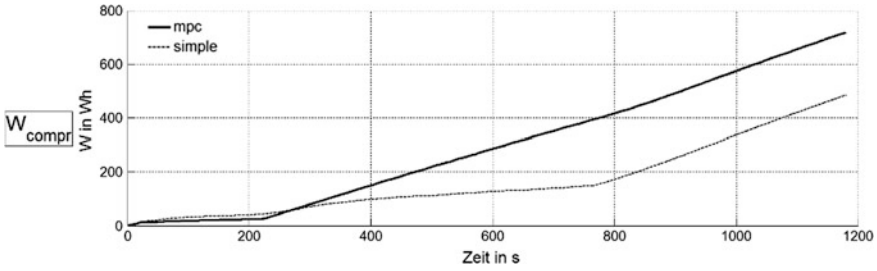

Fig. 5.15 Energy consumption compressor, Lotus cycle, MPC, simple control 30 °C

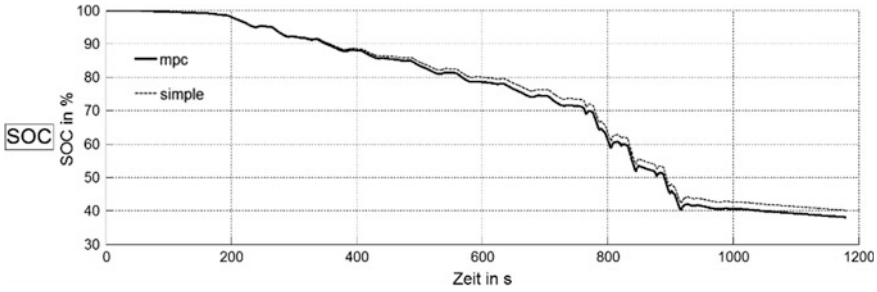

Fig. 5.16 SOC, Lotus cycle, MPC, simple control 30 °C

simple control (Fig. 5.14). In Fig. 5.15 it can be seen that the energy consumption of the compressor of the model predictive control is higher. This leads to a lower SOC at the end of the test cycle (Fig. 5.16). Then increased power demand of the MPC controller is not significant compared to the high power demand of the powertrain for the Lotus cycle.

If the conventional control should not exceed the limits for the cell temperature, the threshold value for the conventional control must be set to 20 °C (Fig. 5.17).

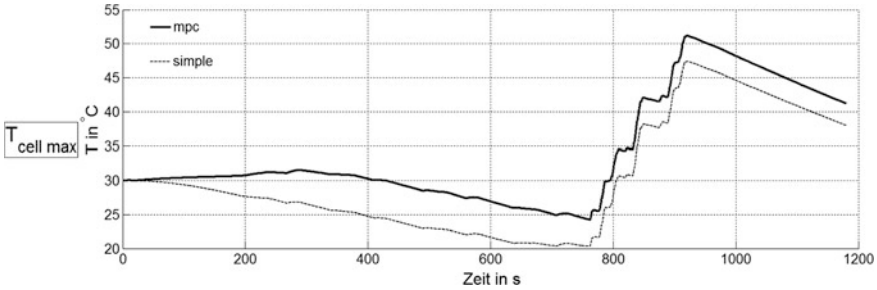

Fig. 5.17 Maximum cell temperature, Lotus cycle, MPC, simple control 20 °C

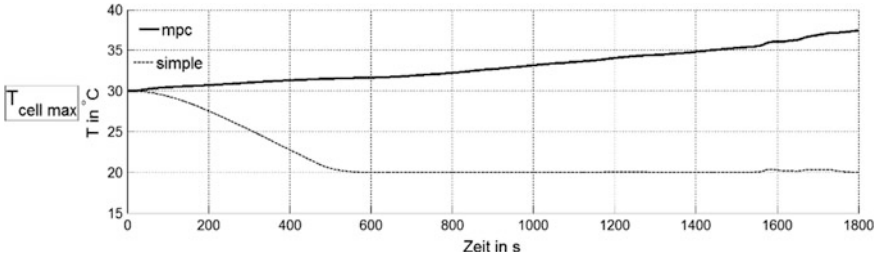

Fig. 5.18 Maximum cell temperature, WLTC, MPC, simple control 20 °C

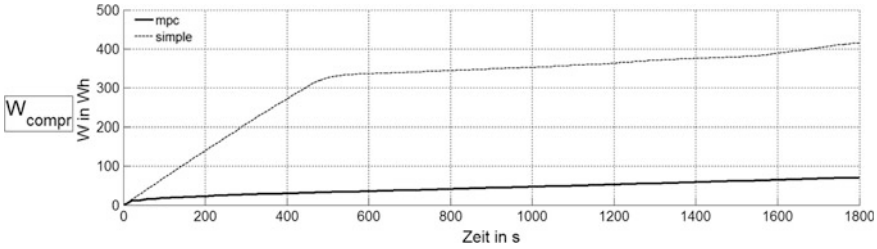

Fig. 5.19 Energy consumption compressor, WLTC, MPC, simple control 20 °C

5.7.2 Comparison Predictive Control and Conventional Control Using WLTC Cycle

Figure 5.18 shows the result for the maximum cell temperature of the battery for the conventional (simple) with a threshold value of 20 °C and model predictive control (mpc) simulating the WLTC. During the simple controller keeps the cell temperature at constant 20 °C, the MPC does not activate Function 5 (cooling with refrigerant compressor) because the predicted battery temperature never exceeds the set limit of 50 °C in this cycle. The energy consumption of the compressor is formed exclusively by the cabin cooling and, in comparison to the simple control, over 300 Wh (Fig. 5.19) can be saved (Fig. 5.20).

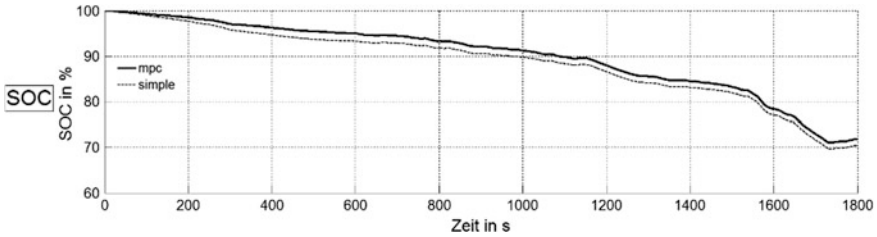

Fig. 5.20 SOC, WLTC, MPC, simple control 20 °C

5.8 Conclusions

The MATLAB/Simulink library of IVI allows to model the entire thermal system of the vehicle and has been integrated into a holistic vehicle model to evaluate the thermal management strategy together with the DMES (Dual Mode Energy Storage).

A thermal management control architecture has been worked out, which allows to develop a holistic thermal management strategy taking all thermal relevant subsystems of the vehicle into account (cooling of powertrain, thermal conditioning of battery and cabin).

A model based approach is used to predict the maximum cell temperature of the battery within a time horizon of 10 min. This approach allows on the one hand an efficient control for low performance cycles and on the other hand a reduction of the maximum cell temperature for high performance cycles.

Acknowledgements The research work of the authors has been partially funded by the European Commission within the project Integrated Control of Multiple-Motor and Multiple-Storage Fully Electric Vehicles (iCOMPOSE) under the Seventh Framework Programme grant agreement №. 608897.

Reference

1. Traussnig AA, Waltenberger M, Klima B, Ennemoser A (2013) Konzeptbewertung und Auslegung der thermischen Betriebsstrategie in einem HEV.—in: 2. VDI-Konferenz "Thermomanagement für elektromotorisch angetriebene PKW". Stuttgart am: 03.12.2013

Chapter 6
Heat Pump Air Conditioning Systems for Optimized Energy Demand of Electric Vehicles

Benedikt Rabl

Abstract The air conditioning system of a passenger car causes significant power consumption. For hybrid and electric vehicles the power consumption for heating of the cabin and windshield (defrosting, defogging) at low ambient temperatures in particular plays an important role, considering that there is only little or no waste heat available. Electric heating of the cabin air drastically reduces the driving range. Additionally, in case of electric vehicles there may be a demand for cooling of the traction battery at high ambient temperatures while in contrary the waste heat of the power electronics could be used for cabin heating at low ambient temperatures if its temperature level is raised by means of a heat pump. This chapter illustrates strategies for the transition of a conventional heating, ventilation and air conditioning (HVAC) system for fuel based vehicles to a more appropriate one for highly electrified vehicles from the standpoint of an effective reduction of energy consumption. The benefits of implementing heat pump technology into the traditional air conditioning system are shown in contrast to systems utilizing electric air heating and a proposition of a vehicles' thermal management system is given, integrating the air conditioning system into an overall vehicle cooling and heating system for an even further reduction of energy consumption. The chapter is complemented with a comparison of two HVAC system topologies regarding their overall annual energy demand for air conditioning and highlighting the implication of heat pump technology from this point of view.

Keywords Electric vehicle · Heat pump · Air conditioning · Energy optimization

Nomenclature

A/C	Air conditioning
air	Concerning cabin air-side
amb	Ambient
COP	Coefficient of performance (6.1)

B. Rabl (✉)
Virtual Vehicle Research Center, Inffeldgasse 21/A, 8010 Graz, Austria
e-mail: Benedikt.rabl@avl.com

© The Author(s) 2018

D. Watzenig and B. Brandstätter (eds.), *Comprehensive Energy Management - Safe Adaptation, Predictive Control and Thermal Management*, Automotive Engineering: Simulation and Validation Methods, DOI 10.1007/978-3-319-57445-5_6

el	Electric
EV	Electric vehicle
EXV	Electronic expansion valve
h	Specific enthalpy ($Jkg^{-1}K^{-1}$)
HP	Heat pump
HT	High-temperature
HVAC	Heating, ventilation and air conditioning
lat	Latent
LT	Low-temperature
MT	Mid-temperature
PHX	Plate heat exchanger
P	Power (W)
$\dot{Q}$	Cooling or heating capacity (W)
r.h.	Relative humidity (%)
sens	Sensible
TXV	Thermostatic expansion valve

6.1 Introduction

A passenger car's air conditioning system is not only a question of comfort but also of safety and energy consumption. Especially for electric vehicles the air conditioning poses a major trade off between comfort and driving range. With driving range being one of the main criteria for customer acceptance of electric vehicles the focus is shifted to optimizing the energy efficiency of the air conditioning system and thereby reducing the energy demand for cooling and heating of the passenger cabin. A proper situation to explain the problem is when driving in colder climates for which the heating demand is high in general. Vehicles with a conventional internal combustion engine can tap the engine's waste heat in order to provide the necessary energy for cabin heating, as shown on the left side of Fig. 6.1.

This is not the case for EVs considering the radically reduced waste heat for electric machines. The same situation applies when the HVAC system is operated in dehumidification mode, which actually is not a real mode that can be set on the control panel but that characterizes situations when the A/C is turned to "ON" and air heating is performed to "reheat" the air passing through the evaporator to agreeable temperatures. This is used especially in regions with generally high humidity and mid-temperatures or for transitional season. Also for driving in heavy rain dehumidification may be performed to keep the windscreen free from mist.

For highly electrified vehicles lacking any fuel based heat source the question is raised on how to compensate for the missing waste heat, which is needed for air heating in both before mentioned operating modes. When carrying over a

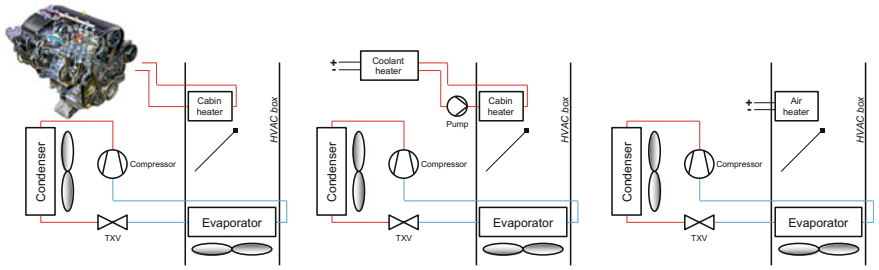

Fig. 6.1 Schematic of a conventional air conditioning system. The cooling circuit of the the internal combustion engine is coupled with the cabin heater (*left*). Schematic of an air conditioning system where the conventional cabin heater is connected to an electric coolant heater (*middle*) or where the cabin heater is replaced with an electric air heater (*right*)

conventional A/C system meant for fuel based vehicles, air heating is in its most simple form accomplished with electric heating elements. These can either be direct air heaters or coolant heaters that connect to the cabin heater via a secondary (coolant) circuit as also shown in Fig. 6.1. Direct air heaters have very low latency, transferring the heating power almost instantaneously to the air, but their heating power is in general restricted to around one kilowatt for automotive use. On the contrary coolant heaters are offered with a considerably higher heating power, which makes them more appropriate for this use than direct air heaters but the secondary circuit exhibits certain delays in heat transfer because of the additional heat capacities introduced by the coolant.

Also, as standard cabin heaters are coolant air heat exchangers in general the latter option would be the one of choice in most cases when pure electrical heating is favored. Concerning the typical use case of a vehicle's A/C system, namely cabin cooling, there is no difference between fuel-based cars, hybrid vehicles or pure electric vehicles in regard to energy consumption. System topologies may differ for sure but the overall system efficiency mainly depends on the single components' efficiencies and the operating strategies. Therefore an approach for the reduction of the overall HVAC system's energy consumption is to find ways to shrink the energy consumption for heating.

6.2 Exploitation of Heat Pump Technology (for xEVs)

Resistance heaters (PTC elements) usually have a coefficient of performance (COP) of about one meaning that there is a one-to-one relationship between electric energy and dissipated heat. The search for more efficient heating solutions for reduction of the energy demand for heating directly leads to heat pump systems, which are known from industrial and residential applications. A heat pump (HP) is a conventional refrigeration circuit like the already discussed A/C system but with

the "benefit" being the heat available at the warm side of the circuit and not the one at the cold side. So *in principle* every air conditioning system installed in a vehicle is already a heat pump but "pumping" the heat from inside the cabin to the outside frontend heat exchanger package so to say to the wrong side of the system when wanting to heat the cabin.

For making this beneficial heat not going lost to the ambient some alterations to the refrigeration circuit and to the whole A/C system have to be done e.g. in the style of Hünemörder [1]. By replacing the cabin heater in the HVAC box with a refrigerant heat exchanger, adding a third heat exchanger to the traditional A/C cycle and by introducing one additional expansion device as shown on the left side of Fig. 6.2, modifications to the overall system are kept minor and an implementation of this topology into existing systems is feasible without further problems.

When operating in A/C mode the system works as every normal air conditioning system does, removing heat from inside the cabin through the evaporator by increasing its temperature level above ambient and rejecting it at the frontend heat exchanger. When the operating mode is changed to heat pump the frontend heat exchanger becomes the system's evaporator, absorbing heat from the ambient which is brought to a higher temperature level by the compressor and rejected into the cabin air at the cabin heater afterwards.

The increase in efficiency gained by implementing heat pump functionality into the A/C system is remarkable in general as seen later on. The coefficients of performance for heating are calculated according to Eq. (6.1) and they depend mainly on the combination of working fluid and operating range regarding temperature of evaporation and condensation. The right side of Fig. 6.2 gives an example on the coefficients of performance of an air source heat pump system for a range of evaporation and condensation temperatures. At extreme operating points, i.e. high condensation temperature and low evaporation temperature the heat pump system may not be beneficial anymore.

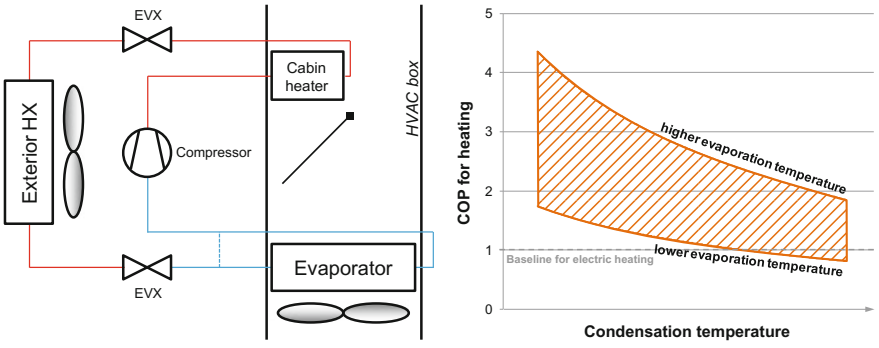

Fig. 6.2 Simple implementation of the heat pump technology into an automotive HVAC system based on Hünemörder [1] (*left*). Example for a range of the COP for heating of air source heat pumps depending on the condensation and evaporation temperature (*right*)

$$COP_{heat,HP} = \frac{\dot{Q}_{heat}}{P_{Compressor}} \tag{6.1}$$

Also regarding the dehumidification operation a big advantage of heat pump systems compared to conventional systems equipped with electric heaters can be shown. Therefore an exemplary dehumidification process is shown in Fig. 6.3. Ambient air of high humidity (Point 1) passes the evaporator and it is cooled below its dew point to a lower temperature (Point 2). This change of state is given by the blue line. Formation of dew or condensate means that the water vapor solved into the air changes its thermodynamic state from gaseous to liquid. Like all phase changes also this one involves a certain amount of latent heat that must be absorbed in addition to the sensible heat by the refrigerant in the evaporator. The latent and sensible enthalpies of cooling are noted in Fig. 6.3 by $\dot{h}_{lat,cool}$ and $\dot{h}_{sens,cool}$. The excess condensate is separated from the system and the air is eventually heated again at the cabin heater to a temperature higher than the one of ambient (Point 3) before entering the vehicle cabin.

Usually for A/C systems the latent heat of condensation is meant to be disadvantageous because it requires additional evaporator capacity and therefore increasing compressor power. Regarding the dehumidification operation, this heat is *lost* when using electric cabin heaters. On the contrary a heat pump system as the one described above can make use of the latent heat from condensation of water

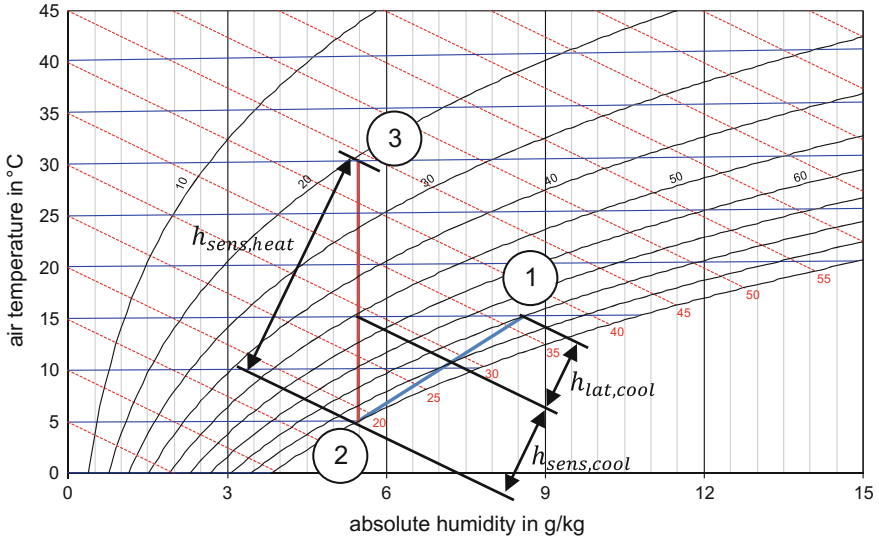

Fig. 6.3 Dehumidification process for ambient air of 15 °C and 80% r.h. being cooled to 5 °C and reheated to 30 °C afterwards. Dehumidification occurs between points 1 and 2 and the enthalpies for cooling can compensate for parts of the enthalpy for heating

vapor in such a way that depending on the operating conditions only little to almost no heat must be absorbed or rejected at the frontend heat exchanger and all the heat from air cooling is passed in total to the cabin air.

Following results are given for an operating case in which reheating is done at ambient conditions being 15 °C and 80% r.h. Three different temperatures for the air exiting the cabin heater were chosen between 20 °C and 40 °C. With $\dot{m}_{air} \cdot h \equiv \dot{Q}_{air}$ and a definition of the coefficient of performance for dehumidification operation according to Eqs. (6.2) and (6.3) (which are considering the benefits of the dehumidification process as the latent heat of condensation plus the difference in sensible air temperature between ambient and outlet of the cabin heater) the impact of using heat pump technology over electrical heating can be drastically illustrated not only for the automotive domain. Equation (6.2) returns the COP of reheat if pure electrical heating is applied and considering a COP of electrical heating with one by stating $P_{el,heat} \equiv \dot{Q}_{sens,heat}$ whereas Eq. (6.3) returns the COP of reheat for heat pump systems.

$$COP_{dehumidification,el} = \frac{\left|\dot{Q}_{sens,heat} - \dot{Q}_{sens,cool}\right| + \dot{Q}_{lat,cool}}{P_{Compressor} + P_{el,heat}} \tag{6.2}$$

$$COP_{dehumidification,HP} = \frac{\left|\dot{Q}_{sens,heat} - \dot{Q}_{sens,cool}\right| + \dot{Q}_{lat,cool}}{P_{Compressor}} \tag{6.3}$$

The difference in efficiency for reheat operation may be even larger compared to the one for heating and it is shown in Fig. 6.4.

These results look quite good on paper but utilization of heat pump technology solely as replacement for electrical heaters is not the answer to everything. Based on the knowledge that a heat pump system with the appropriate topology enables for cooling *and* heating the thoughts on implementing HP functionality into the A/C

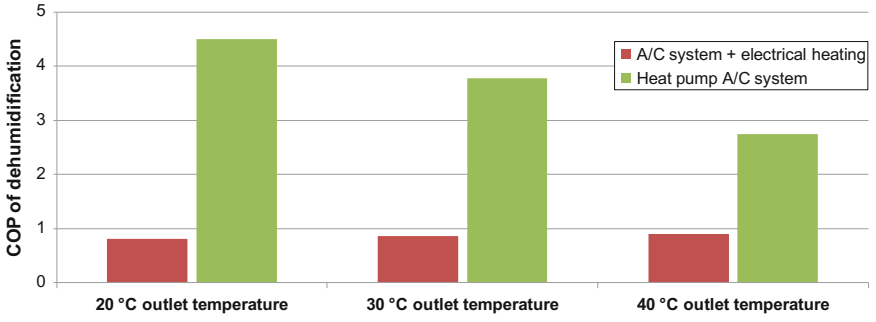

Fig. 6.4 Example of the COP for dehumidification at three different air temperatures at the outlet of the cabin heater for a conventional A/C system with only electric heating compared to an A/C system with heat pump functionality

system can be developed further when it comes to the reduction of the vehicle's overall energy consumption.

6.3 Multi Circuit A/C Systems with Heat Pump Functionality

Long distance travelling capability of electric vehicles is becoming more and more one of the high priority topics amongst OEMs because it is a big deal in customer acceptance as well. One charge of the battery should deliver the same driving range as one gas filling. The "range anxiety" starts to grow into people's heads when they turn on the air conditioning in winter and see the remaining driving distance drop to nowhere. Also, when talking about long distance travelling a higher average driving speed can be assumed in general. Higher speed implies higher propulsion power and therefore increasing electrical loads on the drive train components. Due to the higher heat fluxes in the components their temperatures rise quicker than for urban driving. In contrast to fuel based vehicles an EV has a lot of temperature sensible components like its traction battery, the power electronics, etc. All of these components want to be operated within their own optimal temperature ranges or otherwise control units will start de-rating so temperatures stay within certain limits. Active temperature conditioning of the most crucial components comes to the fore.

This section portrays the HVAC system as an instrument for something more than just comfort requirements. The system shall no longer be viewed as an isolated part of the automobile but as part of the vehicles cooling and heating system instead for which a new and different, also a more elegant "overall thermal management strategy" has to be created. Heat pump technology opens the doors for using not only the ambient air as medium for rejection or absorption of thermal energy but tapping various components inside the vehicle to be used as heat sources and heat sinks. This is accomplished by integration of the refrigerant heat pump cycle into the cooling system. Traditional cooling systems are restricted to ambient temperature as lower boundary for heat dissipation, so the components being cooled will always have a temperature above this one. But what if ambient temperature is outside of the components optimal temperature range, which is a quite common case in summer or winter? Batteries in general don't like cold. They react with decreased capacity (thus reduced driving range) and reduced maximum discharge current, and shortening of lifetime occurs if electrical currents drawn from the battery are too high. On the other side thermal runaway of modern traction batteries has to be avoided in any case. So technically speaking for teasing out the maximum performance of the battery while respecting passenger safety, considerations for cooling and heating of the battery are advisable. The situation is not as critical for the rest of the power train components as in general only thermal overloads need to be prevented for de-rating not to begin.

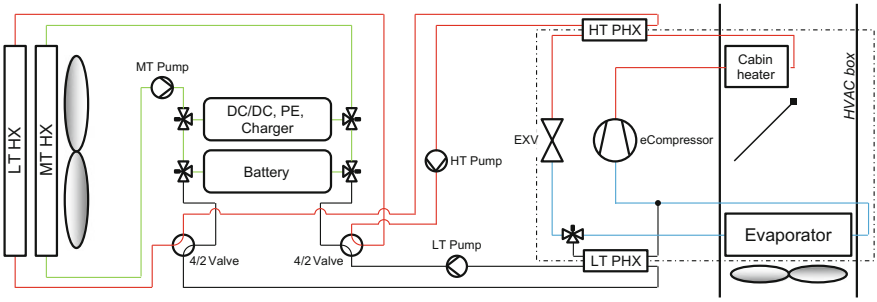

Fig. 6.5 Proposition of a vehicle cooling and heating system incorporating the A/C heat pump cycle into the vehicle's cooling system. Operating mode is set to A/C with the power train components being cooled by the mid-temperature circuit. (Refrigerant cycle indicated by the dot-dashed rectangle, not all components shown for clarity)

With these new requirements cooling system topologies have to be more flexible than the traditional concept of fixed heat sources and sinks within the cooling circuit. Higher flexibility involves more complexity in the systems' topology for sure but it may allow the system to change between source and sink on a per component basis in the ultimate expansion stage. Figure 6.5 gives an example of how such a proposed system topology may look like that is, besides incorporating the air conditioning for cabin climatization, allowing for cooling of all the power train components either passively or actively and additionally allowing for heating of the battery. Only the parts of the system that are relevant for air conditioning are directly implemented into the refrigerant circuit, which is highlighted in Fig. 6.5 by the dot-dashed rectangle.

All other components are connected to the refrigerant cycle by secondary circuits via two plate heat exchangers (PHX), one at the high temperature (HT) side and one at the low temperature (LT) side. The main reasons for doing so are on the one hand that electronics are generally liquid cooled making their integration possible without alterations to existing components and on the other hand that handling and planning of a refrigerant circuit involves higher complexity than of a coolant circuit. Also through this approach the refrigerant circuit can be kept small in size opening the possibilities for some interesting alternative working fluids. Two 4/2-way valves on the coolant side allow for switching between different operating modes, shifting heat sources and heat sinks to the right sides of the system.

In summertime air conditioning may be performed by the conventional refrigerant cycle. The drive train components are either cooled passively with the mid-temperature (MT) coolant circuit or, if ambient temperature exceeds a certain level, actively with the low-temperature (LT) coolant circuit for which the refrigerant cycle must be enabled. When active cooling is required by the thermal strategy but air conditioning is not wanted by the passengers the evaporator for cabin air is bypassed. Also, active cooling of the battery is possible while the rest of the power train components are cooled by the MT cycle yielding for energy

savings. Excessive heat in the refrigerant cycle is rejected at the LT heat exchanger to the ambient.

Heat pump mode in wintertime utilizes the LT heat exchanger as heat source when heating from ambient. If required by the thermal strategy the power train components may be heated in addition to the vehicle's cabin. This feature is of particular interest when considering the preconditioning of the vehicle. Besides climatization of the cabin (defrosting of windscreen and dehumidifying and heating of cabin air) also the battery can be brought to optimal operating conditions, increasing performance as well as driving range. Also in cold ambient conditions the components of the power train may require cooling. In this case the proposed system can tap them as heat sources by means of the heat pump cycle utilizing the dissipated heat for cabin heating. Depending on the amount of dissipated heat and the required heating capacity the system may completely go without ambient air as heat source. This option is advantageous at ambient temperatures below zero to prolong the frosting of the frontend heat exchanger so to keep system efficiency up. *Motor cooling is not limited by low temperatures, efficiency is the better the cooler winding is (temperature dependence of ohmic resistance of temperature). Why not to cool it by antifreezing mixture? The winding is sensitive to steep temperature changes but not to low temperatures themselves.*[1]

To put a number on the increase in efficiency when using heat pump technology in automotive HVAC systems a research project was conducted at the VIRTUAL VEHICLE Research Center. The main interest was to carry over a traditional A/C system known from fuel based cars and do as little alterations to the system for adding heat pump functionality and therefore adapting it to electric drive trains. Based on a cost-only view for series production of such a system one would choose the conventional system with additional electric heating as standard components can easily be adopted for electric vehicles without reducing comfort for the passengers. However turning the focus of attention towards energy consumption changes the situation in favour of alternative systems, cf. Lemke [2].

6.4 Annual Energy Demand of Automotive HVAC Systems

The annual energy consumption analysis is a more descriptive way to justify the selection of a system topology than a plain comparison of efficiencies for certain operating conditions. The energy savings potential can be conveniently represented.

[1] Absolutely correct, motor cooling is not limited by low temperatures, but heat pump efficiency is due to the frosting of the frontend heat exchanger if ambient air is heat source (at temperatures below zero degree celsius the heat exchanger will be blocked by ice in about 15–20 minutes).

So instead of cooling the motor with ambient air (this would be a "waste of waste energy" if the cabin needs to be heated) the motor can be cooled by the heat pump cycle and its waste heat can be harvested for heating purposes.

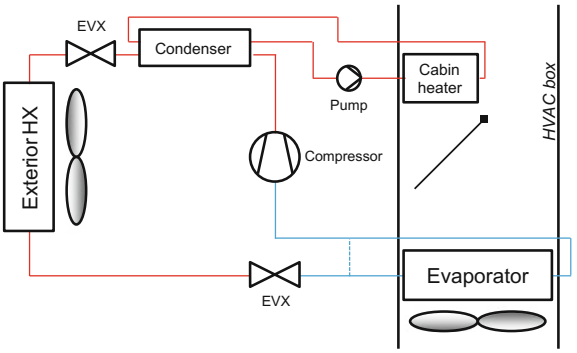

Fig. 6.6 Heat pump air conditioning system considered for calculation of annual energy consumption using a conventional HVAC box with coolant cabin heater

For this study a heat pump system according to Fig. 6.6 was set up on a climatic test bench at the VIRTUAL VEHICLE Research Center. Following Hühnemörder [1] a conventional A/C cycle was complemented with an additional heat exchanger and a second expansion device. The newly introduced HX is a plate heat exchanger that connects to the traditional secondary circuit of the cabin heater. With these little alterations to the A/C cycle it was possible to implement HP functionality on the one hand and to utilize a conventional HVAC box without modifications on the other side. Test bench measurements were conducted to deduce system efficiencies at various ambient conditions in A/C, HP as well as dehumidification mode.

Results for system efficiency were then applied to simulation. The system was coupled with a cabin model for consideration of transient behavior during cool down or heat up and of influence (heat flows) from the environment. The calculation of the overall energy demand of the A/C HP system is done by a method developed from Steiner et al. [3]. In this method the system has to meet boundary conditions regarding air temperature and air mass flows inside the cabin according to DIN 1946-3. Ambient conditions are chosen for the geographically region of interest and they are provided to the simulation on basis of meteorological data, including temperature, relative humidity and solar radiation for every hour of the year. Operating times and modes of the system are deduced from ambient conditions as well as general vehicle driving statistics.

Figure 6.7 depicts the annual energy demand for the heat pump air conditioning system mentioned above in comparison to the same system with only electric heating (as mentioned in the introduction) for three different geographical locations within Europe—Graz, Athens and Helsinki—to cover a broader spectrum of ambient conditions for the analysis.

The advantage in energy savings of the HP A/C system, which a plain comparison of COPs can't depict enough, is clearly visible. Depending on the region a reduction of the overall energy consumption for air conditioning of the passenger compartment of at least 35% compared to the conventional system with pure electric heating is possible. Also remarkable is the energy savings potential in dehumidification mode compared to heating mode for which a reduction in energy consumption of more than 70% can be achieved. Considering the simplicity of the

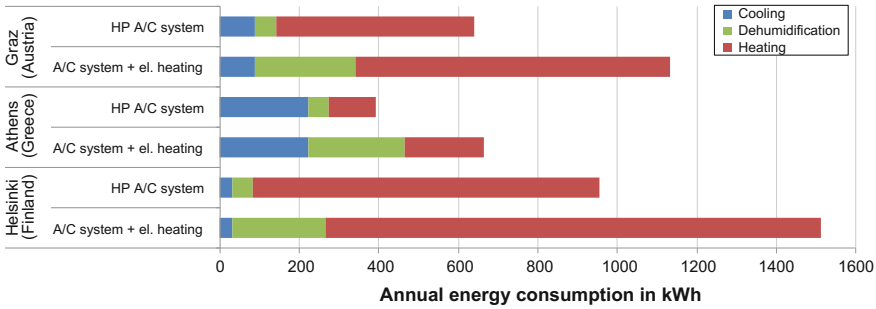

Fig. 6.7 Annual energy demand for air conditioning of a conventional A/C system with only electric air heating in relation to an A/C system with heat pump functionality for different climatic regions

heat pump A/C system in this calculation it stands to reason that more complex systems can achieve even higher energy savings. Bearing in mind that this calculation only covers the energy demand for air conditioning of the vehicle's cabin, figures may change once more in favor of a multi circuit A/C system when considering not only air conditioning but the overall energy demand for cooling and heating of the vehicle.

6.5 Conclusion

When carrying over a conventional A/C system from fuel based vehicles to electrified ones and by replacing the heat source for the cabin heater with an electric heater, heavy losses in travelling distance have to be accepted in case of high heating demands. With only minor modifications to the refrigeration cycle heat pump functionality can be added to the system, leading to drastic improvements in system efficiency whenever heating is required.

Combining the heat pump air conditioning system with parts of the vehicle's thermal management system would lead to a superior cooling and heating system integrating the coolant circuits and the refrigerant cycle into one unit. Depending on the topology of such a system it would be possible to use different components of the vehicle, e.g. the traction battery or the power electronics as additional heat sources besides ambient air or even as heat sinks. With a proper thermal management strategy considering both, passenger comfort and thermal management of the power train components, major advantages can be drawn from such a system by shifting thermal loads between cabin, components and ambient minimizing heat dissipation to the ambient.

A study conducted at the VIRTUAL VEHICLE Research Center suggests that an implementation of heat pump functionality into the air conditioning system

could lead to a reduced energy consumption for air conditioning of at least 35% compared to a traditional air conditioning systems with pure electric air heating, however the results strongly depend on the system topology and on the heating demand. For climates with only little need for cabin heating other system topologies may be more advantageous.

Future trends will not only have to consider systems design but also control strategies for such systems, as heat flows in the whole vehicle have to be directed to the right places at the right times. Predictive controllers will manage to improve overall energy consumption by estimating these heat flows before they occur and by taking the right measures in systems control. Also the integration of heat storing materials (phase change materials) will contribute to a further increase in energy efficiency. Such materials allow for load equalization by storing heat (either warm or cold) at certain times and releasing it whenever needed. Concerning the passenger cabin, future improvements could be a better insulation of the cabin, not only for a reduction in heating and cooling capacities but also for comfort reasons.

Future—using heat accumulators (molten wax?). Better thermal insulation of cabin and windshield? De-frosting and de-fogging is not important during preconditioning phase only but during the whole trip, especially if more passengers use the car.

Acknowledgements This work was accomplished at the VIRTUAL VEHICLE Research Center in Graz, Austria. The authors would like to acknowledge the financial support of the COMET K2—Competence Centers for Excellent Technologies Programme of the Austrian Federal Ministry for Transport, Innovation and Technology (bmvit), the Austrian Federal Ministry of Science, Research and Economy (bmwfw), the Austrian Research Promotion Agency (FFG), the Province of Styria and the Styrian Business Promotion Agency (SFG).

They would furthermore like to express their thanks to their supporting industrial and scientific project partners, namely AVL List GmbH and to Graz University of Technology.

References

1. Hünemörder W (2004) Elektrisch betriebene Wärmepumpe für Fahrzeuge mit dem Kältemittel R744 (CO_2). TWK Symposium Standklimatisierung und Wärmepumpenheizungen im KFZ 2004
2. Lemke N (2010) E-Kfz-Klimatisierung unter verschiedenen Klimabedingungen – Simulation und energetische Betrachtung. Kfz-Klimatisierung bei elektrischer Mobilität, Karlsruhe, 2010
3. Steiner A, Graz M, Rieberer R (2010) Hocheffizientes Kühl- und Heizsystem für Elektro- und Hybridfahrzeuge basierend auf dem umweltfreundlichen Kältemittel CO_2 (R744)

Chapter 7
Thermal Management of PEM Fuel Cells in Electric Vehicles

Michael Nöst, Christian Doppler, Manfred Klell and Alexander Trattner

Abstract The increasing number of fuel cell electric vehicles (FCEV) on the roads will considerably contribute to CO_2 emission reduction and reduction of harmful air pollutants of the transport sector. FCEVs are seen as the future "long distance" and "all purpose" alternative to existing pure battery electric vehicles. The general objective in the FC development is to significantly reduce the costs and system degradation in order to increase the market penetration of FC vehicles. In addition to that, a critical issue represents an adequate thermal management and demand oriented cooling of FCEVs to avoid safety issues, degradation and a decrease in efficiency during operation. Proton exchange membrane fuel cell (PEMFC) can only tolerate a small temperature variation. Two factors are critical when designing a cooling system for PEMFCs. Firstly, the nominal operating temperature of a PEMFC is limited to roughly 80 °C. This means that the driving force for heat rejection is far less than in an internal combustion engine. Secondly, nearly the entire waste heat load must be removed by an ancillary cooling system because the exhaust streams contribute little to the heat removal. Several technical research publications and patents regarding effective cooling strategies are reviewed in this chapter. In the beginning, the thermodynamic characteristics of the heat generation and cooling requirements in a PEMFC stack are discussed. This is followed by outlined advantages, challenges and progresses of various cooling techniques with focus on liquid cooling. Finally, further research needs in this area are presented.

M. Nöst (✉)
IESTA—Institute of Advanced Energy Systems & Transport Applications, 8010 Graz, Austria
e-mail: michael.noest@iesta.at

M. Nöst · C. Doppler
Virtual Vehicle Research Center, Inffeldgasse 21/a, 8010 Graz, Austria

M. Klell
Graz University of Technology, 8010 Graz, Austria

M. Klell · A. Trattner
HyCentA Research GmbH, Inffeldgasse 15, 8010 Graz, Austria

© The Author(s) 2018

D. Watzenig and B. Brandstätter (eds.), *Comprehensive Energy Management - Safe Adaptation, Predictive Control and Thermal Management*, Automotive Engineering: Simulation and Validation Methods, DOI 10.1007/978-3-319-57445-5_7

Keywords PEMFC cooling system · PEMFC cooling strategies · Fuel cell thermal management

Nomenclature

BoP	Balance of Plant (Auxiliaries)
FC	Fuel Cell
GDL	Gas Diffusion Layer
HT	High Temperature
HX	Heat Exchanger
LT	Low Temperature
RDE	Real Driving Emission
PEM	Protone Exchange Membrane
ICE	Internal Combustion Engine
H_2	Hydrogen
FCEV	Fuel Cell Electric Vehicle
EV	Electric Vehicle
HVAC	Heating Ventilation and Air Conditioning
PEMFC	Proton Exchange Membrane Fuel Cell

7.1 Introduction

The major challenges for future road transport and therefore the global automotive industry are (i) Enabling individual mobility, (ii) Reduction of the energy consumption and (iii) Decarbonisation. To meet these challenges, electric vehicles with battery and fuel cell technology will be the key enabler. Pure battery electric vehicles are suitable for smaller vehicles and short ranges (urban) whereas fuel cells are more appropriate for larger vehicles with longer ranges and higher power demand. This review focuses on the cooling requirements and techniques of proton exchange membrane fuel cells (PEMFC) for automotive applications.

A PEM fuel cell produces waste heat which amounts to slightly less than its electric power output, thus leading to an energy efficiency of about 60%. Moreover, PEM fuel cells can only tolerate a small temperature variation. Current PEM fuel cells operate in the temperature range of 60–80 °C.

Two factors are critical when designing a cooling system for PEM fuel cells. Firstly, the nominal operating temperature of a PEMFC is limited to roughly 80 °C. This means that the driving force for heat rejection is far less than in an internal combustion engine. Secondly, nearly the entire waste heat load must be removed by an ancillary cooling system because the exhaust streams contribute little to the heat removal. These two factors necessitate relatively large radiators in automotive fuel cell systems. Furthermore, providing space for the radiators and the associated air

handling ducts represents a significant design challenge. Up to 50% of the delivered energy must be released via the cooling circuit [1].

The heat management system must be designed in a well targeted manner that keeps the stack cool via a system as small and light as possible.

With the advantages of high power density, rapid startup and low operating temperature, the PEMFC is considered to be the most promising candidate for the next generation power source for transportation [2]. The development of reliable, efficient and cost-effective FCs will be achieved by radically new and innovative development steps and technologies, especially regarding durability and costs [3]. Although a very high energy conversion efficiency of PEMFCs, a significant amount of heat generated, approx. the same amount of heat than the electrical power output [4] has to be removed to avoid overheating of the critical components, especially the membrane. As mentioned above, the operation temperature range for current PEMFCs is usually from 60 to 80 °C. Higher temperatures could provoke the degradation of the membrane and decrease the performance of the stack [5]. Lower temperatures are not favorable for the reaction kinetics and may also cause flooding due to lower water saturation pressures at lower temperatures, which is a major concern from the water management perspective [6–8].

Reference [9] outlines, that a cooling system design has direct impact in meeting the durability, cost, and performance targets for commercialization.

The present work is aimed at promoting the development of more effective cooling strategies by presenting a critical review of the reported cooling techniques and systems.

This review is sectioned as follows. Firstly, the thermodynamic characteristics of the heat generation and cooling requirements in a PEMFC stack are introduced. Then the advantages, challenges and progress of various cooling techniques with focus on liquid cooling are outlined. Finally, further research needs in this area are presented.

7.2 Functionality of PEMFC

The fuel cell as an electrochemical energy converter is able to directly convert the inner chemical energy of the fuel, usually hydrogen, into electrical energy. Thus the efficiency of the fuel cell is considerably higher than that of the combustion engine, where the conversion of the chemical energy first into heat is limiting the efficiency through the Carnot cycle. On the other hand the chemical processes of the fuel cell demand the use of catalysts and highly pure hydrogen, pressures, temperatures, and humidity have to be controlled within tight limits.

The scheme of a fuel cell is given in Fig. 7.1. Hydrogen is supplied to the anode via the GDL (gas diffusion layer). In an oxidation the hydrogen is split into protons and electrons there using a catalyst. The anode being the negative pole here supplies electrons to an electrical consumer. The protons cross the PEM (proton electrolyte

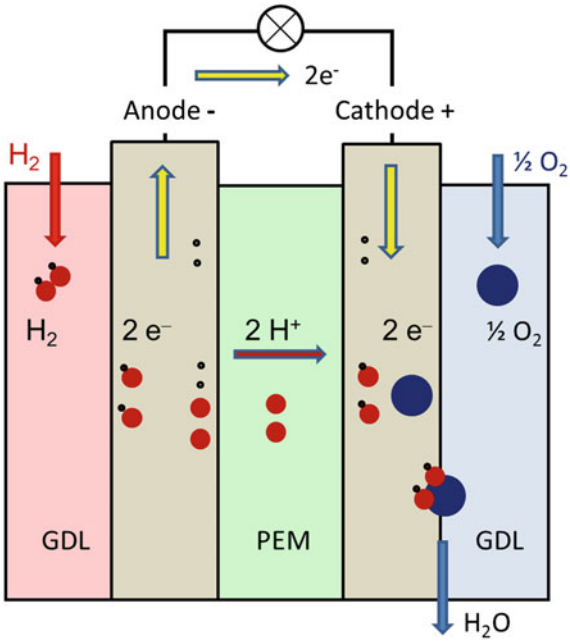

Fig. 7.1 Principle of PEMFC

membrane) to the cathode. There oxygen usually from ambient air is reduced using a catalyst and with the protons yields water.

$$H_2 \rightarrow 2\,H^+ + 2\,e^- \quad 1/2\,O_2 + 2\,H^+ + 2\,e^- \rightarrow H_2O \tag{7.1}$$

Reduction at the Cathode (Plus-pole):

$$1/2\,O_2 + 2\,H^+ + 2\,e^- \rightarrow H_2O, \quad E^{01} = 1.25\ \text{V} \tag{7.2}$$

Oxidation at the Anode (Minus-pole):

$$H_2 \rightarrow 2\,H^+ + 2\,e^-, \quad E^{02} = 0\ \text{V} \tag{7.3}$$

Resulting Redox-Reaction:

$$H_2 + 1/2\,O_2 \rightarrow H_2O, \quad E^0 = E^{01} - E^{02} = 1.25\,\text{V} \tag{7.4}$$

The thermodynamic characteristics of the fuel cell can best be explained using the voltage-current-diagram, see Fig. 7.2.

At standard conditions reaction (7.3) yields a reaction enthalpy of $\Delta_R H^0_m = -241.8$ J/mol_H_2 if the product water remains gaseous (lower calorific value). The negative reaction enthalpy divided by the number of electrons of the

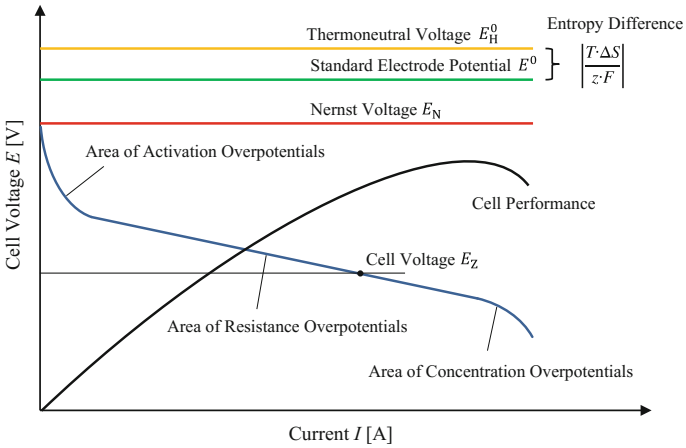

Fig. 7.2 Voltage-current-diagram or polarization curve

reaction z and the Faraday Constant F = 96485.3 C/mol gives the so called thermoneutral voltage $E_H^0 = 1.25$ V. Only the free reaction enthalpy $\Delta_R G_m^0 = \Delta_R H_m^0 - T\Delta_R S_m^0 = -228.6$ J/mol_H_2 can be converted into electrical work, which corresponds to the standard electrode potential E^0 = 1.18 V. The difference $T\Delta_R S_m^0$ quantifies the heat loss to the surroundings. If real temperature and pressure conditions are taken into account, the standard electrode potential E^0 is reduced to the so called Nernst voltage E_N:

$$E_N = E^0 - \frac{R_m \cdot T}{z \cdot F} \cdot \ln \frac{a_{H_2O}}{a_{H_2}\sqrt{a_{O_2}}} \tag{7.5}$$

a is the activity (corresponding to the partial pressure with the ideal gas), R_m = 8.3145 J/mol the ideal gas constant. The theoretical thermodynamic efficiency of the fuel cell is given by:

$$\eta_{th} = \frac{\Delta_R G_m^0}{\Delta_R H_m^0} = 1 - \frac{T\Delta_R S_m^0}{\Delta_R H_m^0} = \frac{E^0}{E_H^0} = 0.945 \tag{7.6}$$

This value of 94.5% thermodynamic efficiency for the PEMFC applies at standard and idle conditions with no current flowing. If a current is applied, the stack voltage is reduced by a number of irreversible losses like the activation over-potential, the resistance over-potential and the concentration over-potential.

Practically the fuel cell is operated in the range of the linear resistance over-potential yielding a cell voltage E_Z.

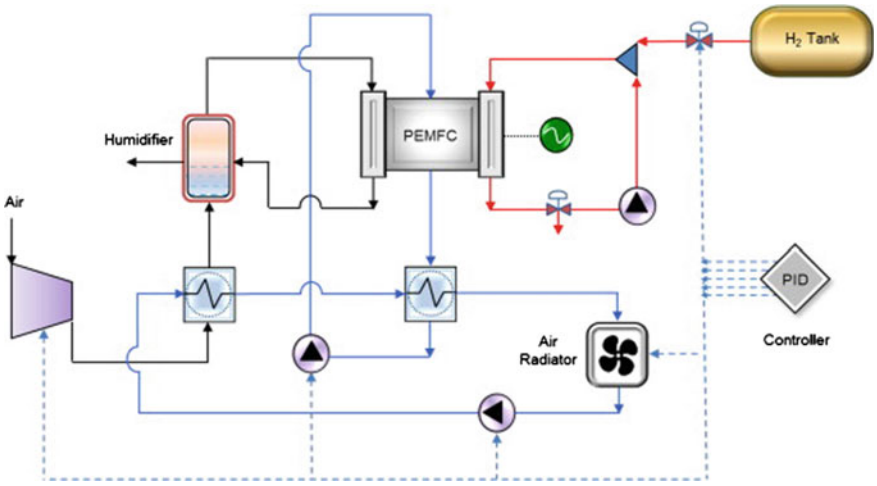

Fig. 7.3 PEMFC system [19]

The practical cell efficiency is given by the relation of the cell voltage E_Z to the thermoneutral voltage E^0:

$$\eta_Z = \frac{E_Z}{E_H^0} \tag{7.7}$$

In practice the efficiency of a single PEMFC can reach values of up to 70% [10]. As the voltage of the fuel cell is limited, a number of cells are combined to form a fuel cell stack. This poses a number of challenges, as pressures, temperatures, and mass flows of the media have to be controlled within tight limits. In order to operate the fuel cell stack properly, it is necessary to control a number of auxiliary components (balance of plant—BoP). Figure 7.3 gives an overview of these components consisting of the hydrogen supply system and the air/oxygen supply system, water and thermal management systems, and the control unit. The air supply system consists of an air filter, an air blower or compressor, and a humidifier. The water and thermal management system controls the temperature and the humidity of the fuel cell stack.

7.3 Characteristics and Heat Transfer of PEMFC

The achievement of higher efficiencies with PEMFC systems represents a key aspect in order to enhance the market share of fuel cell electric vehicles. In principle, the overall efficiency of a PEMFC system depends on the stack characteristics (see polarization curve in Fig. 7.2) and the respective power consumption of the

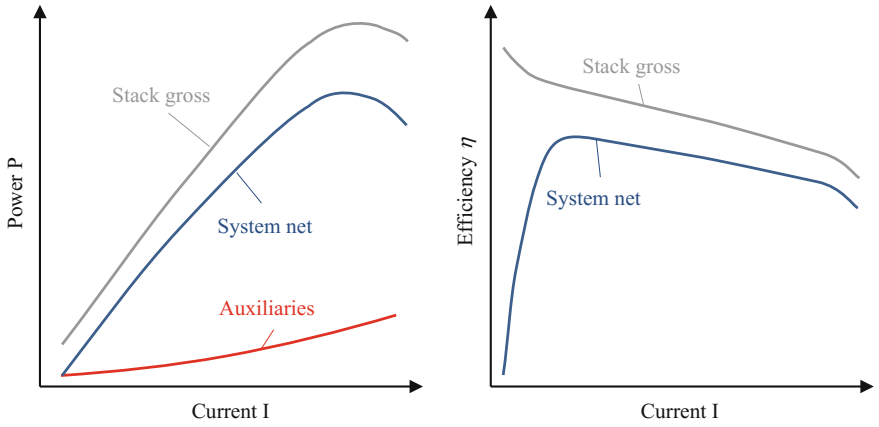

Fig. 7.4 Power and efficiency characteristics over electrical current

required auxiliary systems the so called BoP-components (air compressor, water pump, radiator, H_2 recirculation pump, etc.). Figure 7.4 presents the power and efficiency characteristics versus electrical current. The stack power is basically determined by the polarization curve. Stack power increases with higher electrical current until the maximum is reached. A further increase of electrical current results in lower power as the voltage of the polarization curve decreases drastically.

Overall fuel cell system net power results from stack power minus required power of auxiliaries. Present FC stacks achieve a power density of up to 3.1 kW/dm^3 by volume and 2 kW/kg by mass [11]. A further enhancement is the objective of many research projects. Moreover, a reduction of power consumption of auxiliaries is required and different concepts of BoP-components are investigated. The power consumption of the auxiliaries usually shows an exponential trend on electrical current. Main power consumer of the auxiliaries is the air compressor which compresses the air from ambient to cathode operation pressure of the stack. Cathode operation pressures usually range from a few mbar to 2000 mbar excess pressure and over-stoichiometric air-to-fuel ratios around 1.5–2.5 are generally applied. Basically, higher air pressure on the cathode side and higher air mass flow result in increased operating voltage at any particular current which further enhances stack gross efficiency. Nevertheless, the increase of stack efficiency is often repealed by lower mechanical efficiency as higher power is required for the air compressor. The mechanical efficiency considers the efficiency influence of the auxiliaries and represents the factor between stack and system efficiency. It is calculated by the power of system net to power of stack gross.

With PEMFC the stack efficiency is highest at very low electrical currents (part load operation) and decreases almost linearly with increasing current. By contrast, system net efficiency is lowest at very low electrical currents as the influence of auxiliaries is predominant (low mechanical efficiency). Highest system net efficiency is achieved in part load conditions with values up to 60% [12]. At very high

electrical currents system efficiency decreases again. Hence, many operation strategies of electric vehicles aim to shift the operation point to highest efficiency area by hybridization with batteries.

Despite the high system efficiency of fuel cells, high amounts of waste heat energies have to be transferred from the system. 5–15% of the energy input to the FC is lost as waste heat through the exhaust and 40–45% of input energy is converted to heat and transferred to the coolant system. Hence, the amount of heat is only slightly less than its electric power output.

Current PEMFCs operate in the temperature range of 60–80 °C. Basically, higher coolant temperature positively influences the polarization curve but the nominal operating temperature is limited to roughly 80 °C in order to avoid damages of the proton exchange membrane.

Figure 7.5 presents the heat flows inside a fuel cell system at a higher load point during a real-driving cycle. In this load point ∼43% of input energy is converted to heat and transferred to the coolant system. Depending on BoP-system configuration

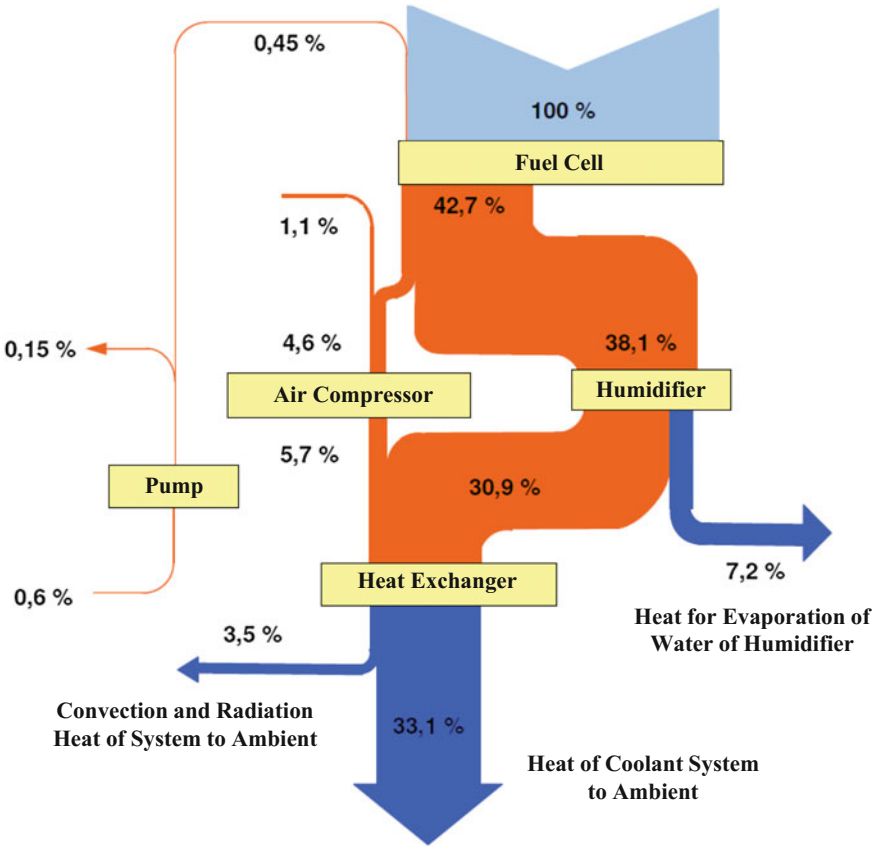

Fig. 7.5 Heat flows at higher load point during real-driving cycle [20]

some parts require cooling or use heat for a proper function. The shown system uses an external humidifier for humidification of cathode air. For evaporation of the water approximately 7% of input energy is required as heat. Present automotive systems try to avoid external humidifiers for efficiency and cost reasons [13]. Hence, higher amount of heat has to be transferred by the heat exchanger. Moreover, air compressor and pump also deliver heat to the coolant system. Overall 33% of the input energy has to be transferred as heat to the ambient by the heat exchanger.

These relatively low coolant temperatures in combination with the high amount of heat necessitate relatively large radiators in PEMFC electric vehicles. This represents a significant challenge regarding packaging and aims for sophisticated thermal management systems.

7.4 Cooling Requirements and Techniques Within a PEMFC Automotive

A typical low-temperature PEMFC with working temperatures clearly below 100 °C has an efficiency of up to 60% as mentioned before. As there is hardly any natural rejection of heat (which is minimum 40% of energy input like shown in Fig. 7.5) via exhaust gases various methods for the dissipation of the heat have been applied in the past. The following list gives an overview of the different approaches. The values in the brackets represent the FC power class for the proper approach.

- Cooling with cathode air flow via natural and forced convection (<300 W)
- Separate Air Flow (<2 kW)
- Heat spreaders also called edge cooling or passive cooling (<5 kW)
  - With highly conductive materials
  - With heat pipes
- Water cooling, using sensible heat of the coolant (>5 kW)
  - Deionized water, requires an ion exchanger
  - Antifreeze/coolant, lower heat capacity than pure water
- Phase change cooling, uses latent heat of the coolant
  - Evaporative cooling with water (500 W < 75 kW)
  - Cooling via boiling requires media with low boiling temperature (e.g. 1 kW)

Due to the power classes of an automotive PEMFC (>50 kW) and in terms of practicality the only reasonable solution with wide experience is the water cooling, to which deeper insight is generated via this chapter.

As medium either water or a water/glycol mixture is used for liquid cooling. The use of water in liquid cooling of a FC has the advantage of the very high specific

heat capacity of 4.182 kJ/kgK compared to air with 1.005 kJ/kgK and 50/50% water/glycol with <3.5 kJ/kgK.

Special attention in water cooling must be given to the electrical conductivity of the water/coolant. As the conduction in coolant can lead to current leakage in the stack or degradation of the bipolar plates the electrical conductivity has to be reduced. This can be either achieved via an ion-exchange resin or partly with filters with activated carbon particles or inert gas injection to purge oxidation products from the coolant.

The cooling channels for the water are integrated in the bipolar plate (see Fig. 7.6). The bipolar plate is the outer structure of the PEMFC and has several functions like the heat transfer from the MEA (Membrane Electrode Assembly) to the cooling circuit. In order to meet with these requirements, the conductivity must

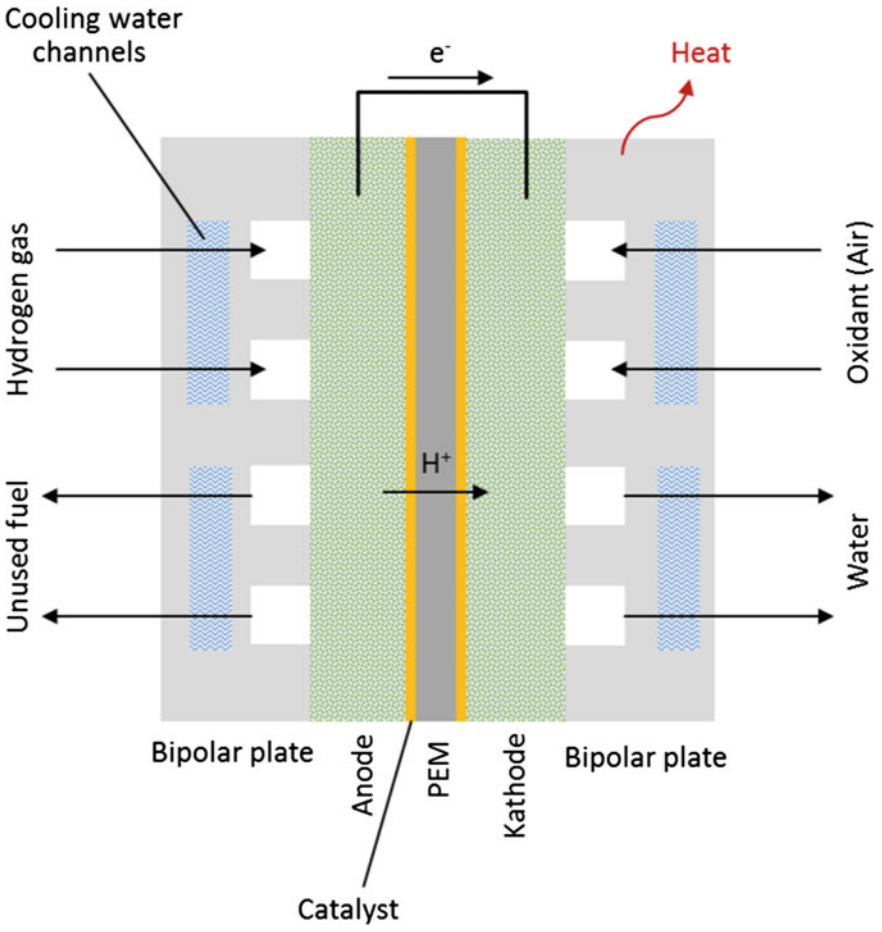

Fig. 7.6 PEMFC Architecture with cooling channels

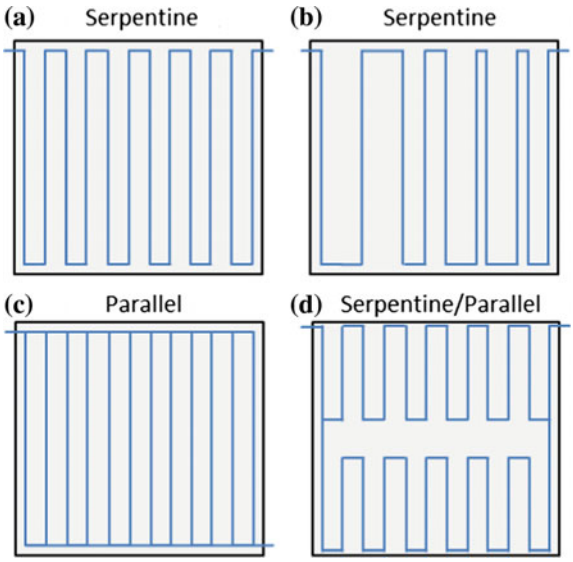

Fig. 7.7 Different cooling flow field design in a fuel cell bipolar plate

be as high as possible, this can be achieved by the non-corrosive and commonly used graphite.

In terms of efficiency and durability it is highly favorable to keep the temperature uniform across the MEA. A uniform temperature profile across the stack was topic of several investigations [1] (Fig. 7.7).

These significant efforts—devoted to improve cooling flow field design—all came to the result that the serpentine design has a much better distribution of coolant flow.

Beside of a good uniformity of temperature the pressure drop must be kept low. Corresponding to several investigations it can be said that the parallel design goes along with lower pressure losses whereby the tradeoff (heat uniformity vs. pressure losses) can be seen as further optimization potential.

Next to the optimization of liquid coolant flow field design, also the coolant channel geometry can be arranged in order to gain better conductivity between die the bipolar plate and the coolant.

Reference [14] developed a so called chaotic 3D channels with chaotic laminar flow inside the channels. It is reported that the efficiency is much higher due to Nusselt number 4–7 time higher by even lower pressure losses.

Another approach was established by Honda, namely the V flow stack structure. While the hydrogen and air is transmitted vertically, the coolant flows horizontally across the bipolar plates. According to Hondas statement the cooling layers could have been reduced by its half and the weight density output could have been increased by 67%. This method has led to a significant reduction of weight and size of the PEMFC stack [15] (Fig. 7.8).

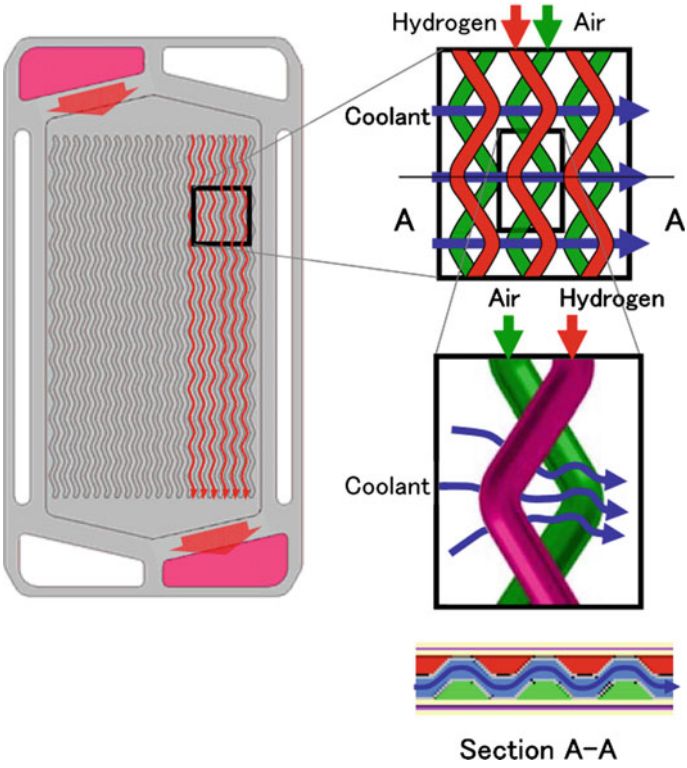

Fig. 7.8 Honda's PEMFC stack cooled by wave flow channels, copyright [15]

7.5 Cooling Circuits and Comprehensive Thermal Management

Beside of an adequate cooling channel layout the circuit architecture of the cooling system must be chosen. The system design of the BoP has a significant impact towards the efficiency of a PEMFC and the electrical power consumption of the auxiliaries. This system influences the parasitic vehicle power consumption as well as the size and weight of the stack.

In the following 4 diagrams different proposals for a cooling circuit for a PEMFC are given.

Concept 1 is to be seen as the most common approach, see Fig. 7.9. This system is also called 2-circuit system as there is one low temperature (LT) cycle for the e-motor and the power electronics, whereat especially the latter is in need of lower coolant temperatures which doesn't allow any satisfying use of one overall circuit architecture. The second circuit serves for cooling the stack and is called high temperature (HT) circuit. The system is driven by an electrically controlled pump; a particle filter can be used to avoid fouling of the PEMFC and the HX. Then the

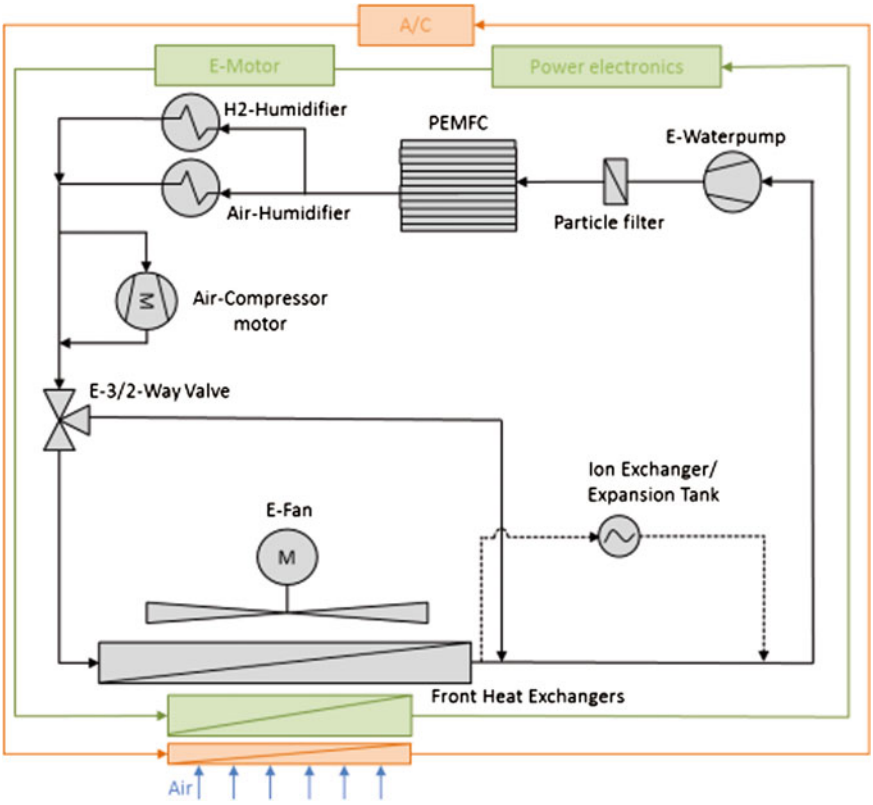

Fig. 7.9 Concept 1, conventional cooling circuit for a PEMFC

temperature control of the humidifiers is common with the release of heat prior absorbed form the FC. In a next step the compressor, respectively the intercooler (if existing), for the reactant air is conditioned. Via convection at the radiator the heat is released to the ambient air. Subsequently an ion exchanger is used in case of no use of glycol within the cooling circuit. This assembly ensures to reduce i.e. soda-ions and restock the water with potassium-ions. For this reason the water loses most of its electrical conductibility.

Concept 2 comprises of a second water circuit and an internal water/water HX, see Fig. 7.10. In the course of this architecture the control of the heat release is made by the pump control in the second circuit and not via a thermostat valve which is left out. The two-circuit-solution makes it possible to implement elements like the humidifier, air compressor or intercooler either in the internal or even in the external circuit. With this higher degree of freedom the components can be positioned in the most favorable temperature zone (inner circuit has a higher temperature level). This allows a more specific layout design and opens up new possibilities for tailor made solutions. Certainly, it must be mentioned that this advantages go along with more complexity and significant increase of weight.

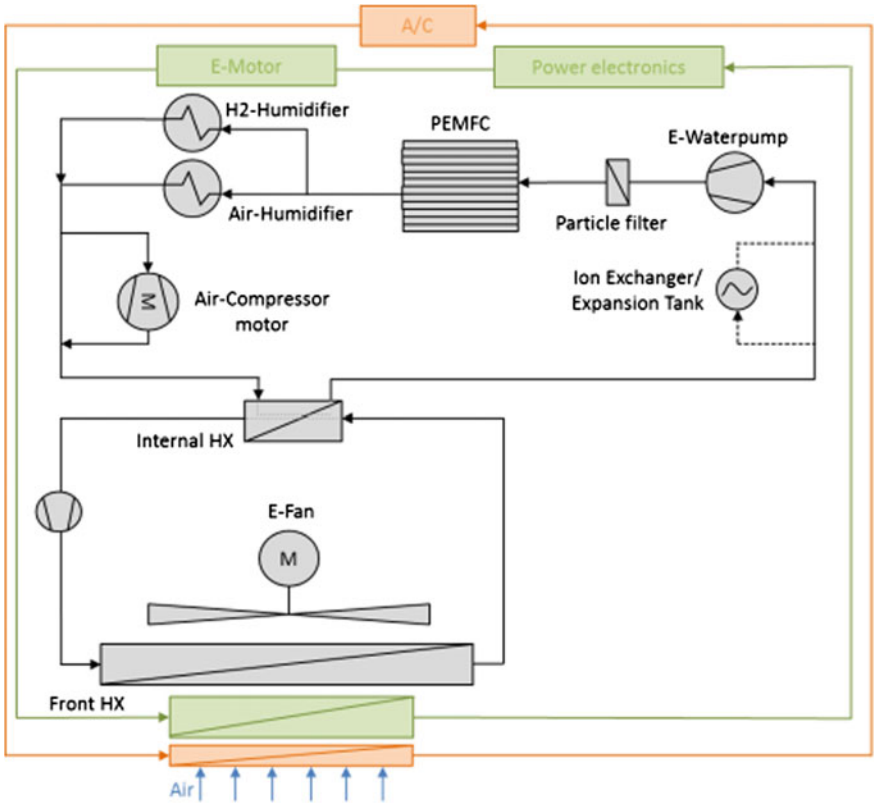

Fig. 7.10 Concept 2, PEMFC cooling circuit with a second HX

Concept 3 comprised of a waste heat recovery system which realizes to reuse the rejected heat and increases the thermodynamic efficiency of the PEMFC-system, see Fig. 7.11.

Reference [16] shows a feasibility study with different cooling agents, namely R123, R245fa and R134a, water and ethanol. This combined heat and power solution was investigated via ex situ tests whereat the PEMFC was loaded with constant current. The feasibility has been proved while obtaining an additional 4% in thermal efficiency of the overall system.

Concept 4 shows a novel approach for increasing the cooling efficiency of the HT-cooling circuit of the FC, see Fig. 7.12. By the use of an additional heat exchanger between HT- and LT-circuit respectively HT- and A/C-circuit extra cooling performance can be gained. On the one hand, this goes along with higher (and for FC very important) cooling performances; on the other hand this leads to an increase of the total system efficiency because of better utilization of the proper cooling capacities. It is required to execute vast prior investigations towards

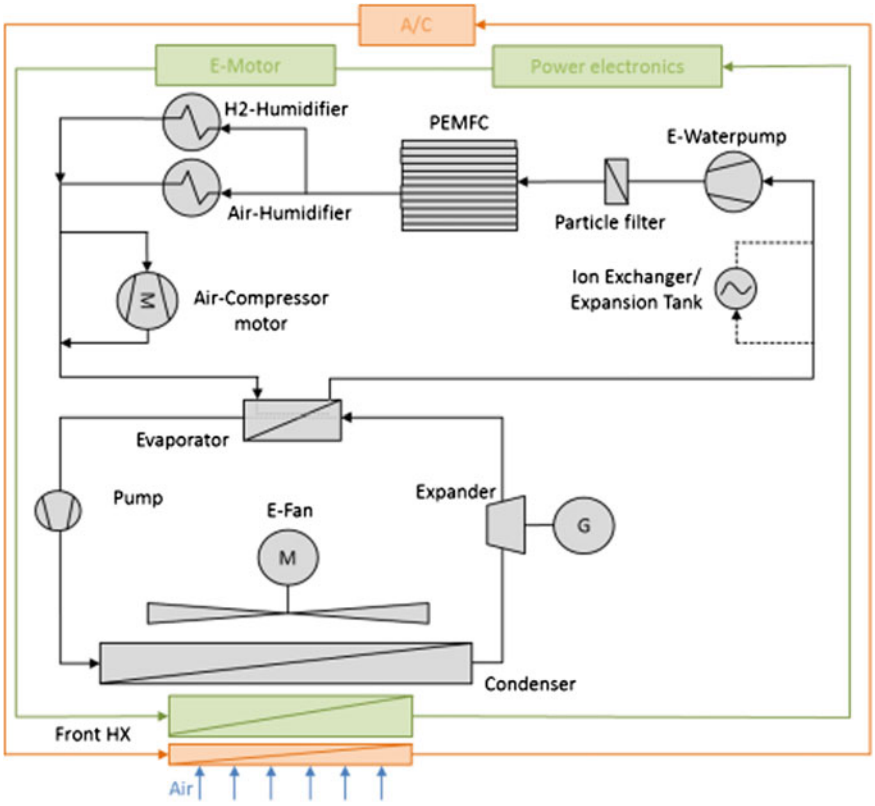

Fig. 7.11 Concept 3, PEMF cooling circuit with ORC for waste heat recovery

control—and operation-strategies in order to have a resilient validation for the temperatures in the cooling/conditioning cycle.

The prior concepts all consist of a pump, a fan, a radiator and a valve. In order to optimize the system in general suggestions are made in the following (valid for all 4 concepts, mentioned above).

7.5.1 Pump

Two control circuits for the pump are proposed. On the one side the pressure of the coolant shall be controlled, on the other side the temperature difference at in—and outlet of the stack shall be kept constant in operation.

Pressure differences between coolant, H_2 and air must be avoided as a matter of principle in a FC for adequate operation. Especially in cases of purging (cyclic, empting of H_2) the pressure in the system significantly decreases. At the same time

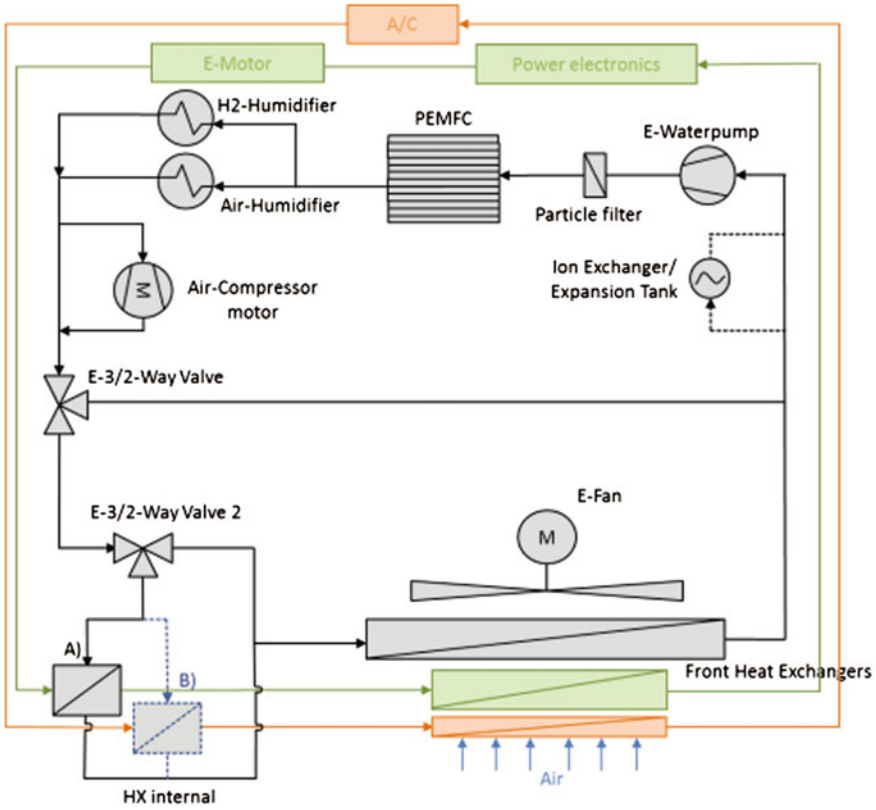

Fig. 7.12 Concept 4, PEMFC cooling circuit with additional HX with A/C or LT-circuit

the pump power control of the pump must be lowered. Pressure difference between the coolant and gas (H_2 as well as air) must be kept below 50 kPa.

The second control keeps the temperature difference between inlet and outlet of the stack module in a defined range (usually between 4 and 7 K). This measure is to be done for a highest uniformity of the temperature profile within the stack. This temperature control superimposes the pressure control. Together with the valve and fan control the stack temperature profile can be kept within the specified temperature regions for low degradation and high efficiency.

7.5.2 Fan

The fan shall be integrated via a hood to avoid leakage flow beside the heat exchangers (HXs). Like the electrical water pump, the fan shall be driven by stack module voltage (300–450 V). It shall consist of an electric control which enables

the fan when too high temperatures occur in the stack module. Especially events like stop-and-go and mountainous routes require major cooling capacity, whose power consumption can kept low via intelligent control strategies.

The increase of more air volume by more power is limited because the increase of the volume involves the rise of power consumption with the factor three. The pressure characteristic of a fan shall be as flat as possible which means that in the fan's downtime nearly no influence towards the dynamic pressure (natural stream) shall be given (overblowing of fan).

7.5.3 Valve

As valve a wax thermostat with a temperature depending characteristic can be used. Though, it is recommended to use an electronic controlled valve, which allows more flexibility in terms of different conditioning modes. Especially in system 4 in Fig. 7.12 the two proposed valves are used for specific cooling strategies which require fully controllable valves with a proportional way characteristic.

7.5.4 Radiator

The radiator is the main component in response for the convection of heat. As the coolant inlet temperature of the FC has to be below 80 °C the requirements for heat dissipation are much higher than with combustion engines. Therefore the enlargement of the HX is highly favorable. Experimental as well as computational studies [17] revealed the high influence of the HX-size, whereat optimized radiator sizes increase the heat rejection with more than 50%.

One interesting solution towards optimum air velocity may be to install one big HX with two fans which cover the major surface of the radiator. The fans shall have a very steep characteristic, at which the HX is configured for maximum heat release with fan operation.

In order to allow heat rejection in low operation modes an additional HX is applied at the very front end which is not subject to the steep fan characteristic and allows a high dynamic pressure operation.

Evaluation of cooling system components with the interaction of the PEMFC can be made either via experimental tests or via simulation. As the simulation is more cost efficient experiments shall be made solely for the validation.

For example an analytical evaluation via one-dimensional modeling can be examined. This concludes the multi-zone calculation of the thermal network, each zone representing physical and chemical phenomena's for the appropriate illustration of hydraulic and thermic behavior. The heat source, namely the PEMFC, can be modelled with a phenomenological method (1D), quasi dimensional method (0D) or non-dimensional method like neuronal, polynomial and mean value models.

The heat release from the FC is transferred to the cooling circuit, whereat interactions between the water circuits and the fuel cell are shown. This allows the optimization of the cooling circuit with respect to optimum FC-temperatures with the possibility of investigating different ambient conditions and road profiles. Especially mountainous roads with steep inclinations and at the same time at very high ambient temperatures have to be subject to benchmarks, not only for the optimization but even for a component protection. Here, the simulation offers wide varieties and a fast acquirement of results with low expenditure.

7.6 Conclusion/Further Research Needs

High power requirements of PEMFC stacks while limited space at automotive applications are the significant challenges for a cooling system for FCEVs.

The problem becomes more severe due to the small temperature difference between the PEMFC stack and the ambient air, and an almost negligible heat removal by the product streams. The heat generation, its removal and the resulting temperature distribution within the cell components directly affect the interfacial properties, local heat generation rate, and water transport [18].

A number of cooling strategies and techniques have been developed and applied in practice for PEMFC stacks with different power ratings. These cooling strategies are summarized in this article. As reviewed in this work, significant advancements have been made in cooling of PEMFC stacks.

Liquid cooling has been widely and successfully applied in automotive PEMFC stacks.

7.6.1 Further Research Needs

It is evident, that a cooling system design has direct impact in meeting the durability, cost, and performance targets to promote their commercialization under wide range of ambient conditions, from high ambient temperatures to extremely frigid conditions in colder climates [9].

Some of the future issues are summarized below [18]:

- Fundamental understanding of the thermal properties and heat transfer characteristics of PEMFC components through in situ and ex situ experimental investigations.
- Optimization of the coolant and reactant flow configurations to achieve the desirable distribution characteristics of local current density, temperature and water content in the PEMFC at low cost and improved efficiencies.
- Improving heat transfer efficiency of radiators for automotive PEMFC stacks to reduce their sizes.

- Developing a coolant that has a high ionic resistance, does not degrade over the lifetime of the stack, and has a low viscosity for reduced pumping power.
- Further improvements by adaption of the circuit design—like shown in the 4 concepts (Figs. 7.9, 7.10, 7.11 and 7.12), to increase the heat rejection. Especially the coupling with the HVAC system, which can generate considerably more cooling performance, shows high potential.
- The use of heat accumulators inside the cooling system to stabilize the temperature.
- Sprinkling of condensed water from exhaust gas to improve cooling performance of a radiator by evaporation of water (also known in diesel plants with two-stage turbocharging and intensive water condensation in an intercooler).
- Further increase of stack efficiency and enhancement of coolant temperature.

References

1. Noreikat KE, MTZ Wissen 11. Brennstoffzelle, Antriebsstrang und Infrastruktur, Apr 2013, p 327
2. Li X (2006) Principles of fuel cells. Taylor & Francis, New York
3. Wang Y, Chen KS, Mishler J, Cho SC, Adroher XC (2011) A review of polymer electrolyte membrane fuel cells: technology applications, and needs on fundamental research. Appl Energy
4. Fuel Cells (2000) Fuel cell vehicles (from auto manufacturers). http://www.fuelcells.org/info/charts/carchart.pdf; 2011
5. Zhang A, Kandlikar SG (2011) A critical review of cooling techniques in proton exchange membrane fuel cell stacks. Department of Mechanical Engineering, Rochester Institute of Technology, USA
6. Li H, Tang Y, Wang Z, Shi Z, Wu S, Song D, et al (2008) A review of water flooding issues in the proton exchange membrane fuel cell, J Power Sources
7. Dai W, Wang H, Yuan X-Z, Martin JJ, Yang D, Qiao J, et al (2009) A review on water balance in the membrane electrode assembly of proton exchange membrane fuel cells. Int J Hydrogen Energy
8. Jiao K, Li X (2011) Water transport in polymer electrolyte membrane fuel cells. Prog Energy Combustion Sci
9. DOE (2007) Fuel cells technologies program: multi-year research, development and demonstration plan: planned program activities for 2005–2015. http://www1.eere.energy.gov/hydrogenandfuelcells/mypp/pdfs/fuel_cells.pdf
10. Frano B (2005) PEM fuel cells: theory and practice. Elsevier. ISBN:0-12-078142-5
11. Itoga M, Hamada S, Mizuno S, Nishiumi H. et al (2016) Development of fuel cell stack for new FCV, SAE Technical Paper 2016-01-0529
12. DOE—U.S. Department of Energy, FY (2015) Progress report for the DOE Hydrogen and Fuel Cells Program, DOE/GO-102015-4731
13. Hasegawa T, Imanishi H, Nada M, Ikogi Y (2016) Development of the fuel cell system in the mirai FCV. SAE Technical Paper 2016-01-1185. doi:10.4271/2016-01-1185
14. Lasbet Y, Auvity B, Castelain C (2006) Chaotic heat exchanger for PEMFC cooling applications. J Power Source
15. Matsunaga M, Fukushima T, Ojima K (2009) Powertrain system of honda FCX clarity fuel cell vehicle. EVS24, Stavanger, Norway, 13–16 May 2009
16. He T, Shi R, Zhuge W (2016) Waste heat recovery of a PEMFC system by using organic rankine cycle. Department of Automotive Engineering, Tsinghua University, Beijing

17. Eichlseder H, Klell M (2012) Wasserstoff in der Fahrzeugtechnik. Erzeugung, Speicherung, Anwendung. (Hydrogen in Vehicle Technology, Production, Storage, Application), 3rd edn. Springer Vieweg Wiesbaden, Berlin
18. Zhang G, Kandlikar SG (2012) A critical review of cooling techniques in proton exchange membrane fuel cell stacks. Int J Hydrogen Energy 37:2412–2429, Elsevier
19. Rabbani A, Rokni M (2013) Dynamic characteristics of an automotive fuel cell system for transitory load changes. Sustainable Energy Technol Assessments 1:34–43, Elsevier
20. Berger O (2009) Thermodynamische Analyse eines Brennstoffzellensystems zum Antrieb von Kraftfahrzeugen. Dissertation, Universität Duisburg-Essen